Heinrich Pette Institute

Leibniz Institute for Experimental Virology

The role of the murine cytomegalovirus protein M28 in cross-species infection

Dissertation

submitted to the

Department of Chemistry

Faculty of Mathematics, Informatics and Natural Sciences

University of Hamburg

In fulfillment of the requirements

for the degree of

Doctor of Natural Sciences (Dr. rer. nat.)

by

Kerstin Pawletko

born in Krefeld

Hamburg 2020

Prof. Dr. Wolfram Brune (First Reviewer)

Prof. Dr. Peter Heisig (Second Reviewer)

Date of oral defense: 08.05.2020

Table of contents

1 Abstract

Cytomegaloviruses (CMVs) have co-evolved with their respective hosts for many years and are known to be strictly species specific. While CMVs can infect cells of a foreign host, they cannot replicate in them, and the underlying mechanisms of the species restriction remain poorly understood. Recently, it was shown that murine CMV (MCMV) can be adapted to human epithelial cells, a phenotype attributed to adaptive mutations in several genes. While comprehensive analysis revealed that inhibition of apoptosis, dispersion of PML-nuclear bodies, and prevention of E2F-mediated gene transcription are important for crossing the species barrier in human epithelial cells (RPE-1), the replication of these adapted viruses was still attenuated in human fibroblasts. To date, why MCMV replication is restricted in human fibroblasts had not been addressed. Preliminary studies indicated that MCMV M28 is an important factor in species specificity.

The aim of this study was to investigate the function and molecular mechanism of M28 in cross-species infection in human fibroblasts. In this study, I identified M28 as a novel host range determinant important for the fibroblast adaptation. Specific introduction of missense or stop mutations in M28, in addition to others, promoted efficient replication in human fibroblasts, whereas replication of MCMV-M28stop in murine fibroblasts was not impaired. In this study I could show that M28 is expressed with early kinetics, localizes to the cytoplasm, and binds to the SHC-transforming protein 1 (SHC1). SHC1 is an essential scaffold protein of the epidermal growth factor receptor (EGFR) and other receptor tyrosine kinases. It is phosphorylated upon EGFR stimulation and activates mitogen-activated protein kinases (MAPK) and phosphoinositide-3-kinase/AKT signaling pathways, which are involved in cell cycle regulation, proliferation, and survival. During infection, M28 interacts with SHC1 and prevents its phosphorylation thus restraining further downstream signaling of MAPK/ERK and PI3K/AKT. However, in primary MEFs phosphorylation of SHC1 was not affected in the presence or absence or M28, suggesting another mechanism of action in murine fibroblasts. Moreover, a transient knockdown of SHC1 in infected MRC5 cells reduced viral titers of an MCMV mutant lacking M28. Taken together these results suggest that expression of M28 restricts viral replication in human fibroblasts by binding to SHC1 and inhibiting downstream signaling. Conversely, SHC1 functions as a pro-viral factor in MCMV cross-species infection of human fibroblasts.

2 Zusammenfassung

Cytomegalieviren (CMV) haben sich über die Jahre mit ihrem Wirt parallel entwickelt und sind als strikt Spezies-spezifisch bekannt. CMV ist in der Lage Zellen artfremder Spezies zu infizieren, kann sich jedoch nicht in ihnen vermehren. Die zugrunde liegenden Mechanismen der Spezies-Spezifität sind bisher nur unzureichend verstanden. Kürzlich wurde gezeigt, dass eine spontan entstandene murine CMV (MCMV) Mutante in humanen Epithelzellen repliziert und die Fähigkeit der Replikation mit dem Auftreten adaptiver Mutationen in mehreren Genen einhergeht. In umfassenden Studien wurde gezeigt, dass die Inhibierung apoptotischer Signalwege, die Zerstörung von *PML-nuclear bodies* und die Unterdrückung von E2F-vermittelter Gentranskription für die Überwindung der Spezies-Barriere in humanen Epithelzellen eine bedeutenden Rolle spielen; eine effiziente Replikation in humanen Fibroblasten jedoch weiterhin stark eingeschränkt war. Bisher konnte nicht ausreichend geklärt werden welche zugrunde liegenden Mechanismen für die attenuierte Replikation in humanen Fibroblasten verantwortlich sind. Vorläufige Studien wiesen darauf hin, dass das MCMV protein M28 ein wichtiger Faktor für die Spezies-Spezifität ist.

Das Ziel dieser Arbeit war es die Funktion und den molekularen Mechanismus von M28, als potenzielle Determinante des Wirtspektrums, zu untersuchen. In dieser Studie konnte ich M28 als eine neue Determinante des Wirtspektrums identifizieren, die für die Überwindung der Spezies-Barriere in humanen Fibroblasten eine bedeutende Rolle spielt. Die Einführung spezifischer M28 *missense* oder stop Mutationen, neben anderen Mutationen, förderten die effiziente Replikation in humanen Fibroblasten. Die Replikation einer M28 defizienten Mutante in murinen Fibroblasten jedoch nicht beeinträchtigt war. M28 konnte als frühes Protein (*early*) identifiziert werden und ist im Cytoplasma lokalisiert. Dort bindet M28 an das *SHC-transforming protein 1* (SHC1). SHC1 ist ein zelluläres Adapterprotein des *epidermal growth factor receptors* (EGFR) und anderen Rezeptor- Tyrosinkinasen. Durch die Stimulierung von EGFR mit Wachstumsfaktoren wird SHC1 phosphoryliert, aktiviert Mitogen-aktivierte Proteinkinasen (MAPK) und die Phosphoinositid-3-Kinase/AKT-Signalwege, die an der Regulierung des Zellzyklus, der Proliferation und apoptotischen Signalwegen beteiligt sind. Während der Infektion interagiert M28 mit SHC1, verhindert die Phosphorylierung von SHC1 und hemmt die stromabwärts liegenden Signalwege MAPK/ERK und PI3K/AKT. In murinen Fibroblasten wurde die Phosphorylierung von SHC1 in Gegenwart oder Abwesenheit von M28

13

jedoch nicht beeinträchtigt, das auf einen anderen molekularen Mechanismus in murinen Fibroblasten hindeutet. In humanen Fibroblasten führte ein transienter *Knockdown* von SHC1 zu einer eingeschränkten Replikation und niedrigeren viralen Titern einer M28 defizienten Mutante. Zusammenfassend deuten die Ergebnisse darauf hin, dass die Expression von M28 die virale Replikation in humanen Fibroblasten über die Bindung an SHC1 einschränkt, um die weiteren stromabwärts gerichtete Signalwege zu beeinträchtigen. Umgekehrt konnte SHC1 als ein pro-viraler Faktor identifiziert werden, der an der Anpassung von MCMV an humane Fibroblasten beteilig ist.

3 Introduction

3.1 Cytomegalovirus

3.1.1 Epidemiology and pathology

Clinical signs characteristic of cytomegalovirus infection were firstly reported in 1904 and named as cytomegalic inclusion body disease (CIBD) [1]. 50 years later, CMV was isolated and propagated by Margaret Smith and Thomas H. Weller [2, 3]. Human cytomegalovirus (HCMV) is one of the most important human pathogens in immunocompromised individuals such as organ transplant or HIV infected patients. In the case of congenital infection, cytomegalovirus is the most common cause of long-term disabilities, like mental retardation and sensorineural hearing loss in newborns [4, 5]. Transmission from primarily infected mothers to the fetus occurs in 30-40% of cases, whereas only a small number (0,6-1,4%) of seropositive mothers transmit the virus either during gestation, delivery or later on via breast feeding [6-8]. In the general population, the virus is transmitted via body fluids, such as urine, saliva, breast milk, semen, vaginal fluids, and blood transfusions [9]. The worldwide seroprevalence of HCMV ranges from 40- 100% depending on the socioeconomic status of the region and hygienic habits [6, 10] (Figure 1). A recent study performed in Germany reported a cytomegalovirus seroprevalence of 57% with a higher seroprevalence for women (62%) than men (51%) [11].

The course of infection in immunocompetent individuals is mainly subclinical, with mostly mild and flu-like symptoms that spontaneously regress due to efficient viral control by the immune system. Nevertheless the virus is not eradicated, and the acute phase of the infection is followed by a latent infection in which the virus remains lifelong in the body with occasional sporadic reactivation events [12]. In rare cases, cytomegalovirus infection can also lead to mononucleosis-like illness. On the other hand, in immunocompromised patients like AIDS- or organs transplant patients, both HCMV infection and reactivation can lead to severe diseases like pneumonitis, hepatitis, myocarditis or cardio-vascular diseases [8]. Due to the development of HIV specific treatment with highly active antiretroviral therapy (HAART), the risk of severe complications of an HCMV infection in HIV patients has decreased over time [13]. Unfortunately, HCMV is still an important morbidity factor in patients undergoing hematopoietic stem cells transplantation and in seronegative patients receiving a solid organ from seropositive donors [14].

The therapeutic strategies are limited: both infected immunocompromised patients and congenitally infected newborns can be treated with the first line antivirals ganciclovir or its derivate valganciclovir. In the case of viral resistance, foscarnet or cidofovovir may substitute ganciclovir. All of these antivirals target the DNA polymerase complex and thereby inhibit viral replication. However, all mentioned antivirals have strong side effects like myeloid- and nephrotoxicity and cannot be applied during pregnancy nor in patients severely ill [5, 15, 16]. Recently, a new antiviral, letermovir, has been discovered and approved for CMV prophylaxis treatment in transplant recipients in 2018. LTV targets the viral terminase complex components pUL56 and pUL89 and inhibits viral DNA processing and packaging. LTV can be an alternative treatment in case of viral resistance against other antivirals [15]. However, first case studies reported emergence of a CMV resistant strain after allogeneic hematopoietic-cell transplantation during secondary prophylaxis with LTV [17]. Therefore, the awareness and prevention of an HCMV infection is of high importance as no vaccine is available.

Figure 1: Worldwide seroprevalence of HCMV in adults [18].

3.1.2 Classification and Structure

A hallmark of all herpesviruses is their large DNA genome, their ability to persist in the host and establish a lifelong latency after a primary infection. Additionally, herpesviruses are classified into alpha-, beta- and gamma- subfamilies, depending on the different replication properties, cell tropism and host range. The prototypic of alpha-herpesviruses is Herpes Simplex Virus 1 (HSV-1), characterized by a very fast replication cycle and a broad host range. Human and murine cytomegaloviruses are the most representative members of the sub-family beta-Herpesvirinae [19]. A characteristic shared by CMV is the strict species-specificity, which means the virus can only replicate in cells of its own or closely related host species [20]. The strict species-specificity likely resulted from co-evolution of CMVs with their respective hosts and reflects the optimal adaptation of the viruses to their natural environment. Due to the strict host range, HCMV cannot be studied in animal models and instead the murine CMV (MCMV) infecting mice is used for *in vivo* studies [21]. Finally, gamma-herpesviruses are represented by Epstein-Barr virus (EBV) and Kaposi's sarcoma associated herpesvirus (KHSV), both viruses have a narrow host range and a slow replication cycle.

Irrespectively on their classification in alpha-, beta- or gamma- subfamilies, herpesviruses share a common structure of the viral particles. The genome consists of a large double stranded linear DNA (dsDNA) genome. For MCMV, the genome is about 230 kb in size and encodes at least 170 open reading frames (ORF) [22]. The genome is enclosed by an icosahedral nucleocapsid, which is surrounded by a protein matrix layer, which is called the tegument. Tegument proteins are released into the cell immediately after viral entry and function as important host-cell factors, which for instance modulate intrinsic cellular defenses [23, 24]. The virion particle is 200-300 nm in diameter and surrounded by a lipid-membrane layer containing several glycoprotein complexes, which are important for the attachment and entry of the virus into the host cell [25] (Figure 2).
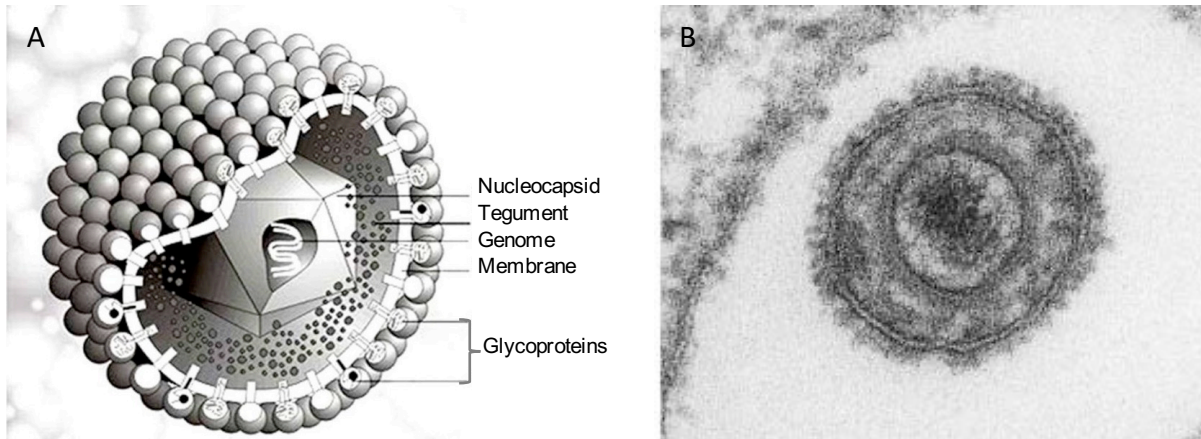
Figure 2: Virion structure of a cytomegalovirus particle.

A Schematic of a CMV particle including the indicated structures: genome, membrane, nucleocapsid, tegument and glycoproteins http://www.virology.net/big_virology/bvdnaherpes.html **B** Electronic microscopic image of HCMV [26].

3.1.3 Gene expression and replication

Cytomegaloviruses have a very strict host range, but a broad cell tropism. They can infect and replicate in different cell types, for example fibroblasts, epithelial cells, endothelial cells, monocytes/macrophages, smooth muscle cells, neuronal cells, neutrophils, and hepatocytes [27]. The whole replication cycle of HCMV occurs within 72- 96 hours and in comparison, MCMV completes its replication cycle in 24 hours. The following steps of the replication cycle are described for HCMV as a model. The replication cycle is initiated by the attachment of the particle to the cell. This process occurs via the adsorption of gB or gM/gN to heparin sulfate proteoglycans (HSPGs) on the surface of the host cell [28, 29].

Once the particle is attached to the plasma membrane, viral entry into the target cell is mediated by the glycoprotein complexes gB, gH and gL, which interact with tyrosine kinase receptors [28] (Figure 3). The specific receptor for HCMV is controversial, and until now while EGFR, PDGFR and neuropilin have been described as main receptors, Integrins are considered as co-receptors [30-33]. After interaction with the receptors and co-receptors, the viral envelope either fuses with the plasma membrane in a pH- independent manner, or instead with the endosomal membranes, surrounding the viral particles that are internalized via endocytosis or macropinocytosis [34]. After internalization the viral capsid and tegument proteins are released into the cytoplasm (Figure 3).

The viral capsid is transported along microtubules towards the host cell nucleus. The viral DNA is delivered into the nucleus through the nuclear pores and a cascade of viral gene expression is initiated [35]. Meanwhile, important tegument proteins counteract host cell immune responses and regulate important gene regulatory functions [24].

Once the viral genome has entered the host cell nucleus, the virus can establish a lytic infection, complete the replication cycle or instead establish latency and persist lifelong in a "silent" state. Latency mostly occurs in hematopoietic stem cell precursors and myeloid cells where the virus genome persists as episomal material, transcriptionally repressed and therefore incapable to express immediate early genes [12, 36]. On the other hand, during the lytic phase, viral genes are highly expressed and follow a strictly temporally ordered cascade. First of all, the immediate early (IE) proteins are transcribed and act as transcriptional factors and trans-activators of early proteins (E) (Figure 3). Afterwards, the immediate early proteins IE2 (HCMV)/IE3 (MCMV) and the early proteins, encoded by gene regions UL112/113 (HCMV) and M112/113 (MCMV), accumulate in close proximity to promyelocytic leukemia protein-associated nuclear bodies (PML-NB), and recruit other viral factors, like the viral polymerase to form the viral replication compartments [37, 38]. Viral DNA replication is initiated at the origin of lytic replication (ori_{Lyt}) and proceeds with a rolling cycle mechanism [39, 40]. In parallel to the replication of the viral genomes, the late genes are expressed, and the viral structural proteins are produced. Viral DNA and nucleocapsid proteins associate in the nucleus and give rise to the capsids that move to the cytoplasm, where they enter the viral assembly compartment (vAC) for final association with the tegument proteins. Tegumented capsids acquire their final envelope by budding into the Golgi apparatus containing glycoproteins. Finally, virus containing vesicles fuse with the plasma membrane, and viral particles are released into the extracellular space (Figure 3).
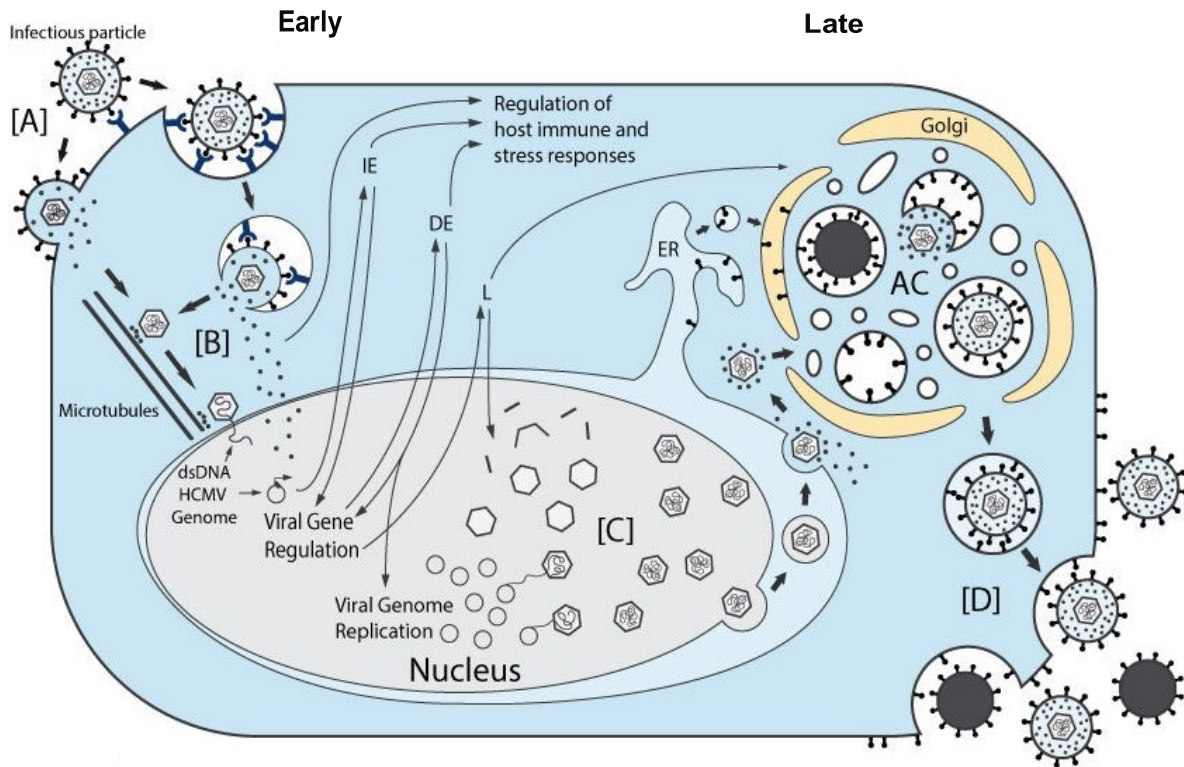
Figure 3: Replication cycle of cytomegalovirus.

Schematic steps of the CMV replication cycle. Detailed steps are described in text. viral assembly compartment (vAC), endoplasmic reticulum (ER), Golgi dense bodies (black), IE immediate early-, DE delayed early-, L late genes [41].

3.1.4 Factors counteracting innate sensing and viral restriction

3.1.4.1 Interferon response

The induction of interferons (IFN) is known to restrict HCMV and MCMV replication [42, 43], while abrogation of the interferon response promoted efficient replication of HCMV [44]. Several observations indicated that interferon secretion might restrict viral replication in foreign hosts, in particular in human fibroblasts [45]. On the other hand cytomegalovirus has co-evolved with its host for many years and developed efficient counteraction mechanisms to overcome host cell restriction factors, transcription inhibition and even cell death [19]. Even though, it still remains elusive whether MCMV counteraction of the antiviral state operates in the same fashion in foreign host cells.

The process of viral entry is sufficient to trigger the first defense mechanisms of a target cell. Cellular sensing of microbial components results in the activation of innate and intrinsic immune responses devoted to restrict viral replication, even at the cost of sacrificing the entire cell. The viral DNA is one of the pathogens associated molecular patterns (PAMPS)

recognized by pattern recognition receptors (PRRs), for instance Toll-like receptors (TLRs), interferon inducible protein 16 (IFI16) or cyclic GMP/AMP synthase (cGAS).

The activation of these DNA sensors results in the induction of type I Interferons, release of pro-inflammatory cytokines, like tumor necrosis factor (TNF)-alpha, and activation of viral restriction factors. [46-48]. Initiation of the antiviral response starts with the recognition of the virus by PRRs, like TLRs, RNA sensors RIG-I receptors (RLR), NOD-like receptors (NLRs), or AIM2-like receptor. Activation of TLRs leads to the activation of interferon regulating factor 3 (IRF3) and nuclear factor kappa B (NF-κB) and in turn induction of type I IFNs. TLR engagements by HCMV PAMPs induce the expression of cytokines like IL-6 and IFN-β via activation of NF-κB [49-51].

The MCMV protein M35 modulates type I IFN induction by targeting NF-κB signaling downstream of PRRs [52]. Upon stimulation of interferon receptors, the activation of the janus kinase (JAK) results in phosphorylation of signal transducer and activator of transcription 1 (STAT1) and STAT2 proteins. Subsequently binding to IRF9 and translocation to the nucleus can induce interferon stimulated genes (ISG). HCMV and MCMV encode two antagonists to target IFN signaling via STAT proteins. While HCMV IE1 forms a complex with STAT1/2 and prevents induction of IFN, the MCMV protein M27 targets STAT2 for proteasomal degradation [53, 54].

Viral dsDNA can be also recognized by cGAS [47, 55, 56]. Binding of cGAS to viral dsDNA produces the second messenger cyclic guanosine monophosphate-adenosine monophosphate (cGAMP). cGAMP binds and activates ER-resident stimulator of interferon genes (STING) and associates in the ER-Golgi with TANK-binding kinase 1 (TBK1). The binding of TBK1 leads to phosphorylation of STING and the recruitment of interferon regulatory factor 3 (IRF3). This subsequently induces the expression of IFN-β, which restricts CMV replication [56, 57]. HCMV multifunctional protein UL82 (pp71) interacts with STING and iRhom2 to inhibit complex formation of STING-TBK1-IRF3 and therefore circumvents the induction of IFN-β and ISG56 [58]. More recently, two candidates, pUL31 and pUL42, have been identified to target cGAS by inhibiting DNA binding and oligomerization via direct interaction [59, 60]. MCMV m152 was identified to impede the translocation of STING from the ER to the Golgi compartment and thereby inhibits the type I IFN response [61].

Protein kinase R is a dsRNA sensor, induced by IFN and can recognize RNA intermediates, produced during CMV replication [62, 63]. The activation of PKR in the cytosol causes the

phosphorylation of the α subunit of the eIF2 translation initiation factor (eIF2α), which in turn silences the global protein translation in the cell and restricts the progeny of new viruses [63]. By interacting with PKR and preventing phosphorylation of elF2α, MCMV proteins m142 and m143 avoid protein synthesis shutoff and promote viral replication [64-66]. This mechanism seems to be conserved between HCMV (TRS1, IRS1) and MCMV (m142, m143) proteins [67].

3.1.4.2 Nuclear domain 10

Promyelocytic Leukemia protein associated nuclear bodies (PML-NB), which are also referred as nuclear domain 10 (ND10), are nuclear structures composed of several proteins like PML, death-domain associated protein (Daxx), and SP100 [68]. ND10 are involved in essential cellular functions such as regulation of gene transcription, proliferation, senescence, apoptosis, and DNA damage response [69, 70]. Infection of human RPE-1 cells with an human cell-adapted MCMV/h1 resulted in increased dispersion of ND10 structures indicating a role in cross-species infection [71]. During CMV replication, ND10 structures were found in close proximity to viral replication compartments, suggesting an important role for viral replication. Indeed, ND10 structures are described to restrict viral replication of HCMV and MCMV by silencing immediate early gene transcription [37, 72, 73]. It was shown that knockdown of ND10 components lead to increased IE gene expression [68, 72]. To counteract ND10 restriction, CMV has evolved a mechanism to disrupt ND10 structures by the viral IE1 protein [74]. Moreover, CMV replication can be also restricted via the repression of the major immediate early promoter (MIEP) by histone deacetylase complexes (HDACs) [75, 76]. One component of ND10 nuclear bodies is Daxx. Daxx is described as a repressor of IE gene expression by inactivation of the viral DNA chromatin via the action of HDAC [77, 78]. The multifunctional protein pp71 is able to target Daxx for proteasomal degradation and therefore relieve its repressive effect from the MIEP and promote IE gene expression [79].

3.1.4.3 Apoptosis

Another strategy used by the host cell to avoid viral replication and progeny of new viral particles is to induce programmed cell death. Increased apoptosis was observed during MCMV infection in human cells while inhibition of apoptosis allowed replication in foreign host cells [80]. Apoptosis is one of several programmed cell death pathways, next to necroptosis and

pyroptosis. Apoptosis is characterized by morphological changes of the cell, like cell shrinkage, DNA fragmentation, and nuclear condensation. The apoptotic pathway is rather complex and is regulated by an essential family of cysteine proteases called caspases. The pathway can be activated by intrinsic or extrinsic stimuli. The extrinsic pathway is activated by the binding of a ligand like FasL or tumor necrosis factor α (TNF-α) to death receptors at the plasma membrane. This leads to subsequent activation of firstly initiator caspases, caspase-8 or caspase-10 and then executor caspases caspases-3 and -7, that account for the degradation of cellular components and DNA.

The intrinsic pathway is triggered by stimuli like cellular stress, growth factor deprivation, or DNA-damage, and is regulated by B-cell lymphoma 2 (BCL-2) family members. This pathway is characterized by mitochondrial outer membrane permeabilization caused by the pro-apoptotic proteins BCL-2 homologous antagonist killer (BAK) and BCL-2-associated X protein (BAX). This results in release of cytochrome C, which leads to the final activation of caspase-9 and caspase-3. The anti-apoptotic protein BCL-xL and myeloid leukemia cell differentiation protein (MCL-1) can efficiently sequester BAX and BAK and prevent apoptotic cell death [81, 82].

In order to ensure efficient viral replication CMV has evolved numerous strategies to circumvent induced apoptosis. Several proteins of HCMV and MCMV have anti-apoptotic functions: for examples the protein UL37x1 (vMIA) blocks the FAS-mediated apoptotic pathway downstream of caspase-8 activation and sequesters pro-apoptotic protein BAX at the mitochondrial membrane [83, 84]. The functional homolog in MCMV, m38.5, also binds to BAK and prevents permeabilization of the outer mitochondrial membrane [85, 86], whereas m41.1 (vIBIO) prevents BAK oligomerization [87]. The extrinsic pathway is targeted downstream of death receptors by the protein pUL36 (vICA) during HCMV or by M36 during MCMV infection, which inhibits caspase-8 activation [88-90]. MCMV encodes a multifunctional protein called M45 (vIRA), which binds receptor-interacting protein 1 (RIPK1) and RIPK3 and prevents necroptosis by inhibiting TNF receptor signaling [91, 92].

3.1.5 Manipulation of the cell cycle by cytomegalovirus

3.1.5.1 Cell cycle of mammalian cells

During their life, cells proceed through a sequence of phases, called the cell cycle. These phases include periods of cell growth, during which proteins are produced and DNA is replicated, followed by cell division, when a cell divides into two daughter cells. Strict regulation of the cell cycle ensures equal division of the cell constituents (cytoplasm, organelles, and intact genome) and prevents uncontrolled cell proliferation, which can lead to malignant transformation. The regulation is mainly controlled by a family of protein kinases, called cycle-dependent kinases (CDKs) and its regulatory cyclin subunits [93]. The phasic presence of CDKs is controlled by the anaphase-promoting complex (APC), an E3-ubiquitin ligase, which targets CDKs for proteasomal degradation. In addition to APC, phosphorylation of cyclins and CDKs is another mechanism to regulate the cell cycle .

The cell cycle is divided into four phases, G1, S, G2, and mitosis (M) phase with an optional G0 phase. Due to the complexity, the following steps are described in a simplified way. The G0 phase is described as a quiescent or resting cell state in which cells have exited the cell cycle. The cycle starts with the G1 phase which involves expression of cyclin D, complex formation with CDK4 or CDK6, and in late G1 phase the phosphorylation of the retinoblastoma protein (pRb) family member pRb, p130, and p107 [94]. This results in the release of E2F-dimerization protein (DP) transcription factors from E2F-responsive promoter regions and subsequently expression of cyclin E and progression of the cell cycle. This process drives the cell cycle, once they have passed the restriction point at G1/S phase, independently of growth factors into S phase in which the cellular DNA is duplicated [95]. S phase is characterized by the expression of cyclin A and binding to CDK2, which in turn initiates DNA replication. After DNA replication the cell enters G2 phase, which includes the induction of cyclin B and CDK1 association. During G2, the cell synthetizes macromolecules, grows in size and prepares for the mitotic phase, when the genetic material is segregated into two daughter cells. To ensure correct segregation of spindles and to avoid transmission of genomic abbreviations, cells have to pass three checkpoints at the transition from G1 to S phase, during S phase, and from G2 to M phase. In case of genomic abbreviations, the cell cycle is arrested, and DNA damage repair mechanism are induced. These checkpoints are mediated by two important proteins p53 and pRb [96].

3.1.5.2 Cell cycle alteration by CMV

CMV is a master in manipulating the cell to ensure a suitable environment for its long replication cycle. During its long co-evolution with the host, CMV has acquired the capacity to exploit several strategies to alter the cell cycle, without interfering with cellular DNA replication. It was observed that induction of E2F-target genes, such as cyclin E and B as well as PCNA are detrimental for viral replication of MCMV in human RPE-1 cells. Therefore, modulation of cell cycle components might be a mechanism to overcome the species barrier of MCMV [97]. Moreover, it is likely that cell cycle regulation, in particular the duration and timing, differs in murine and human cells.

HCMV can infect cells during all cell cycle stages but IE1 expression is only induced in G0 and early to mid G1 phase [98, 99]. HCMV pushes the cells towards the G1/S transition by altering RNA transcription, proteins that are involved in cell cycle regulation, modulation of cyclin-dependent kinases, posttranslational modifications of proteins, re-localization of proteins and protein stability by degrading them [100]. On the other hand, MCMV can arrest the cell cycle at G1/S or G2/M phase and can express IE3 independently of the cell cycle phase [101] (Figure 4). It was observed that HCMV replicates efficiently in a so-called *pseudo G1 phase* which includes inhibition of cellular DNA-synthesis but expression of specific G1, S, and M phase gene products [99, 102-105]. For instance, during infection the induction of cyclin E, activity of CDK2, accumulation of cyclin B, as well as low expression levels of cyclin A and D were observed [102, 104, 106, 107] (Figure 4). Over the years, several CMV proteins have been identified to modifiy the cell cycle. The multifunctional protein pp71 was described to target hypo-phosphorylated pRb for proteasomal degradation. Moreover, the viral kinase pUL97 phosphorylates pRb. In both scenarios E2F/DP- transcription factors are released, which results in expression of E2F-responsive genes and progression of the cell cycle [108, 109] (Figure 4).

Recently, our group showed that the murine homolog of HCMV pUL117, M117, interacts with E2F-transcription factors and activates E2F-target genes like cyclin E and PCNA while cells are arrested at G1/S phase. Cells infected with M117 deficient virus cannot arrest the cell cycle in G1, progress to S phase and instead arrest cells in G2/M phase [97]. The human CMV homolog pUL117 acts in a different way by targeting the mini-chromosome maintenance complex to suppress cellular DNA synthesis [110]. The viral protein IE1 is able to arrest the cell cycle in G2/M phase and S phase and the IE2 protein can block the cell cycle at the G1/ S transition.

However, most studies were not done in context of infection. Deborah Spector's group was able to show that during infection with IE2Δ aa33-77 mutant, cyclin E levels were altered [111] (Figure 4).
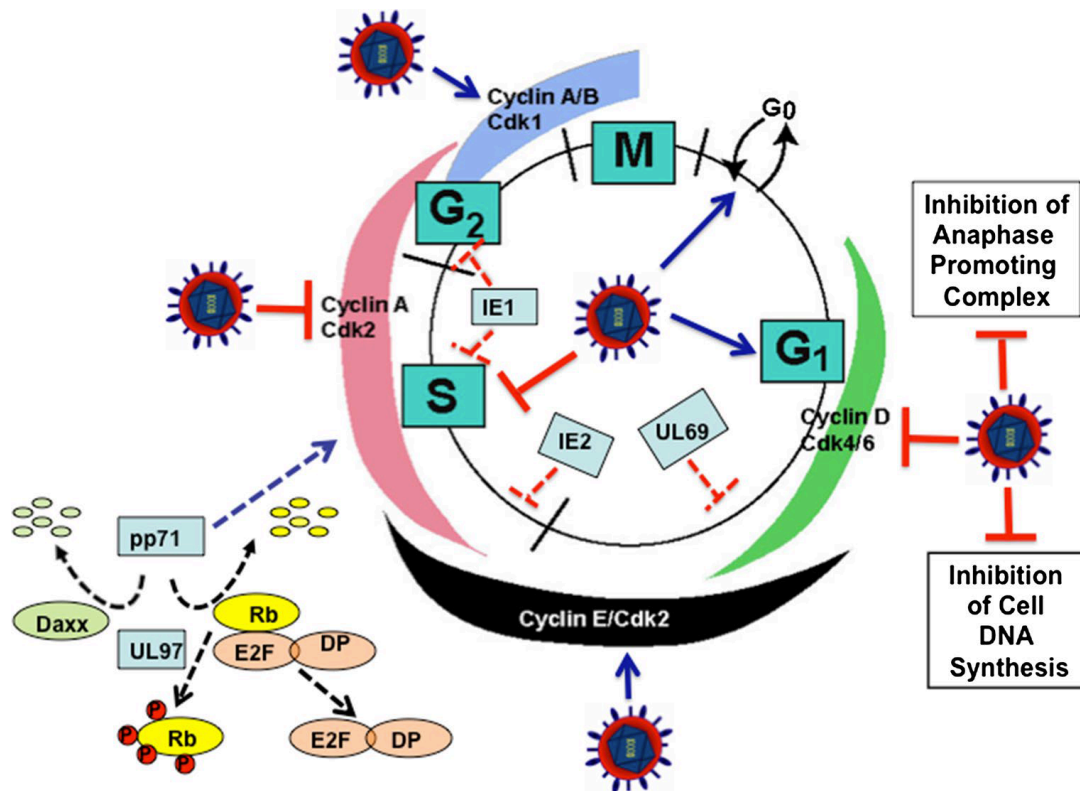
Figure 4: Modulation of the cell cycle by cytomegalovirus proteins.

CMV is able to promote the cell cycle towards G1/S phase to ensure a suitable environment for viral replication, which includes inhibition of cellular DNA synthesis, inhibition of the APC, upregulation of cyclin E and B, and low levels of cyclin A. The tegument protein pp71 can target pRb for proteasomal degradation and pUL97 can phosphorylate pRb. This results in the release of E2F/DP-transcription factors and progression towards S phase. The viral protein IE1 can arrest the cell cycle in G2/M and S phase, and IE2 can inhibit the cell cycle at the G1/S transition. pUL69 can arrest the cells with a G1 DNA- content [100].

3.1.5.3 LIMD1 as potential cell cycle regulator

The LIM domain containing protein 1 (LIMD1) belongs to the Zyxin protein family and can shuttle from the nucleus to the cytoplasm. It is described as a scaffold protein for signal transduction and cytoskeletal mechano-transduction [112, 113]. LIMD1 is a tumor suppressor and has been found in many malignant tumors such as breast, lung, and neck squamous cell

carcinomas as well as in patients with acute leukemia [114-117]. Moreover, LIMD1 is involved in hypoxic regulation of Hypoxia-inducible factor 1-alpha, which is an important key player in tumorigenesis, proliferation, and malignancies [118, 119]. E2F-transcriptions factors interact with DP proteins and can have activating and repressive effects on promoter regions with an E2F-response element. E2Fs act downstream of pRb and are involved in cell cycle progression, DNA repair and apoptosis [120]. Sharp and colleagues were able to show that the protein LIMD1 carries a pRb-binding site (Figure 5) and can interact with pRb to inhibit E2F-mediated transcription. The binding of LIMD1 to E2F has in turn repressive effects on E2F- target genes, with E2F responsive promoters. Furthermore, LIMD1 can reduce tumor growth and inhibit proliferation *in vitro* and *in vivo* [115]. More recently LIMD1 was observed being phosphorylated during mitosis by CDK1 and c-Jun NH2-terminal kinases 1/2 (JNK1/2). Lack of LIMD1 resulted in a shortened mitosis phase and progression of the cell cycle [121]. In the context of viral infection, the EBV LMP1 protein upregulates LIMD1 via IRF4 and NF-κB during latency [122]. Due to these findings, LIMD1 could be a potential target to regulate E2F-dependent cell cycle regulation during cross-species infection.
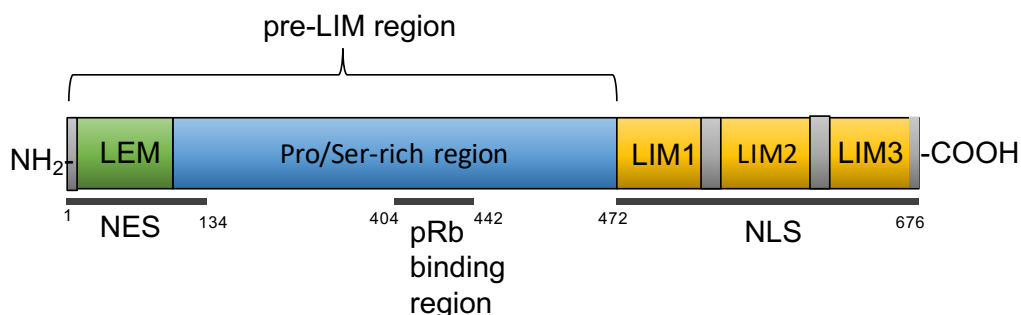
Figure 5: Predicted protein structure of LIMD1.

The LIMD1 protein contains three LIM domains located at the C-terminus, a proline/serine rich region and a N-terminal region with a LEM domain. It contains a pRb binding site at position aa 404-44 as well as a nuclear export signal (NES) at position 54-134 [115]. modified from http://atlasgeneticsoncology.org/Genes/GC_LIMD1.html

3.1.6   Modulation of receptor tyrosine kinase signaling during CMV infection

3.1.6.1   Receptor tyrosine kinases

Receptor tyrosine kinases (RTKs) are cell surface receptors extensively investigated since their first discovery more than 40 years ago. Human RTKs can be classified into 20 subfamilies and participate in diverse functions, such as proliferation, cell survival, and cell cycle control. However, the mechanism of action and the key components are conserved among different

species [123]. Some well described RTKs are the platelet derived growth factor (PDGFR), epidermal growth factor (EGFR), vascular growth factor (VEGFR), insulin-like growth factor (IGFR), and fibroblasts growth factor receptor (FGFR). The activation of RTKs by ligands or the internalization of the receptor, trigger different signaling pathways, which are important for efficient entry or replication of viruses. Several studies revealed that downstream signaling of RTKs is modulated by viruses to escape from host defense mechanism [124]. The fact that activation of RTKs regulates proliferation, cell cycle and survival, known mechanism important for crossing the species barrier of MCMV, investigations of RTK-mediated signaling could be of particular interest.

3.1.6.2   Epithelial growth factor receptor

The activation of EGFR leads to the initiation of many different signaling cascades for instance, RAS, mitogen activated protein kinases (MAPK), Phosphoinositide 3-kinases (PI3K)/AKT (Proteinkinase B), mammalian target of rapamycin (mTOR) or JAK/STAT pathways [123]. It starts with binding of a ligand (e.g. EGF, TGF-alpha) to the extracellular receptor, which is generally followed by the dimerization of the extracellular domains and activation of the intracellular kinase domain. This results in autophosphorylation of the receptor and phosphorylation by other kinases, such as proto-oncogene tyrosine-protein kinase (c-Src) or focal adhesion kinase (FAK). Phosphorylation causes the recruitment of other signaling proteins or adapters, for instance SHC-transforming protein 1 (SHC1) and growth factor receptor-bound protein 2 (GRB2) to the receptor [125-127]. Moreover, ligand activation of EGFR leads to its internalization and translocation to endosomes [128]. Adapter proteins do not function as effector kinases, but recruit and activate in turn other proteins, which activate further downstream signaling.

3.1.6.3   SHC adapter protein 1

The SHC1 protein is an adapter protein that plays a role in mitogen activation of protein kinases, differentiation, and survival signaling by different receptors. This includes signaling through growth factor signaling receptors, Integrins, antigen receptors, cytokine receptors, G-protein coupled receptors, or insulin receptors [129]. SHC1 is mainly localized into the

cytoplasm and is recruited to the plasma membrane upon ligand binding. In addition, SHC1 and EGFR were also observed in endosomes upon ligand stimulation [130].

The protein is involved in different signaling pathways, like RAS-MAPK/ERK or PI3K/AKT signaling, which regulate proliferation and cell survival. The tyrosine-phosphorylation of SHC1 at position Y239/240 was described to activate c-MYC expression as well as regulation of cell cycle progression via Integrins [131, 132]. SHC1 is ubiquitously expressed with three isoforms of 46, 52, and 66 kDa (Figure 6), which are produced by alternate translational start sites and splicing [133] [134]. They all contain a conserved N-terminal PTB as well as a CH1 and a C-terminal SH2 domain (Figure 6). Moreover, three tyrosine phosphorylation sites exist at the CH1 domain, Y239, Y240 and Y317, which serve as a binding site for the protein GRB2 to activate the RAS-MAPK/ERK pathway and PI3K-AKT signaling [135-137]. It was observed that SHC1 binds to the GRB2-associated binding protein 1 or 2 (GAB1/2), which is involved in PI3K-AKT signaling [138]. SHC1 mediates Insulin growth factor-I (IGF)-stimulated PI3-kinase/AKT activation via complex formation of SHC/GRB2/GAB2 in vascular smooth muscle cells [139] [140]. Besides RAS-MAPK/ERK and PI3K/AKT signaling SHC1 regulates oxidative stress responses and cytoskeleton rearrangements [141].

Moreover, SHC1 plays also an important role during virus infections. Middle T antigen from polyomavirus interacts with SHC1 and GRB2, which resulted in GAB1 phosphorylation , PI3K activation, and caused a tumorigenic phenotype of cells [142]. The disruption of the SHC1/GRB2 complex during Abelson murine leukemia virus infection, affected cell proliferation [143]. Nevertheless, the HSV-1 VP11/12 protein also interacts with SHC1, p85, and GRB2 and modulates AKT activation however the interaction with SHC1 showed only a minor effect on downstream signaling [144, 145].
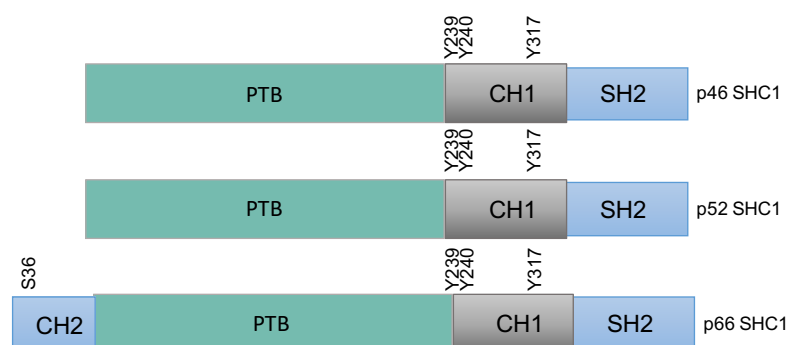
Figure 6: Schematic of SHC proteins.

SHC1 is expressed with three isoforms 46-, 52-, and 66kDa due to alternate translational start sites and splicing. They all contain a conserved N-terminal PTB as well as a CH1 and a C-terminal SH2 domain.

Three conserved tyrosine phosphorylation sites exist at the CH1 domain at position Y239, Y240 and Y317. In addition, the large isoform p66 is shown with an additional serine phosphorylation site at the CH2 domain at position S36. modified from [141]

3.1.6.4 RAS-MAPK/ERK pathway

The RAS-MAPK/ERK pathway is involved in many cellular mechanisms, such as proliferation, inhibition of apoptosis, differentiation and migration. For those reasons, in particular inhibition of apoptosis or regulation of the cell cycle, targeting of the EGFR-mediated signaling might be supportive for MCMV to cross the species barrier. The activation of the RAS-MAPK/ERK pathway starts with a ligand binding to EGFR, which in turn dimerizes and auto-phosphorylates. It binds either directly to GRB2, phosphorylates SHC1 or phospholipase C gamma 1 (PLC-γ1). GRB2 is recruited to SHC1 and EGFR, followed by binding to son of sevenless 1 (SOS1), a guanine nucleotide exchange factor, which activates the GTPases RAS and RAF (Figure 7). Activation of RAF and RAS is followed by phosphorylation of the kinases MEK1/2, which in turn phosphorylate the serine/threonine kinases ERK1/2. Once ERK1/2 is phosphorylated, it translocates to the nucleus or stays in the cytoplasm and activates several target genes. For instance, in the nucleus, it acts as a transcription factor and leads to the activation of target genes like ELK1, c-fos, c-Jun (AP-1), cyclin D, c-MYC, cAMP-response element binding protein (CREB) and anti-apoptotic genes of the BCL-2 family [125]. AP1 can bind to the promoter region of cyclin D and promotes cell cycle progression at G1 phase [146] (Figure 7).

3.1.6.5 PI3K pathway

The PI3K downstream effector of EGFR regulates motility, metabolism, proliferation and survival. Promotion of survival via the downstream signaling of PI3K might be of particular interest to limit apoptosis in human fibroblasts during cross-species infection [80]. After stimulation of EGFR, GRB2 or SHC1 bind to GAB1/2 and recruit the p85 regulatory subunit of PI3K, which in turn binds to the p110 catalytic domain. The binding results in conversion of PIP_2 into PIP_3, recruitment of phosphoinositide-dependent kinase 1 (PDK1) and phosphorylation of AKT by PDK1 and mTORC2. Target genes important for survival are induced or anti-apoptotic genes are inhibited, for instance, inhibition of pro-apoptotic genes like caspase-9 or BAD (Figure 7).

Moreover, AKT phosphorylation results in upregulation of pro-survival myeloid leukemia 1 protein (MCL-1) [125, 147]. The activation of AKT can also lead to phosphorylation and inhibition of CDK inhibitors p21^{CIP1} and p27^{KIP} leading to cell cycle progression towards S phase [125, 147, 148].
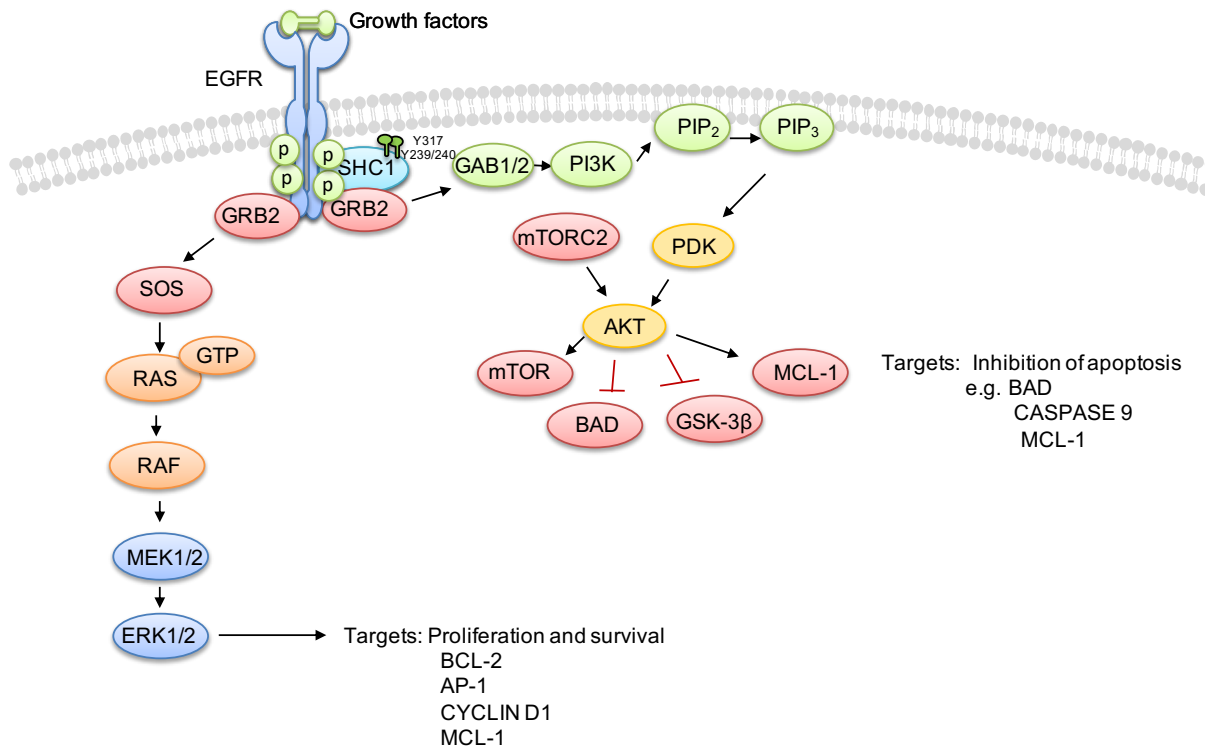
Figure 7: EGFR-mediated signaling downstream of SHC1.
EGFR binds a ligand (growth factor), dimerizes and auto-phosphorylates. It then binds directly to GRB2 or phosphorylates and recruits SHC1 to the plasma membrane. GRB2 binds SOS, which in turn activates the GTPases RAS and RAF. RAF phosphorylates and activates the kinases MEK1/2, which phosphorylates ERK1/2. Activated ERK1/2 acts in the nucleus as a transcription factor to regulate AP-1, c-MYC, cyclin D, and other anti-apoptotic genes of the BCL-2 family. GRB2 can also recruit GAB1/2 to activate PI3K. The binding results in conversion of PIP$_2$ into PIP$_3$ and recruitment of AKT and its phosphorylation by PDK1 and mTORC2. AKT inhibits other proteins involved in apoptosis inhibition of BAD or induces the ani-apoptotic protein MCL-1.

3.1.6.6   Modulation of EGFR-mediated signaling by cytomegalovirus

EGFR-mediated signaling, in particular RAS-MAPK/ERK and PI3K/AKT pathways are known to be modulated by numerous viruses [149-151]. Several studies showed that cytomegalovirus impairs EGFR signaling. Moreover, the entry receptor being important of HCMV is controversial discussed like EGFR, Integrins as Co-receptors, and PDGFR [28, 30-33, 152]. The

glycoprotein gB was observed to activate EGFR, while gH interact with Integrins, leading to further downstream signaling [152, 153].

However, the importance of EGFR downstream signaling is greater during the establishment of latency and reactivation of HCMV in CD34$^+$ hematopoietic progenitor cells (HPCs). The proteins pUL138 and pUL135 interact with EGFR. pUL138 enhances cell surface expression and signaling of EGFR while pUL138 promotes the turnover and inhibition of EGFR and PI3K facilitates reactivation of HCMV [154]. More recently, Felicia Goodrum's group defined the mechanism in more detail. The pUL135 interacts with the host adapter proteins CIN85 and affects EGFR trafficking and turnover to regulate latency [155]. The inhibition of MEK/ERK, STAT, or PI3K/AKT downstream of EGFR resulted in increased viral reactivation of latent infected CD34$^+$ HPC, whereas HCMV diminishes EGFR downstream signaling in productive infection of fibroblasts [156].

During HCMV infection, MEK/ERK signaling is upregulated in CD34$^+$ HPCs and contributes to the upregulation of the pro-survival protein MCL-1, decrease of the pro-apoptotic BIM and PUMA and thus preventing cell death. [157, 158]. However another group showed that, in the context of a productive infection, HCMV induces activation of ERK1/2. It was described that ERK1/2 phosphorylates IE2, with this modification being important for its transactivation function [159-161]. Specific inhibition of MEK1/2 upstream of ERK1/2 reduced viral titers and replication [162]. During HSV-1 infection, ERK1/2 is activated and translocated in a spatio-temporal fashion that mediates G1/S phase progression and promote efficient viral replication [163]. These studies show that also during productive HCMV and HSV-1 infection, ERK1/2 is important for efficient replication.

Little is known about MCMV and EGFR signaling. However, in a mouse salivary gland organ culture model it was shown that EGFR was highly expressed in salivary glands tumors and ERK1/2 phosphorylation was necessary for MCMV-induced pathogenicity in submandibular salivary glands [164]. The PI3K pathway is also described to play a role during cytomegalovirus infection. Activation of PDGFR upon entry of HCMV leads to IE1 and IE2 mediated phosphorylation and activation of AKT at later times [32, 165]. Moreover, specific inhibition of PI3K during HCMV infection, reduced expression levels of IE and E genes as well as decreased viral replication [166]. Another study showed that MCMV activates PI3K signaling, and specific inhibition of this pathway reduced salivary gland pathology [164]. PI3K dependent

activation of the pro-survival MCL-1 protein prevents HCMV infected monocytes from cell death [167].

3.1.7   Species specificity of cytomegalovirus

CMV species specificity has been known since the first isolation and propagation of MCMV and HCMV in the 1950-70s, as observed by Margret Smith and Thomas H. Weller [2, 3]. The productive infection of CMV is restricted to its natural hosts or closely related host species. For instance, MCMV replicates only in murine and rat cells and likewise HCMV and simian CMV can only replicate in human and chimpanzee cells. The rat CMV strain Maastricht, can only replicate in its native host, rat cells (reviewed in [20]).

It has been often observed that CMV can infect cells of a foreign host but this leads to the expression of only IE, and a few early genes and not complete replication. This phenomenon is described as a post penetration block of viral gene expression and replication, suggesting that cross-species restriction does not result from insufficient entry of the virus [168-172]. However, the underlying mechanisms of the species specificity of CMV still remains poorly understood. A more recent study has shown that apoptosis plays an important role in cross-species infection. It has been observed that MCMV can replicate to low titers in human embryonic kidney cells (HEK293) as well as human embryonic retinoblasts cells (911). Both cell types have been transformed with the adenoviral E1A and E1B genes, which are described as transcriptional activators, cell cycle regulator (E1A) and anti-apoptotic gene (E1B) [173, 174]. The induction of apoptosis can limit late viral gene expression and replication of MCMV in human cells. It has been reported that apoptosis is less induced when viral replication is inhibited [80]. Furthermore, overexpression of an anti-apoptotic gene of the BCL-2 family or overexpression of the viral apoptosis inhibitor vMIA (UL37x1) facilitated MCMV replication in retinal-pigment epithelial cells (RPE-1) [80]. This observation was supported by our laboratory by infection of RPE-1 cells with a spontaneously emerged human cell-adapted MCMV, referred as MCMV/h1, which showed reduced induction of apoptosis [71].

Apart from apoptosis, other studies have proposed PML-NB, also referred as PML-nuclear domain (ND10), as a restriction factor capable of limiting viral replication in foreign hosts [175]. Both the expression of HCMV proteins IE1 and the infection with UV-inactivated HCMV, providing tegument proteins such as pp71, led to MCMV replication in human cells, at least to low titers. This raised the speculation that both proteins could facilitate the disruption of ND10

structures and thereby allow replication of MCMV in a foreign host cell [176]. This hypothesis is in line with the observation that MCMV/h1 disrupts ND10 structures more efficiently than MCMV wild type virus [71].

In our laboratory, stepwise adaptation of MCMV to foreign host cells has been employed to study and identify host range determinants of the species specificity. By whole genome sequencing of MCMVs adapted to human cells, the gene regions M112/113 and M117 have been identified as determinants of viral replication in human cells. However, mutated M112/113 and M117 MCMV did not facilitated replication in RPE-1 cells to the same extent as the human cell adapted MCMV/h1, which indicated occurrence of additional genomic alteration in the genome [71, 97].

The gene region M112/113 encodes the viral early (E1) proteins, which are important for the formation of replication compartments [177]. However, the function of M112/113 in cross-species infection is not clear and it is suggested that mutations in the E1 coding region might impact splicing events and balance or stability of various E1 isoforms [71]. Ostermann et al. showed that the interaction of M117 with E2F-transcription factors downregulates activation of E2F-responsive genes like cyclin E, cyclin A, and proliferating cell nuclear antigen (PCNA) in human cells. Moreover, chemical inhibition of E2F3 facilitated moderate MCMV-wt replication in RPE-1 cells, suggesting that E2F-activation of target genes is detrimental for viral replication in human cells [97].

MCMV/h1 can replicate to high titers in RPE-1 cells, but replication is more restricted in human fibroblasts. In addition, RPE-1 cells, which have been employed to adapt MCMV to human cells, differ in response of IFN-β compared to human fibroblasts [45]. It was observed that plaques formed by MCMV/h1 did not increase in size and regressed after several days in infected MRC5 cells. This observation led to the hypothesis that secretion of cytokines like interferon-β (IFN-β) restricted viral infection to neighboring cells [45]. This idea was supported by a study that Myxoma virus from rabbit, a poxvirus, was able to cross the species barrier by disruption of the ERK-dependent type I interferon induction [178].

The dsRNA sensor Protein kinase R (PKR) is described to be induced by interferons. MCMV mutants deficient in m142 and m143 replicated worse in murine cells when the HCMV homolog TRS1 was expressed instead, provided in cis or trans [66]. Moreover, TRS1 of HCMV and rhesus CMV are only able to inhibit PKR from the respective species, suggesting a potential role of PKR during cross-species infection [179].

By adding IFN-β neutralizing antibodies to MCMV/h1 infected MRC5 cells, followed by passaging them for several times, the virus was able to replicate more efficiently and accumulated additional genomic alterations [45]. MRC5 cells infected with the isolated fibroblast-adapted MCMV (MCMV/h1-fa) did not show any difference on induced IFN-β mRNA levels compared to the parental virus (MCMV/h1) [45]. Complete genome sequencing of two different fibroblast adapted MCMVs (MCMV/h1-fa and MCMV/112-117-fa2) identified mutations in the gene region M28 in addition to other mutations [45, 180]. Introduction of a M28 point mutation into a mutant, carrying mutations in M112/113+M117, was sufficient to increase virus replication in human fibroblasts. These preliminary results ,obtained during my master project, indicated that the gene region M28 is an important factor for the species specificity of CMV [180].

4 Aim of the study

Cytomegaloviruses have co-evolved with their respective hosts for many years and are highly species-specific with a limited host range. Stepwise adaptation of MCMV to human cells has been described as a valuable tool to identify host range determinants of MCMV [45]. Previous studies suggested that induction of apoptosis, disruption of ND10 structures, and more recently E2F-mediated gene regulation are important for the restriction of MCMV replication in human epithelial cells [71, 80, 97]. However, the underlying molecular mechanisms and general principles of counteraction still remain poorly understood. In particular, the underlying mechanisms of the restriction and adaptation of MCMV to human fibroblasts have been not elucidated.

The main aim of this study was to investigate the molecular mechanisms involved in the adaptation of MCMV to human fibroblasts while identifying and characterizing M28 as a potential host range determinant and its function in cross-species infection.

New insights into the principles of adaption of MCMV to other cell types, in particular human fibroblasts, could identify general or overlapping mechanisms of the species specificity of cytomegalovirus. The identification and functional characterization of so far neglected host range determinants will increase our understanding of host cell restriction and intrinsic responses of CMV in general.

5   Results

5.1   Identification of MCMV M28 as a host range determinant

Cytomegaloviruses are opportunistic pathogens with a highly restricted host range. They can only replicate in their natural or closely related hosts [20]. Nevertheless, our group has shown for the first time that MCMV can be adapted to human retinal pigment epithelial cells (RPE-1) by several passaging this virus in cell culture [45]. The capability to efficiently replicate in these cells is associated with adaptive mutations in several genes, including the gene region M112/113 and M117. The RPE-1 cell-adapted MCMVs, (MCMV/h1, MCMV/h2, and MCMV/h3), did not completely cross the human species barrier as its replication remained more restricted in HFF and MRC5 human fibroblasts [71, 97]. Moreover, an MCMV mutant with mutations introduced in the gene region of M112/113+M117 did not lead to efficient replication in human fibroblasts [180]. Preliminary experiments performed during my master project indicated that the gene region M28 could play an essential role for MCMV adaptation to human fibroblasts. However, at that time the molecular mechanism and the function of M28 were still uncharacterized.

Next generation sequencing (NGS) and comparative analyses of whole genomes, obtained from different human cell-adapted MCMVs, revealed that three out of five mutants carried mutations in the gene region M28, among others. This included the RPE-1 cell-adapted MCMV/h3 and two human fibroblasts-adapted MCMV/h1-fa and MCMV/112-117-fa2. All of M28-specific mutations lead to a missense mutation at position 35282 (fa), 34881 (fa2) and 34700 (h3) of ORF M28 (Table 1).

A Adapted virus	Gene /ORF	Position	Sequence difference	Amino acid variance
MCMV/h1-fa	M28	35 282	A -> T	L166Q
MCMV/112-117-fa2	M28	34 881	C -> T	E300K
MCMV/h3	M28	34 700	G -> A	G360V

Table 1: Sequence alterations of M28 gene region of three different human cell-adapted MCMVs.

A: Gene alteration of the ORF M28 revealed via whole genome sequencing of different human cell-adapted MCMVs isolated after several passages of adaptation to human cells. MCMV/h1-fa and MCMV/112-117-fa2 have

been adapted to human MRC5 cells and MCMV/h3 were propagated only in human epithelial RPE-1 cells. Nucleotide positions and ORFs are annotated according to MCMV Smith reference (GenBank NC_004065). **B:** Schematic of M28 protein and specific mutations.

In order to verify the importance of M28 during cross-species infection in human fibroblasts I introduced individually the identified M28 mutations (fa, fa2, h3), by BAC mutagenesis using the *en passant* method. I introduced the mutations into a MCMV-GFP BAC carrying mutations in M112/113+M117 and performed replication kinetics after low MOI infection. Human MRC5 cells were infected with M28 recombinant viruses (M112-117+M28fa, M112-117+M28fa2, and M112-117+M28h3) and were analyzed compared to the parental M112-117+M28wt, the fibroblast-adapted MCMV/h1-fa and MCMV/112-117-fa2 viruses, respectively. In addition, I introduced the M28(fa2)-specific mutation into the wildtype MCMV-GFP to investigate whether mutated M28 alone is sufficient to promote viral replication in MRC5 cells. Interestingly, while the introduction of M28fa alone into MCMV-wt backbone (MCMV-M28fa2) did not facilitate the replication in MRC5 cells, introduction of M28-fa, fa2, and h3 mutations into M112-117 backbone (M112-117+M28fa, M112-117+M28fa2, M112-117+M28h3) led to increased viral peak titers at day 5 compared to the parental M112-117+M28wt virus (Figure 8). Remarkably, introduction of the h3 mutation (M112-117+M28h3) led to the most efficient replication and the highest viral titers compared to other M112-117+M28 mutants (Figure 8). Nevertheless, introduction of M28 mutations did not show the same replication properties as the spontaneously human fibroblast-adapted MCMV/h1-fa or MCMV/112-117-fa2 (Figure 8). A detailed analysis of the gene region M28 revealed that mutations introduced in closer proximity to the C-terminus of the protein conferred a more efficient replication in MRC5 cells (Table 1). This suggests that the C-terminus might be important for the function of the protein. The missense mutations in M28 did not display a conserved pattern among the different human cell-adapted MCMVs. The change from leucine to glutamine (M28fa) seemed to be more relevant from hydrophobic to polar, compared to the change of glutamic acid to lysine (M28fa2) or glycine to valine (M28h3), which conserve the polarity (Table 1A). However, whether the mutations affect the folding or destabilize the protein needs further investigation. All together, these findings validate that M28 is necessary but not sufficient for viral replication in MRC5 cells. Mutations in M112/113, M117 and M28 contribute to the phenotype. These results identify M28 as a novel host range determinant and verifies the importance of M28 in cross-species infection in human fibroblasts.
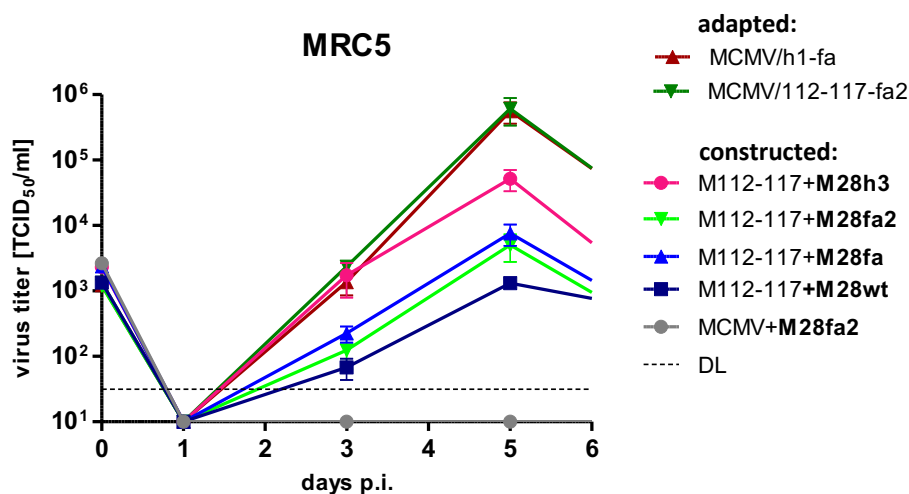
Figure 8: Mutations in MCMV M28 are responsible for efficient replication in human fibroblasts.

Human MRC5 cells were infected at MOI 0.2 $TCID_{50}$/cell with the fibroblast-adapted MCMV/h1-fa and MCMV/112-117-fa2 and recombinant M112-117+M28wt, M112-117+M28fa, M112-117+M28fa2, M112-117+M28h3, and MCMV+M28fa2. Virus inoculum was removed at 2 hpi., cells were washed 1x with PBS and fresh media was added. Viral titers were determined by titration of the supernatant and shown as means ± SEM. DL detection limit

5.2 Characterization of MCMV M28

5.2.1 M28 protein is expressed with early kinetics and localizes to the cytoplasm

M28 is a protein of unknown function and has been only poorly characterized. Kattenhorn and colleagues demonstrated that M28 protein is as a virion-associated protein examined via mass spectrometry analysis [181]. The human CMV homolog pUL29/28 has been described as a protein expressed with early kinetics, localized in the nucleus and cytoplasm, and is incorporated into the virion [182].

In order to obtain more insights into the properties and function of M28, a recombinant MCMV was constructed expressing a C-terminal HA-tagged version of the protein (Figure 9A). Expression kinetics performed in NIH-3T3 murine fibroblasts infected with MCMV-M28wtHA revealed that M28 was already expressed at 2-4 hours pi. with the predicted size of 50 kDa, similar to the expression kinetic of the immediate early 1 (IE1) and early 1 (E1) proteins (Figure 9A).

To specify to which class of viral proteins M28 belongs to, a so-called cycloheximide (CHX)/actinomycin D (ActD) release assay was performed. NIH-3T3 cells were infected and either left untreated or incubated in presence of CHX. CHX is a translation inhibitor, which inhibits only immediate early gene translation but not transcription. Upon removal of CHX translation of only prior transcribed immediate early genes are expressed while ActD inhibits transcription of early genes. With this approach, viral proteins can be classified as IE genes. As shown in Figure 9B, on the contrary of IE1 protein, M28 as well as E1 was not expressed when cells were treated with CHX and ActD, thus indicating M28 does not belong to the class of the immediate early proteins. Furthermore, by treating cells with phosphonoacetic acid (PAA), which prevents viral DNA replication and late gene expression, gB (late gene) expression was inhibited (Figure 9B). However, a M28 band could be detected in Western blot upon treatment with PAA thus confirming that M28 is not a late gene and must be an early protein (Figure 9B). The expression kinetics, the CHX/ActD release assay and treatment with PAA verified that M28 protein can be classified as an early protein (Figure 9).
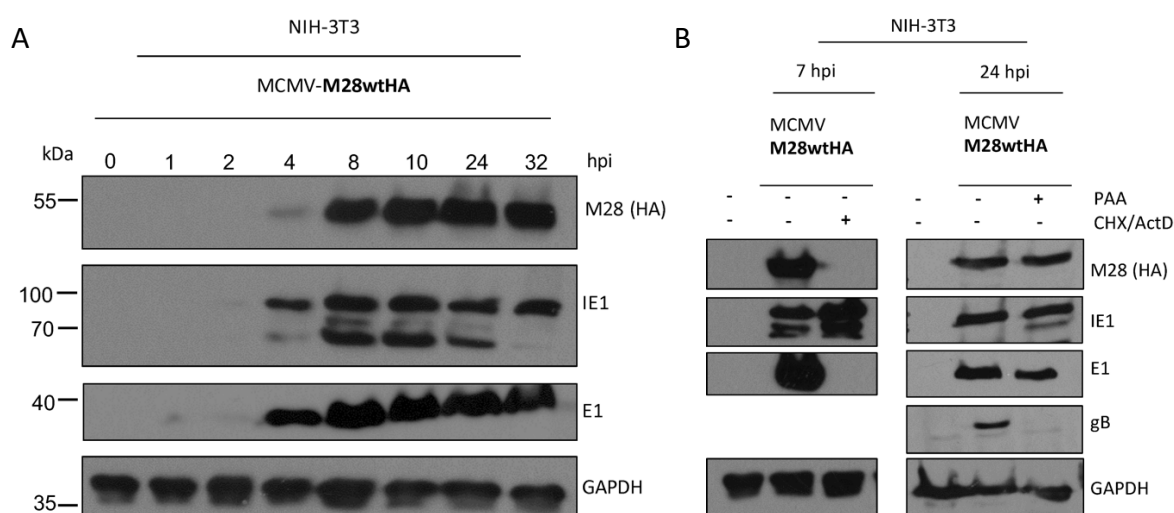
Figure 9: MCMV M28 is expressed with early kinetics.

A: NIH-3T3 cells were infected with MCMV-M28wtHA at MOI of 3 $TCID_{50}$/cell (centrifugal enhancement). Cells were washed and harvested with 2x Laemmli buffer at indicated time points and analyzed via Western blot. M28 was detected using a HA-specific antibody. GAPDH was used as loading control. **B:** NIH-3T3 cells were infected with MCMV-M28wtHA at MOI of 1 $TCID_{50}$/cell (centrifugal enhancement) and either treated or left untreated with CHX (50µg/mL) for 4 hpi., followed by 1x washing with PBS, adding of ActD (5µg/mL), harvested 7 hpi. and probed for immunoblotting. NIH-3T3 cells were infected in presence or absence of PAA (250µg/mL) with MCMV-M28wtHA at MOI of 1 $TCID_{50}$/cell (centrifugal enhancement) and analyzed via Western blot. M28 was detected using a HA-specific antibody. GAPDH was used as loading control.

Since subcellular localization influences protein function, the localization of M28 was investigated. NIH-3T3 cells were infected with MCMV-M28wtHA or M112-117+M28faHA and investigated by immunofluorescence. As shown in Figure 10, both at 6 and 24 hours pi., M28wt was detected predominantly in the cytoplasm of infected cells (Figure 10A). Only in a very small proportion of the infected NIH-3T3, M28wtHA was also detected in the nucleus (data not shown). A comparable analysis performed with recombinant viruses expressing the HA-tagged version of the fa mutated M28 did not indicated any difference between the intracellular distribution of the mutated protein as compared to the wild type (Figure 10A).

The HCMV pUL29/28 homolog of M28 is located in the nucleus at early and in the cytoplasm at later times (72 hpi.) [182], and might share functional similarities with M28. Therefore, I tested the hypothesis whether M28 can shuttle between the two cellular compartments. Since M28 exhibited predominantly a cytoplasmic distribution, even though due to its size M28 (50 kDa) would be able to diffuse into the nucleus. Thus, I assumed that the sequence of M28 could carry a nuclear export signal (NES) that would either actively exclude the protein from the nucleus or inducing the protein to shuttle between the nucleus and cytoplasm. NIH-3T3 cells were firstly treated for 2 hours with Leptomycin B (LMB), a CRM1/exportin1 inhibitor, to prevent active nuclear transport [183]. Cells were infected with MCMV-M28wtHA for 24 hours, fixed with 4% PFA and finally analyzed via immunofluorescence. As shown in Figure 10B, the LMB treatment affected the cellular distribution of M28. As expected MCMV-M28wtHA was detected in the cytoplasm in untreated cells, whereas in cells treated with LMB, M28 was detectable in both the nucleus and cytoplasm, confirming the hypothesis that M28 is exported from the nucleus by a potential NES or by binding to another protein exported from the nucleus (Figure 10B).

Taken together, these findings suggest that, irrespectively on the presence of specific mutations in ORF M28, M28 predominantly localized to the cytoplasm in a cellular compartment topologically distinct from the nuclear viral replication compartments in which M112 and M117 accumulate [71, 97].
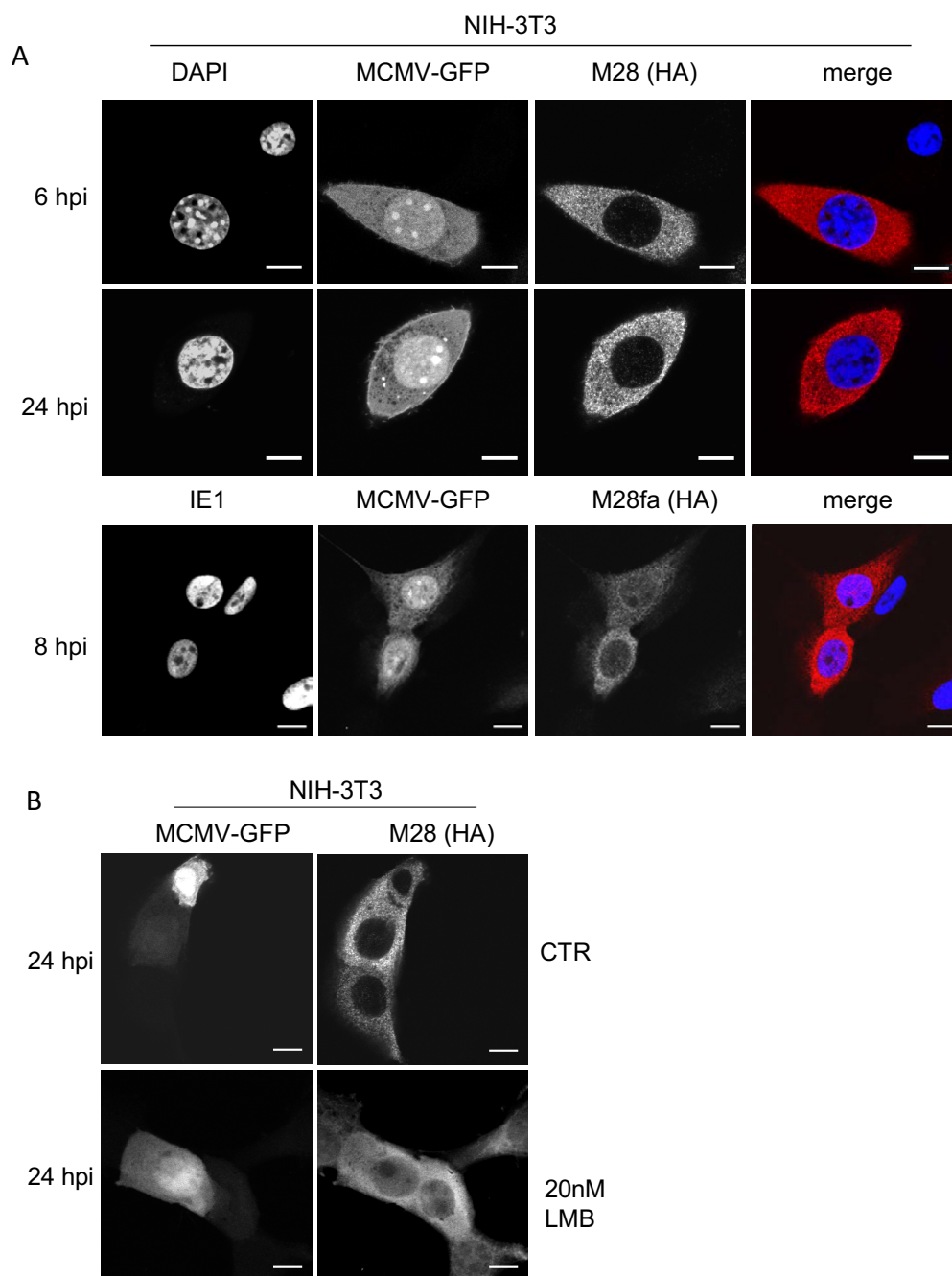
Figure 10: MCMV M28 localizes to the cytoplasm and is excluded from the nucleus.

A: NIH-3T3 cells were infected with MCMV-M28wtHA for 6 and 9 h, or M112-117+M28faHA for 8 h, fixed with 4% PFA and analyzed via Immunofluorescence. M28-HA (red). Nucleus stained with DAPI, MCMV-GFP as infection control, IE1 immediate early protein 1 (blue). **B:** NIH-3T3 cells were treated 2 h before infection either with methanol as control or 20 nM Leptomycin (LMB) (in methanol) and fixed at 24 hpi. with 4% PFA. white bar represents 10μm.

5.2.2   Loss of M28 protein promotes replication in human fibroblasts

In order to address whether M28 mutations can have stabilizing or destabilizing effects on M28 protein, expression levels of wild type and mutant M28 variants were investigated by Western blot (Figure 11A). Notably, when M28 was mutated, lower levels of the protein were detected in infected cells starting from 24 to 48 hours pi., indicating that the stability or expression of the protein might have been affected (Figure 11A). Moreover, I observed that introduction of the M28h3 variant into M112-117 led to the most efficient replication in MRC5 cells, which correlated inversely with M28 expression (Figure 11AB). This observation led to the speculation that a complete lack of M28 protein could be advantageous for replication in MRC5 cells. In order to prove this hypothesis, a stop mutation was introduced at the second start codon of ORF M28 using the backbone of M112/113-117. The replication kinetics showed that the lack of M28 protein promoted efficient viral replication in human fibroblasts and showed a similar phenotype like M112-117+M28h3 mutant (Figure 11B). M112-117+M28h3 reached a peak titer of 10^5 TCID$_{50}$/cell at day 5, whereas introduction of a stop mutation increased the titer by 5-fold. Nevertheless, this result supports the hypothesis that the mutations of M28 can lead to instability of the protein, and low abundance or lack of M28 protein promote viral replication in human fibroblasts.

To assess whether M28 facilitates viral replication specifically in human fibroblasts, the replication phenotype of M112-117+M28stop MCMV was investigated in human epithelial RPE-1 cells as well as in primary human foreskin fibroblasts (HFF) (Figure 12). The mutant M112-117 with wild type M28 (M112-117+M28wt) was not able to replicate in HFF cells whereas a moderate replication was detectable in HFF cells, upon infection with M112-117+M28stop (Figure 12A). In RPE-1 cells both viruses replicated to high viral titers and the lack of M28 in M112-117+M28stop seemed to confer a moderate replicative advantage but reached the same peak titer at day 9 compared to M112-117+M28wt (Figure 12B). These findings suggest that M28 is important for MCMV replication in human fibroblasts but not in human epithelial cells.
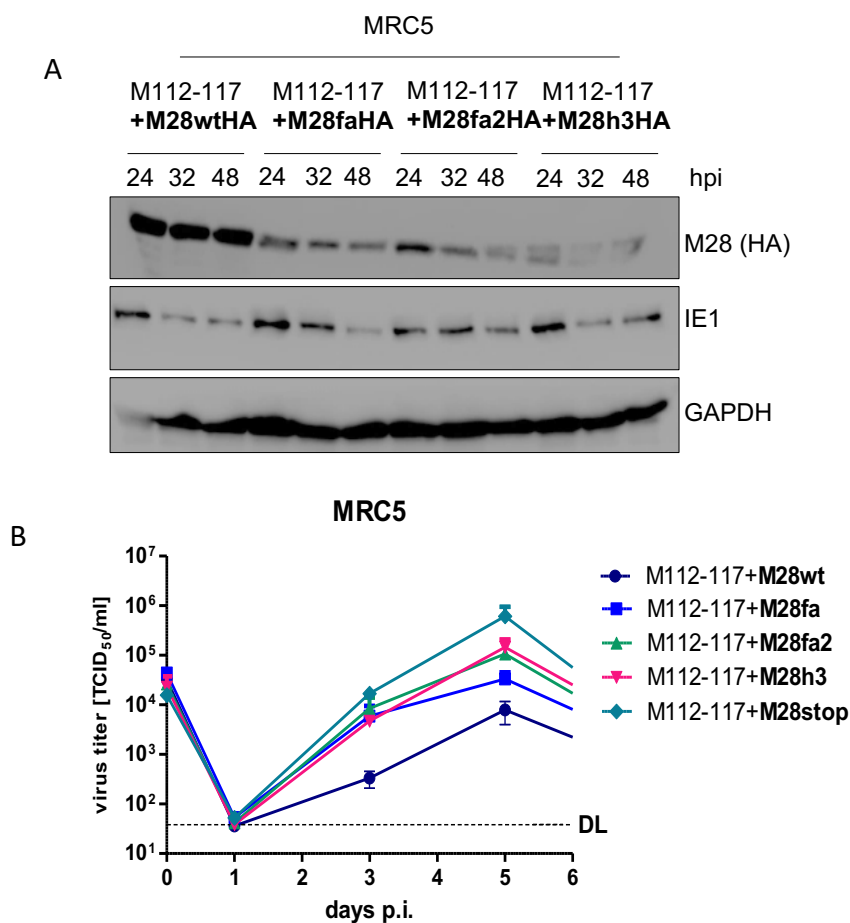
Figure 11: Lack of M28 protein promotes viral replication in human fibroblasts.

A: MRC5 cells were infected at MOI 3 $TCID_{50}$/cell with indicated HA-tagged M112-117+M28 variants, harvested at the indicated time points, and analyzed via SDS-PAGE and Western blot. IE1 was used as infection and GAPDH as loading control. **B:** MRC5 cells were infected at MOI 0.2 $TCID_{50}$/cell to analyze the replication properties of different M28 mutants in the M112-117 mutant backbone. Virus inoculum was removed at 2 hpi.,cells were washed 1x with PBS and fresh media was added. Viral titers were determined by titration of the supernatant and shown as means ± SEM. DL detection limit
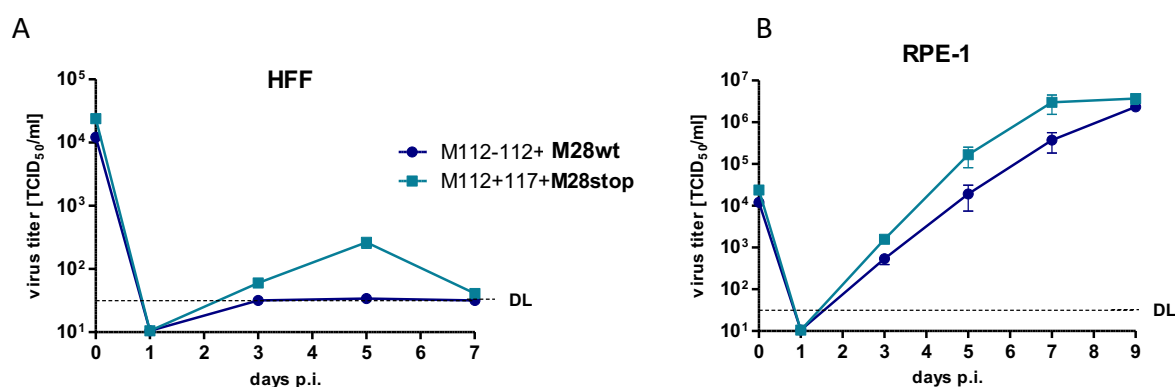
Figure 12: Loss of M28 promotes replication only in human fibroblasts but not in human epithelial cells.

AB: HFF or RPE-1 cells were infected at MOI of 0.2 $TCID_{50}$/cell to analyze the replication properties of M112-117+M28wt or M112-117+M28stop. Virus inoculum was removed at 2 hpi. and cells were washed 1x with PBS. Viral titers were determined by titration of the supernatant and shown as means ± SEM. DL Detection limit

5.2.3 MCMV M28 is not essential for replication in murine fibroblasts

While the loss of M28 resulted in enhanced replication in human fibroblasts, whether M28 was essential for MCMV replication in murine tissue culture remained unclear. Interestingly, the other host range determinant M117 is dispensable for *in vitro* replication in murine cells, but is required for viral dissemination *in vivo*, whereas the large isoform of M112/113 (E1p87) is essential for replication in NIH-3T3 cells [97, 184].

To further investigate whether M28 protein is important for replication in murine cells, viral replication of MCMV-M28wt and MCMV-M28stop virus were investigated in immortalized NIH-3T3 cells, primary mouse embryonic fibroblasts (MEFs), as well as murine SV40-transformed endothelial cells (SVEC4-10). As shown in Figure 13AB, in primary MEFs as well as in immortalized NIH-3T3 cells, MCMV-M28stop replicated to similar titers than MCMV-M28wt. Interestingly, murine SVEC4-10 cells infected with MCMV-M28stop showed a replication defect. At day 4, virus peak titer was 10-fold lower than the titer reached by the virus expressing M28 (Figure 13C). Furthermore, the number of infected endothelial cells in MCMV-M28wt or MCMV-M28stop infected cell cultures was not comparable, indicating that the stop mutant impairs viral replication or even dissemination (Figure 13D). These observations suggest that M28 is not essential for MCMV replication in murine cells and loss of M28 does not affect replication in primary as well as immortalized murine fibroblasts but reduces viral replication in SVEC4-10.
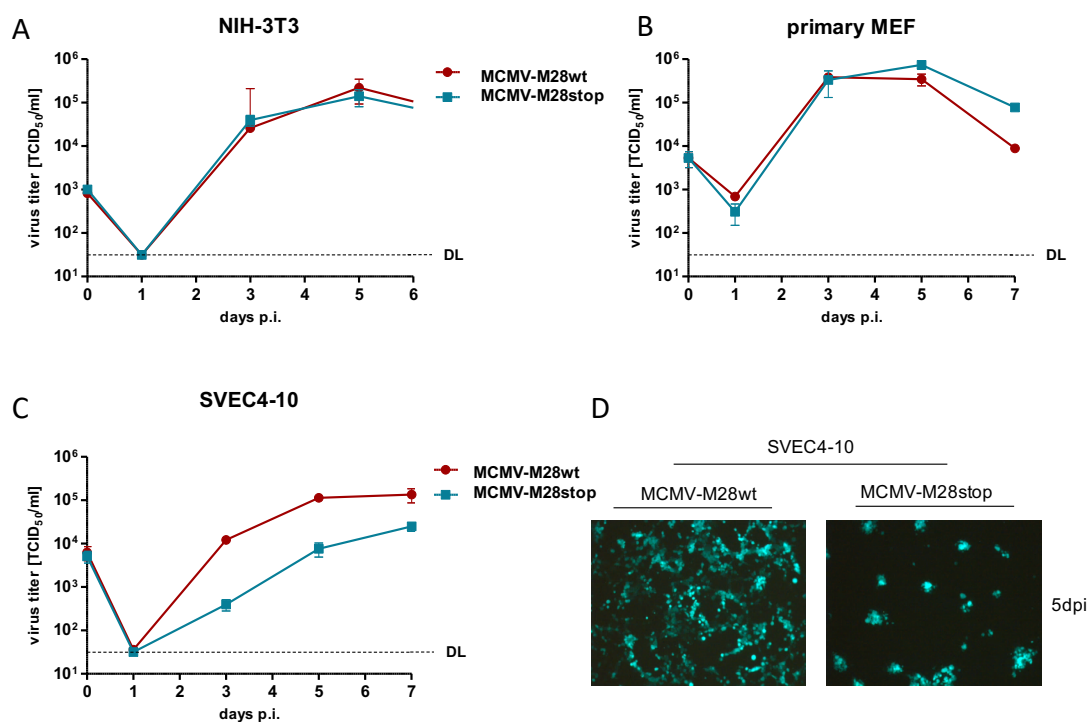
Figure 13: MCMV M28 protein is not essential for replication in mouse fibroblasts.

A: NIH-3T3 cells were infected at MOI 0.02 $TCID_{50}$/cell with MCMV-M28wt or MCMV-M28stop. **B**: Primary MEFs p.2 were infected at MOI 0.02 TCID50/cell with MCMV-M28wt or MCMV-M28stop. **C**: SVEC4-10 cells were infected at MOI 0.02 TCID50/cell with MCMV-M28wt or MCMV-M28stop. Virus inoculum was removed at 2 hpi., cells were washed 1x with PBS and fresh media was added. Viral titers were determined by titration of the supernatant and shown as means ± SEM. DL detection limit **D**: Microscopic pictures of SVEC4-10 cells infected with MCMV-M28wt or MCMV-M28stop (MCMV-GFP) at day 5 pi..

5.3   Identification and characterization of the function of M28 protein

5.3.1   Identification of potential interaction partners of M28

The results obtained so far, indicated that the expression of M28 does not play major roles in murine fibroblasts, however M28 is important in human fibroblasts and its presence restricts efficient MCMV replication in MRC5 cells. In order to identify the molecular mechanism of action of M28, potential interaction partners were identified using a SILAC-based screening for interaction partners. Firstly, in collaboration with Tim Schommartz (HPI, Hamburg) and Stefan Loroch (ISAS, Dortmund), an affinity-purification combined mass-spectrometry (AP-MS) analysis was performed by using stable isotope labeling of amino acids in cell culture (SILAC). NIH-3T3 cells, cultured in either DMEM containing heavy or light isotope labeled amino acids, were infected with HA-tagged (MCMV-M28wtHA) or non-tagged M28 mutant (MCMV-M28wt), respectively.

Afterwards, lysed samples were immunoprecipitated using HA-covalent coupled beads, and MCMV-M28wtHA samples were analyzed vs. non-tagged MCMV samples, to identify interaction partners (Figure 14). Proteins were only considered as potential interaction partners when they were found in both replicates, with minimum of 2 unique peptides, and a $\log_2$ ratio ≥ 2.8. Moreover, to exclude false positive results, a label switch of amino acids was applied, and the experiment was done in duplicates. Proteins that are often found during screening were excluded using *CRAProm*e [185].
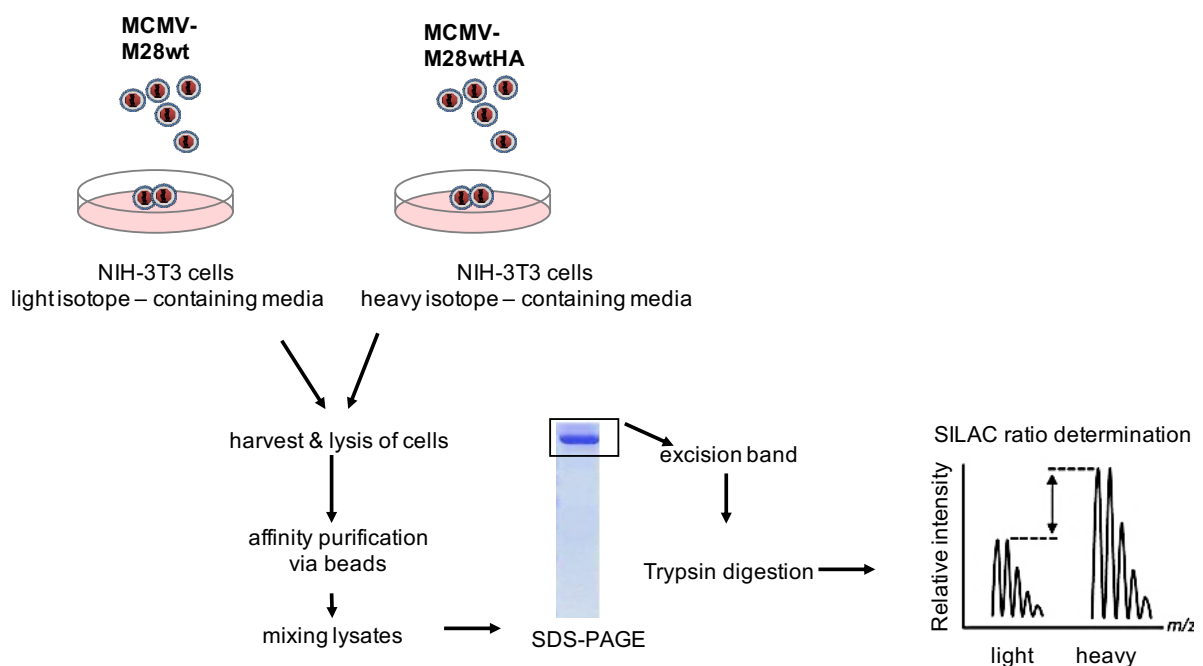
Figure 14: Workflow of SILAC-based AP-MS screening for putative MCMV M28 interacting proteins.

NIH-3T3 cells were cultured with heavy or light isotopes and infected with non-tagged MCMV-M28wt or HA-tagged MCMV-M28wtHA at MOI of 5 $TCID_{50}$/cell. Cell lysates were mixed, run on an SDS-PAGE and the band (containing all proteins) was excised from gel. Isolated proteins were digested, cleaned up and subjected to MS-analysis after affinity purification using HA-covalent coupled beads. modified from www.thermofisher.com

Five candidates fulfilling the criteria were identified to be enriched in the M28HA positive fraction. One of the candidates was the immediate-early protein 1 (IE1). IE1 is the most abundant protein of the IE class and acts as a transcriptional activator of early (E) gene expression. This protein was identified in the screen with 4 and 1 unique peptides over the control (MCMV-M28wt). Despite the high score in the SILAC screen, this candidate was interpreted to be a false positive, as it was very unlikely that the cytoplasmic M28 protein interacts with nuclear IE1, unless M28 would shuttle during infection. Indeed, I could confirm by Co-immunoprecipitation (Co-IP) that IE1 is likely a false positive (data not shown).

Moreover, the protein transcription elongation factor B (elongin B) was identified with 4 and 3 unique peptides compared to MCMV-M28wt. However, by performing Co-IP experiments pulling HA-tagged M28, elongin B could be not detected in Western blot (data not shown). Another candidate that was not analyzed in this study was TSC22 domain family 4, due to the fact that two other proteins appeared to be more promising candidates, which are involved in cell survival and cell cycle regulation: two mechanism important during cross-species infection [80, 97]. LIMD1 could be detected with 7 and 11 unique peptides and was analyzed in more detail. Interestingly, this protein is described as a cell cycle regulator in modulating the interaction of pRb and E2F-trancription factors, by affecting E2F-mediated activation of target genes [115]. Our group demonstrated that MCMV protein M117 interacts with E2F-transcription factors and regulates E2F-dependent transcription to overcome host restriction in human-epithelial cells [97]; this candidate seemed to be relevant.

Finally, the last candidate was the SHC-transforming protein 1 detected with 10 unique peptides in both replicates compared to MCMV-M28wt (Table 2). In response to growth factor stimulation, SHC1 is phosphorylated at position Y239/240 and Y317 to activate RAS-MAPK ERK signaling pathways [129], which are involved in cell cycle regulation, proliferation, and survival [141]. The SILAC-based screening performed in NIH-3T3 cells infected with the mutant M112-117+M28fa-HA did not revealed any significantly enriched interaction partners (data not shown), which could strengthen the hypothesis that mutations in M28 resulted in low abundance of the protein (Figure 11) and therefore loss of potential interactions partners.

| | Accesion number uniprot | Unique peptide count (mascot against uniprot (incl. MCMV) FDR ≤ 1% on PSM level | | | | Enrichment M28wt-HA vs. MCMV-M28wt | |
Description		M28wt-HA heavy replicate 1	M28wt light replicate 1	M28wt-HA heavy replicate 2	M28wt light replicate 2	Replicate 1 ratio (log, heavy/light)	Replicate 2 ratio (log, light/heavy)
M28 protein [M28]	A8E1D9	95	32	110	0	2,8	12,5
LIM domain-containing protein 1 [LIMD1]	Q9QXD8	7	0	11	0	3,8	12,0
SHC-transforming protein 1 [SHC1]	P98083	10	0	10	0	3,9	12,3
Immediate-early protein 1 [IE1]	P11210	4	2	1	0	4,2	8,9
TSC22 domain family protein 4 [T22D4]	Q9EQN3	4	0	8	0	3,7	11,4
Transcription elongation factor B [Elongin B]	P62869	4	0	3	0	3,1	4,0

Table 2: Potential interaction partners identified via SILAC - affinity purification-mass spectrometry (AP-MS).

Stable isotope labeled NIH-3T3 cells (heavy and light) were infected with MCMV-M28wt-HA or non-tagged MCMV-M28wt at MOI 5 $TCID_{50}$/cell. Identified interaction partners are presented with unique peptides, spectrum peptide match, and enrichment tagged MCMV-M28wtHA vs. control non-tagged MCMV-M28wt.

5.3.2 MCMV M28 protein interacts with LIMD1 during infection

Cytomegaloviruses are well known to interfere with the cell cycle in order to establish a favorable environment for viral DNA replication by inhibiting cellular DNA synthesis. HCMV is able to arrest the cell cycle at G1 phase whereas MCMV results in the accumulation of cells in G1/S and G2 phase. The cell cycle arrest goes along with the induction of S phase specific genes to promote viral replication, which enables the virus to not interfere with cellular DNA synthesis [100]. Most of these S phase specific genes are induced via the E2F-Retinoblastoma protein (pRb) axis. LIMD1 is a scaffold protein belonging to the Zyxin family and acts as an adapter for signal transduction, and is involved in cell cycle regulation [112, 114, 115, 186, 187]. LIMD1 is a tumor suppressor and cell cycle regulator, which interacts with pRb resulting in E2F-target gene inhibition [115]. Ostermann *et al.* published that inhibition E2F-dependent gene transcription is important for crossing the species barrier [97]. Therefore, I hypothesized that a potential interaction of M28 with LIMD1 might be beneficial for replication of MCMV in human fibroblasts.

To verify the potential interaction of M28 and LIMD1, I performed Co-IP experiments. Murine NIH-3T3 fibroblasts and human primary fibroblasts (MRC5) were infected with C-terminal HA-tagged M28 mutants for 24 hours. The proteins present in the cell lysate were immunoprecipitated using a HA-specific antibody and whole lysates and IP samples were analyzed via SDS-PAGE and Western blot, using specific antibodies for HA and endogenous LIMD1. As shown in Figure 15, in human as well as in murine fibroblasts infected with MCMV-M28wtHA, both M28 and LIMD1 were detectable in the whole lysate and in the IP fraction, confirming the potential interaction revealed by mass spectrometry analysis (Table 2). On the other hand, the mutated form of M28 (M112-117+M28faHA) was less detectable both in the whole lysates and in the IP fraction, suggesting that the protein was less stable or less expressed and could not interact with LIMD1. As expected, the negative control MCMV-M45HA or MCMV-m142HA was not detected in the IP fraction and no cellular contamination was observed in the IP fraction by staining GAPDH or β-actin (Figure 15AB).

These results suggest that wild type M28wt interacts with LIMD1 in murine and human fibroblasts whereas the mutated form of M28 interacts less efficiently or not at all.
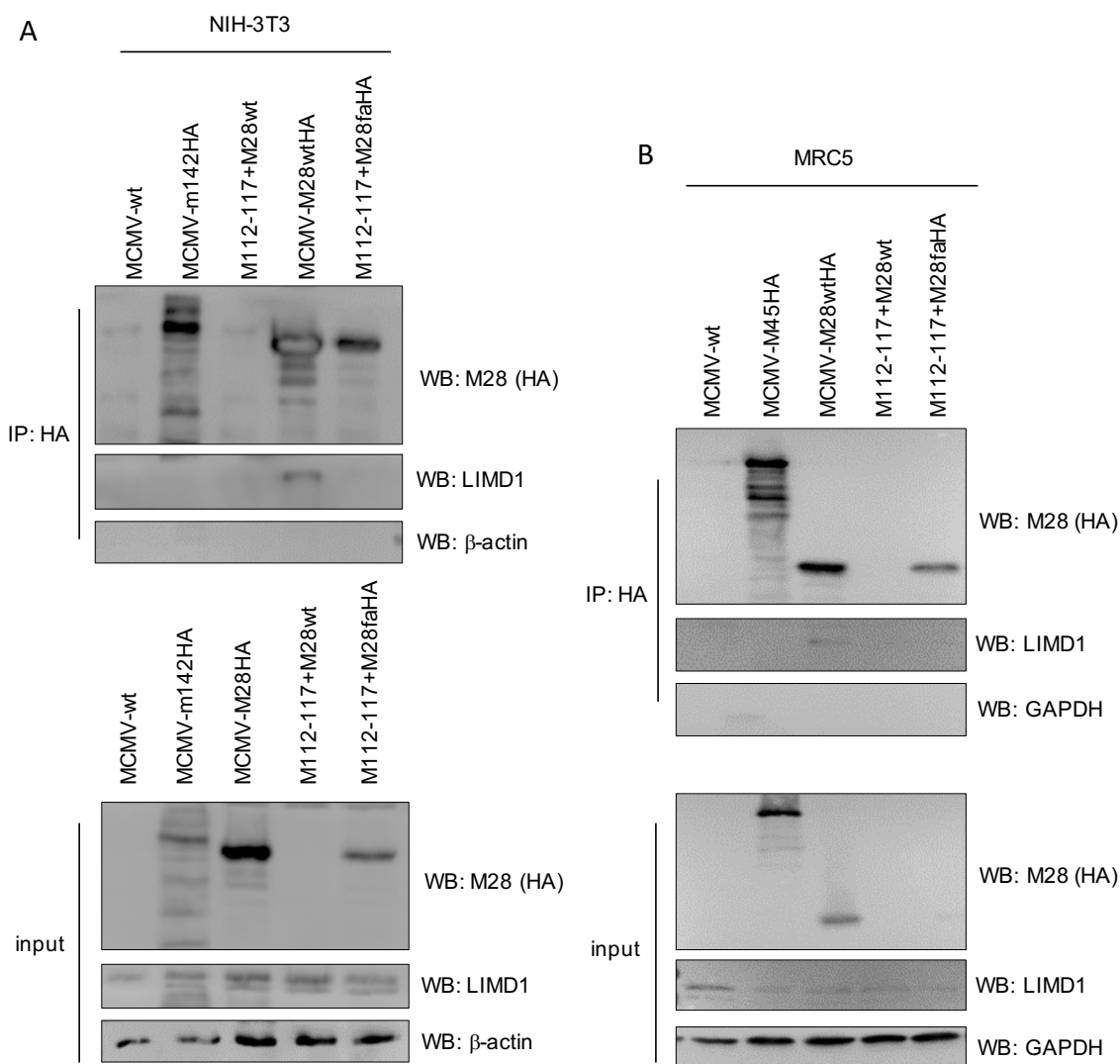
Figure 15: M28wt interacts with LIMD1 during infection in murine and human fibroblasts.

A: NIH-3T3 murine fibroblasts were infected with non-tagged MCMV-wt, M112-117+M28wt, and HA-tagged MCMV-M28wtHA, or M112-117+M28wtHA mutants at MOI 3 $TCID_{50}$/cell and harvested at 24 hpi. in NP-40 buffer. HA-tagged proteins were affinity purified via a HA-specific antibody and corresponding beads. M28 and LIMD1 expression was analyzed via immunoblotting against HA and LIMD1. **B:** MRC5 cells were infected with non-tagged MCMV-wt, M112-117+M28wt (neg. control), and HA-tagged MCMV-M28wtHA, or M112-117+M28faHA mutants at MOI 3 $TCID_{50}$/cell and harvested at 24 hpi. in NP-40 buffer. HA-tagged proteins were affinity purified via an HA-specific antibody and corresponding beads. GAPDH or β-actin was used in both experiments as a loading control and control for unspecific contamination. MCMV-m142HA or MCMV-M45HA, as well as non-tagged mutants were used as additional negative controls.

5.3.3   M28 does not modulate cell cycle regulation

Previous results from our lab showed that regulation of E2F-mediated gene transcription is important for crossing the species barrier in human epithelial cells. Moreover, it was described that the human CMV homolog of M28, pUL29/28 together with pUL38 can arrest the cell cycle

in G0/G1 phase [188]. It could be possible that cell cycle regulation might differ in primary MRC5 cells compared to immortalized human epithelial RPE-cells (Figure 11). I hypothesized that the interaction of M28 and LIMD1 would result in impaired binding of LIMD1 to pRb and therefore allow E2F-target gene expression and progression of the cell cycle. This impaired binding might lead to an inappropriate cell cycle arrest at G1 or G2 phase. In order to investigate whether M28 can modulate the cell cycle, flow cytometry was performed upon labelling of cellular DNA with propidium iodide. NIH-3T3 or HEK293 cells were prepared according to the protocol described in (8.3.9). I transfected cells with the expression plasmids encoding the wild type or the mutated form of M28-HA-tagged protein (M28wt and M28mut (fa)), respectively. A positive control pUL117-HA was transfected as well, which is able to inhibit DNA synthesis [110]. At 24 hours after transfection, cells were proceeded as described in (8.3.9) and stained with mouse anti-HA and fluorophore conjugated secondary antibodies. After exclusion of dead cells and cell aggregates (doublets), the cellular DNA content was investigated in single cells expressing HA (Figure 16).
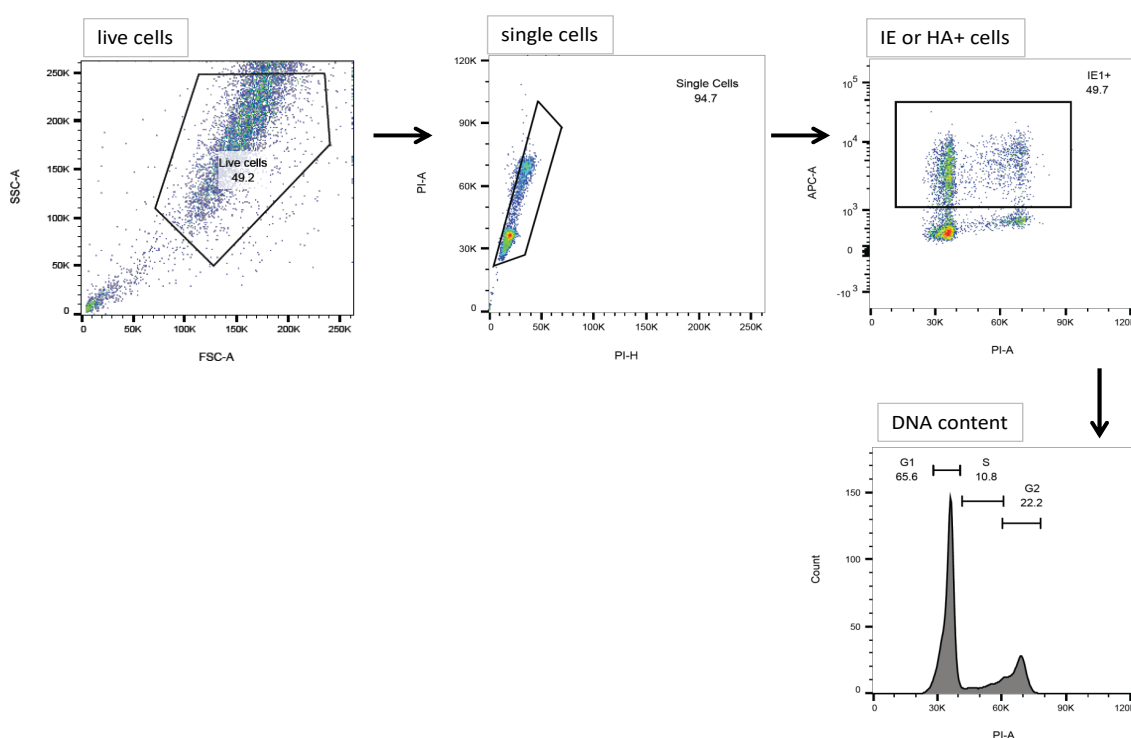
Figure 16: Flow cytometry- Cell cycle gating strategy

Cell cycle phases of different samples were selected with the following gating strategy. First live cells (10000 events) were selected and gated for single cells with IE1 or HA positive staining using specific primary antibodies + mouse AlexaFlour 647 as a secondary antibody. For analysis of specific cell cycle phases, cells were stained with propidium iodide (PI) and DNA content was measured. The number of cells in G1, S, and G2 phase were determined via FlowJo.

As shown in Figure 17, HEK293 cells transfected with M28wt showed 10% less cells in G1 phase compared to M28mut(fa) transfected cells. Conversely, HEK293 cells expressing the M28mut(fa) showed similar G1-DNA content as the positive control pUL117. However, when cells expressed M28wt, more cells were detectable in G2 phase compared to M28mut(fa) and pUL117. Whereas cells expressing the fa-variant of M28 showed 10% more cells in G1 and 10% less cells in G2 phase (Figure 17). These findings indicate that expression of the fa-mutant variant of M28 results only in a slightly stronger accumulation of cells in G1 phase while M28wt expression led to accumulation of few cells in G2 phase. When NIH-3T3 cells were transfected with the same setup of expression constructs, the experiment showed a similar trend, even though differences in cell cycle stages of cells expressing M28wt and M28mut (fa) were less pronounced (Figure 17B). These results indicate that M28 does not alter the cell cycle to a strong extent irrespective of M28 mutation.
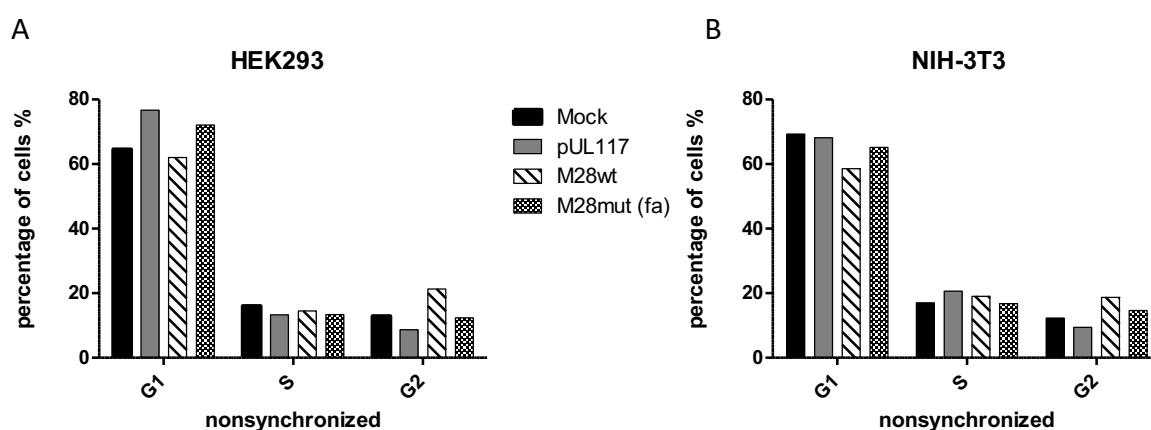
Figure 17: Expression of M28mut (fa) has only a minor effect on the cell cycle in transfected cells.

AB: NIH-3T3 or HEK293A cells were transfected with the indicated M28-HA or control plasmids. HA positive cells were fixed with EtOH at 24 hpt. and stained with HA and anti-mouse AlexaFlour (AF) 647 antibodies. First live cells, single, and HA positive cells were gated and analyzed with different DNA content, identified with propidium-iodide (PI) staining. The number of cells in G1, S, and G2 phase were determined via FlowJo.

In order to analyze the impact of M28 on the cell cycle under more physiological conditions, MRC5 cells were infected with MCMV-wt, M112-117+M28wt, or M112-117+M28fa at MOI of 1 $TCID_{50}$/cell for 24 hours. Samples were stained with anti-IE1 antibodies in order to label infected cells and were further proceeded as described above. MRC5 cells infected with M112-117+M28wt or M112-117+M28fa did not show a drastic difference in the DNA-content in all

cell cycle stages. Cells infected with M112-117+M28wt or M112-117+M28fa accumulated with 13-15% higher proportion of cells in S phase compared to MCMV-wt infected cells (Figure 18). In contrast, more cells infected with MCMV-wt were detected in G1 phase and only a small number in S phase compared to M112-117+M28mutants. However, non-infected cells showed the highest number of cells in G1 and only small proportion of cells in S and G2 phase (Figure 18). These data indicate that expression of different M28 variants does not modulate the cell cycle during infection, which differ marginally from the results obtained in transfection.
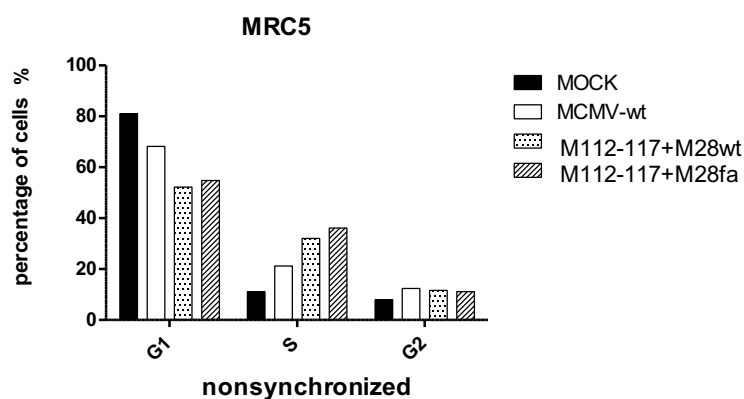
Figure 18: M28 does not affect cell cycle regulation in infected MRC5 cells.

MRC5 cells were infected at MOI 3 TCID$_{50}$/cell with the indicated mutants. IE1 positive cells were fixed at 24 hpi. and stained with IE1 and anti-mouse AF647 antibodies. First live cells, single cells, and IE1 positive cells were gated and analyzed for DNA content by staining with propidium iodide. The number of cells in G1, S, and G2 phase were determined via FlowJo.

5.3.4 M28 does not modulate phosphorylation of pRb during infection

One of the most important regulator of the cell cycle progression is the retinoblastoma protein (pRb), which is also targeted by HCMV pp71 for proteasomal degradation and phosphorylated by pUL97 [108, 109], which results in induction of E2F-responsive genes. So far, a protein fulfilling this function in MCMV has not been described. As previously mentioned, LIMD1 can regulate the cell cycle and E2F-mediated transcription via its binding to pRb, which prevents phosphorylation of pRb and therefore inhibits entry into S-Phase [115, 121].

To investigate whether the interaction of M28 with LIMD1 would result in phosphorylation of pRb, Western blot analysis was performed at different time points after infection using a pRb specific antibody, detecting both the total as well as all phosphorylated forms of pRb. As

phosphorylation of pRb results in a mobility shift in SDS-PAGE, bands of different sizes can be detected as multiple closely spaced bands. Non-synchronized MRC5 cells were seeded and infected at MOI 3 $TCID_{50}$/cell either with M112-117+M28wt or M112-117+M28fa. As shown in Figure 19, while early after infection (6 to 9 hours pi.) both M112-117+M28wt as well as M112-117+M28fa promoted pRb dephosphorylation. At 24 hours pi., pRb seemed to exist in a strong hypo and/or slightly hyperphosphorylated state, which would indicate being cells in early G1 or partially G1/S-phase. A slightly stronger band of pRb at 24 hours post infection was detected in cells infected with M112-117+M28wt as compared to cells infected with M112-117+M28fa (Figure 19).

Taken together these results showed that in transfection as well as infection, irrespective of expression of M28 mutant variant, M28 does not alter the cell cycle and only marginally differences could be detected. Moreover, pRb-phosphorylation is not altered by M28wt nor M28fa variant, suggesting that the interaction with LIMD1 does not affect pRb phosphorylation.
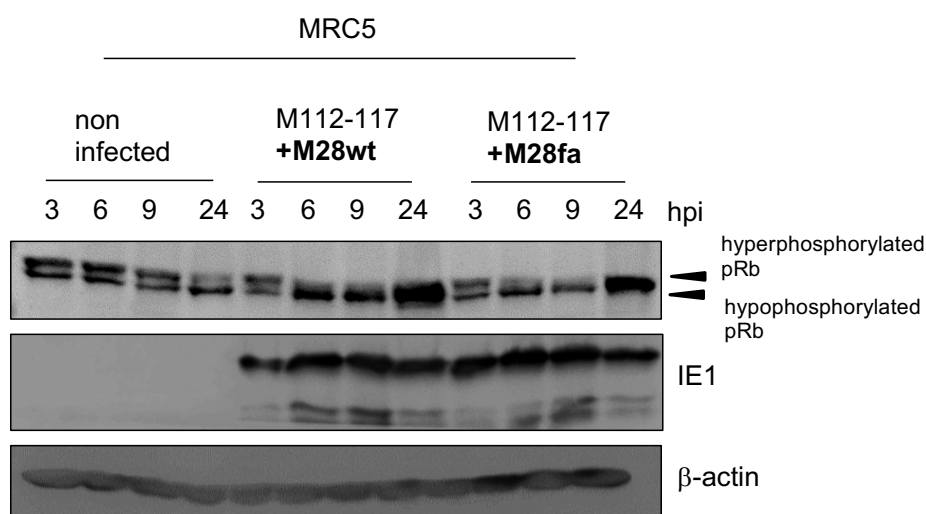
Figure 19: Phosphorylation of pRb is not altered by M28.

MRC5 cells were infected at MOI 3 $TCID_{50}$/cell with M112-117+M28wt or M112-117+M28fa in the presence of 10% FCS, harvested in 2x Laemmli, and analyzed via Western blot. pRb was stained using an antibody specific against all non and phosphorylated forms of pRb. IE1 was used as an infection control and β-actin as a loading control.

5.3.5 M28 protein interacts with the cellular adapter protein SHC1

Apart from LIMD1 I studied another promising potential interaction partner identified via AP-MS using SILAC labeling, the SHC1 protein. SHC1 is localized in the cytoplasm and is well known for its importance during receptor tyrosine kinase signaling, in particular in the RAS-MAPK ERK1/2 and PI3K/AKT signaling [132, 139] [129]. It was already described that the viral protein

VP11/12 of HSV-1 interacts with SHC1, among other adaptors [144]. During HSV-1 infection, ERK1 is phosphorylated to promote cell cycle progression towards G1/S phase and support viral replication [163]. Moreover, HCMV upregulates PI3K and inhibits apoptosis in short-lived monocytes [167]. The fact that downstream signaling of SHC1 regulates cell cycle and apoptosis, known determinants of the species specificity, strengthens the potential importance of SHC1 during cross-species infection.

First of all, I confirmed the potential interaction of M28 with SHC1. Proteins expressed in MRC5 and NIH-3T3 infected cells, capable to bind M28-HA, were pulled down by using HA-specific antibodies covalently bound to agarose beads. In NIH-3T3 and MRC5 cells, which were infected with MCMV-M28wtHA or M112-117+M28wtHA, SHC1 could be detected with all three isoforms in the IP fraction, even though the large isoform was less expressed in NIH-3T3 cells (Figure 20A). However, when cells were infected with M28 mutated forms, SHC1 was less detectable or only detectable after long exposure times (Figure 20AB). This phenomenon could be explained by the fact that mutations in M28 led to low abundance of the protein and therefore less M28 protein could be affinity purified (Figure 11). In summary, M28wt interacts with the adapter protein SHC1 during infection in both human and murine fibroblasts however mutations in M28 seem to impair the interaction with SHC1.
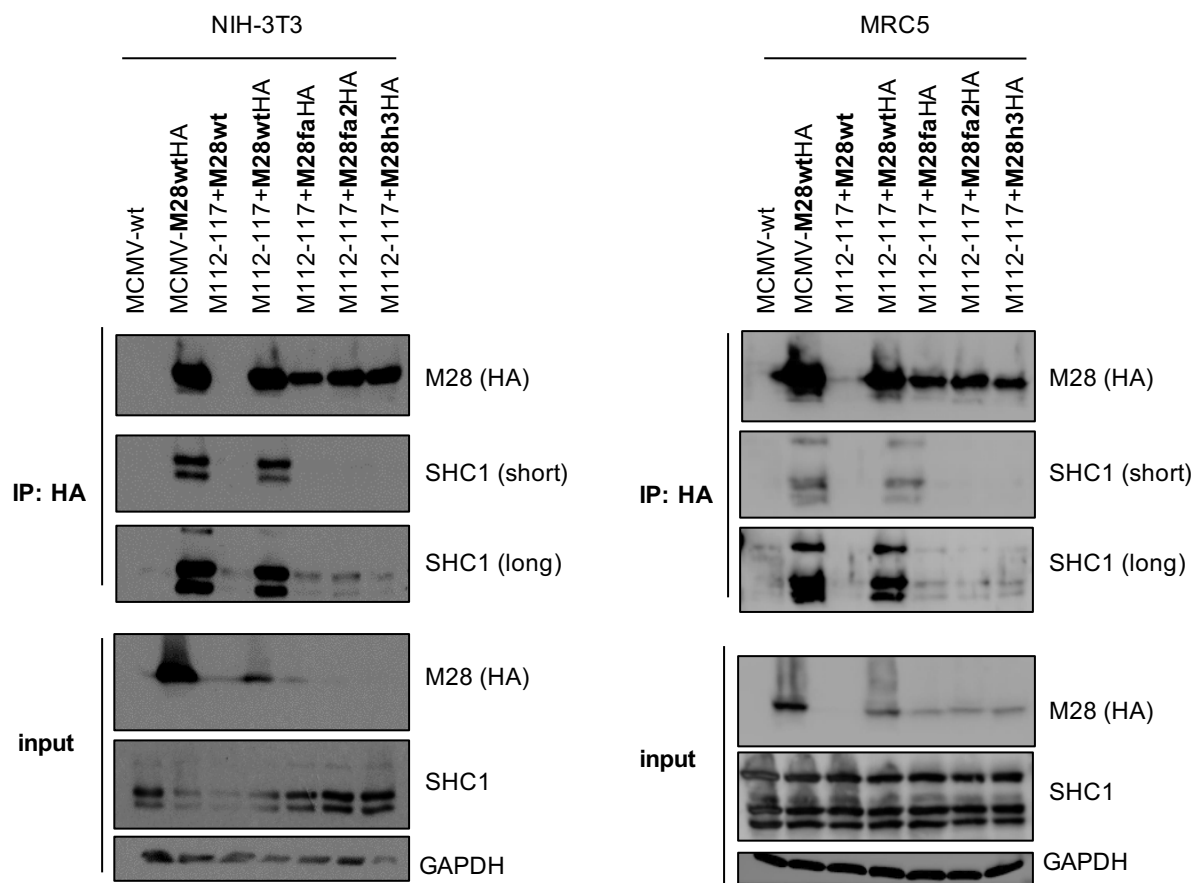
Figure 20: MCMV M28wt interacts with SHC1 during infection.

A: NIH-3T3 murine fibroblasts were infected with non-tagged MCMV-wt, M112-117+M28wt (neg. control) and MCMV-M28wtHA and M112-117+M28variant HA-tagged mutants at MOI 3 TCID$_{50}$/cell and harvested 24 hpi. in NP-40 buffer. Samples were affinity purified using HA-covalent coupled beads and analyzed by Western blot. **B:** MRC5 human fibroblasts were infected with non-tagged MCMV-wt, M112-117+M28wt (neg. control) and MCMV-M28wtHA and M112-117+M28variant tagged mutants at MOI 3 TCID$_{50}$/cell and harvested 24 hpi. in NP-40 buffer. Proteins were analyzed by Western blot, staining HA and endogenous SHC1 proteins with all three isoforms. short: short exposure time, long: long exposure time

5.3.6 M28 prevents phosphorylation of SHC1 in human fibroblasts early during infection

Previous results showed that M28wt interacts with SHC1 in murine and human fibroblasts (Figure 20). It was observed that upon ligand binding to EGFR, SHC1 is tyrosine phosphorylated at position Y239/240 and Y317 (Y313 murine), which results in recruitment of GRB2 to SHC1 and EGFR [135-137]. This activation leads to further downstream activation of PI3K/AKT and MAPK/ERK1/2, which might promote cell cycle regulation and survival [129]. First of all, I wanted to analyze the functional relevance of the interaction of SHC1 and M28 in murine cells. Therefore, I hypothesized that upon growth factor stimulation interaction of M28wt with SHC1 might impair phosphorylation of SHC1 at position Y239/240 and Y313 and modulate further downstream signaling.

To prove this hypothesis, I seeded primary MEFs at passage one, almost confluent, and deprived them from serum for 24 hours. Afterwards, cells were infected either with MCMV-M28wt or MCMV-M28stop in the presence of EGF containing medium to activate EGFR and subsequently phosphorylation of SHC1.

In primary MEFs, stimulated with EGF and infected with MCMV-M28wt or MCMV-M28stop, the phosphorylation levels of SHC1 at position Y239/240 or Y313 were comparable at early and later time points (Figure 21). Moreover, a slight increase in phosphorylation levels were observed in infected versus non-infected cells (Figure 21). In general, in non-infected cells as well as in infected cells, phosphorylation of SHC1 at position Y239/240 and Y313 increased after EGF stimulation but then decreased after 4 hours. Altogether, MCMV-M28wt nor MCMV-M28stop infection did not impaired the phosphorylation of SHC1 upon EGF stimulation suggesting that the interaction between M28 and SHC1 most likely not impede activation of SHC1 in primary MEFs.
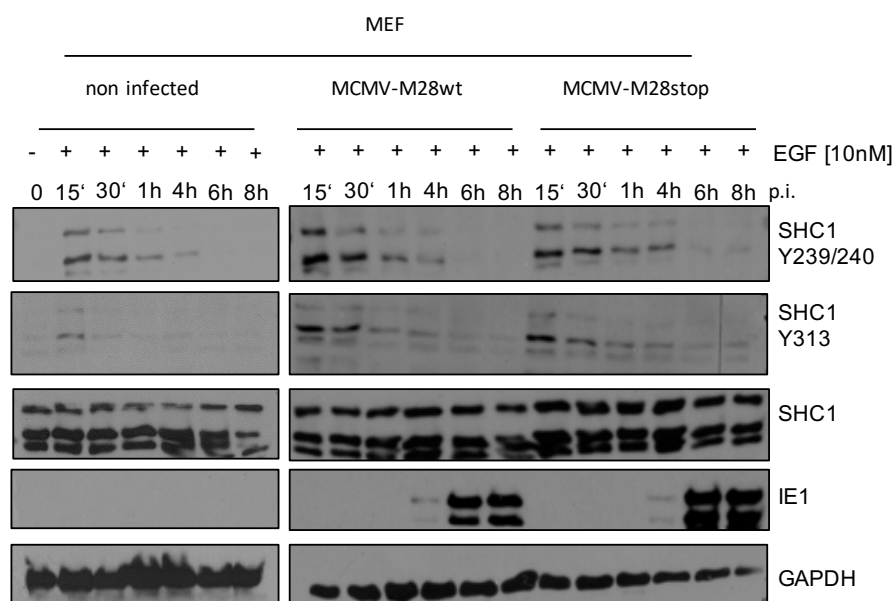
Figure 21: M28 does not affect phosphorylation of SHC1 in primary MEFs.

Primary MEFs p.1 were seeded almost confluent and starved for 24 h without FCS. Cells were infected with MCMV-M28wt or MCMV-M28stop at MOI 3 TCID$_{50}$/cell in media containing 10 ng/mL EGF. Virus inoculum was removed at 2 hpi. and cells were washed 1x with PBS. Cells were harvested with 2x Laemmli buffer and analyzed via immunoblotting. SHC1 phosphorylation was determined using specific antibodies against endogenous SHC1 phosphorylation at position Y239/240 and Y313. Non infected cells were either treated for 15min with or without EGF. IE1 was used as an infection control and GAPDH as a loading control.

Previous experiments performed in primary MEFs did not demonstrate any difference in phosphorylation levels of SHC1 (Figure 21). However, the loss of M28 showed a replication phenotype only in MRC5 cells, but not in murine fibroblasts (Figure 11,Figure 13). Therefore, I hypothesized that the interaction of M28wt with SHC1 might have a different effect on SHC1 phosphorylation in human MRC5 cells. To further investigate whether the expression of M28 and its interaction with SHC1 impede phosphorylation in human fibroblasts, I performed a phosphorylation assay in MRC5 cells infected with M112-117 recombinant M28 mutants. In MRC5 cells infected with M112-117+M28wt, SHC1 phosphorylation was diminished at position Y239/240 (Figure 22A) or Y317, compared to M112-M117+M28h3 or M112-117+M28stop (Figure 22AB). Moreover, it seems that M28stop infection shows a stronger phenotype compared to the M28h3-mutant, which is consistent with the observation that M112+117+M28stop replicates to higher titers than M112-117+M28h3 in human MRC5 cells (Figure 11). This could be explained as the protein of M28h3 is still detectable but to a lesser extent. The phosphorylation of SHC1 was observed early from 15 min up to 4 hours pi. (Figure 22AB). This fast response suggests that the effect observed was modulated by incoming M28 with the virion.

Kattenhorn and colleagues detected M28 as a virion-associated protein via mass spectrometry [181]. The results shown above suggested that SHC1 phosphorylation might be mediated by interaction of SHC1 with the virion associated M28. In order to formally proof that M28 is associated with the virion, I purified virions from cells infected with MCMV-M28wtHA, via a glycerol-tartrate gradient prior to analysis of M28. For this experiment the MCMV tegument protein M45 was used as a positive control. Firstly, the enrichment of pure virions was verified by glycoprotein gB via immunoblotting. While in the unpurified viral preparations, still containing cellular membranes, both full length (FL) and processed forms of gB could be detected (Figure 22C, input). However, in the purified viral particles only the processed form of gB was detectable. M28 as well as the positive control M45 were detected in the whole lysate (input) as well as in purified virions (Figure 22C). These observations confirmed the data obtained by Kattenhorn et al. and suggested that the phosphorylation of SHC1, early during infection, could be modulated by incoming M28 with the virion. MEFs infected with M28 mutants did show a different phenotype in phosphorylation of SHC1 (Figure 21). I speculated that differences of SHC-phosphorylation in MEF and MRC5 cells could be due to differences in abundance of SHC1 or its corresponding receptors in different cell lines. To investigate

whether the expression levels of SHC1 or EGFR differ in MEF, MRC5 cells and other cell types, I seeded equal numbers of cells, determined the overall protein concentration and analyzed the expression levels of SHC1 and EGFR via immunoblotting. Interestingly, the expression level of SHC1 is slightly different in NIH-3T3 cells and primary MEFs compared to human cells (HFF, MRC5, RPE-1). Moreover, EGFR is not detectable in NIH-3T3 cells and only weakly expressed in primary MEFs (Figure 22D). The difference in expression level of EGFR and SHC1 might explain the difference of SHC1 phosphorylation in primary MEF and human MRC5 cells.
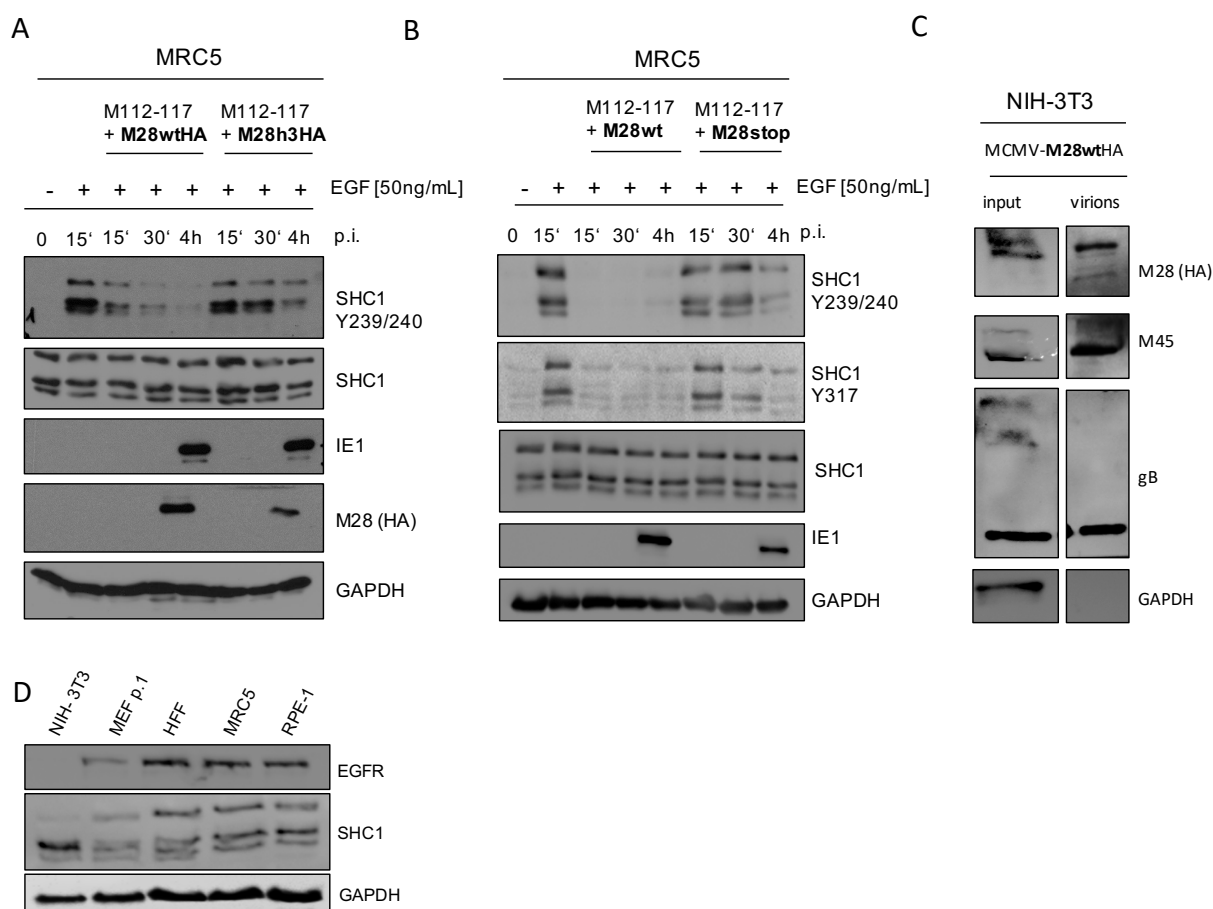
Figure 22: SHC phosphorylation is diminished in presence of M28wt in human fibroblasts.

AB: MRC5 cells were seeded almost confluent and starved for 24 h without FCS. Cells were infected with the indicated mutants at MOI 3 TCID$_{50}$/cell, containing 50 ng/mL EGF. Virus inoculum was removed at 2 hpi., cells were washed 1x with PBS and fresh media without serum was added. Cells were then harvested with 2x Laemmli buffer and analyzed via immunoblotting. SHC1 phosphorylation was determined using specific antibodies against endogenous SHC1 phosphorylation at position Y239/240 or Y317. IE1 was used as an infection control and GAPDH as a loading control. MOCK cells were treated for 15 min with or without EGF. **C:** NIH-3T3 cells were infected to produce a virus stock and cells were collected to analyze the input in the whole lysate via Western blot. After 6 days p.i., virus supernatant was collected, and gradient purified via a glycerol tartrate gradient. Enriched virions were lysed and the abundance of M28wtHA in the virion was determined via immunoblotting and specific antibodies. M45 was used as a positive control for a viral tegument protein. Detection of gB and GAPDH were used to analyze cell contamination in gradient purified samples**. D:** Expression levels of EGFR and SHC1 were analyzed by immunoblotting staining for endogenous SHC1 and EGFR.

5.3.7 M28 restrains activation of ERK1/2 and AKT downstream of SHC1

Stimulation of EGFR with growth factors results in SHC1 tyrosine phosphorylation at position Y239/240 and Y317, which serve as a binding site for GRB2 being recruited to SHC1 and EGFR [135, 137]. Since I could demonstrate that M28wt protein interacts with SHC1 and causes a diminished phosphorylation of SHC1 in MRC5 cells, I hypothesized that the interaction of SHC1 with GRB2 in presence of M28 might be affected. Therefore, I performed a Co-IP experiment of infected cells with M28HA-tagged mutants. Protein lysates were affinity purified by using an antibody against endogenous GRB2 or HA. Unfortunately, the affinity purification of GRB2 was not successful. The pull down of M28HA was difficult to interpret, as the GRB2 staining in Western blot was masked by the light chain, even by using a secondary antibody, which only detected the native IgG (data not shown). Phosphorylation of SHC1 at position Y239, Y240 and Y317 activates the downstream RAS-ERK MAPK and PI3K-AKT pathways [135-137]. Nevertheless, I hypothesized that diminished phosphorylation of SHC1 (Figure 22AB), presumably mediated via the interaction of SHC1 and M28, might impair downstream effectors such as ERK1/2 and AKT.

To determine whether M28 modulates ERK1/2 or AKT signaling downstream of SHC1, MRC5 cells were deprived from serum for 24 hours, treated with EGF and infected with MCMV recombinant mutants M112-117+M28wt or M112-117+M28stop. ERK1/2 and AKT activation was evaluated by Western blot analysis of their respective levels of phosphorylation. As shown in Figure 23, starting at 15 min pi. and until 2 hours pi., cells infected with M112-117+M28wt showed a reduced phosphorylation of ERK1/2 and AKT, in contrast to cells infected with M112-117+M28stop (Figure 23). Phosphorylation of ERK1/2 and AKT was less pronounced in cells infected with M112-117+M28stop than in non-infected cells. At 8 hours pi., ERK1/2 and AKT phosphorylation was almost not detectable and reached the basal level in non-infected and infected cells (Figure 23). The results show that at 4 hours pi., phospho-ERK1/2 is only slightly detectable in cells infected with either M112-117+M28wt, M112-117+M28stop compared to non-infected cells. Phosphorylation of ERK1/2 and AKT at early times corresponds with the timing of SHC phosphorylation immediately after infection (Figure 22), which strengthens the hypothesis that M28 impairs ERK1/2 and AKT activation via the interaction with SHC1. These results suggest that presence of M28 restrains SHC1 phosphorylation and further downstream signaling of ERK1/2 and AKT.
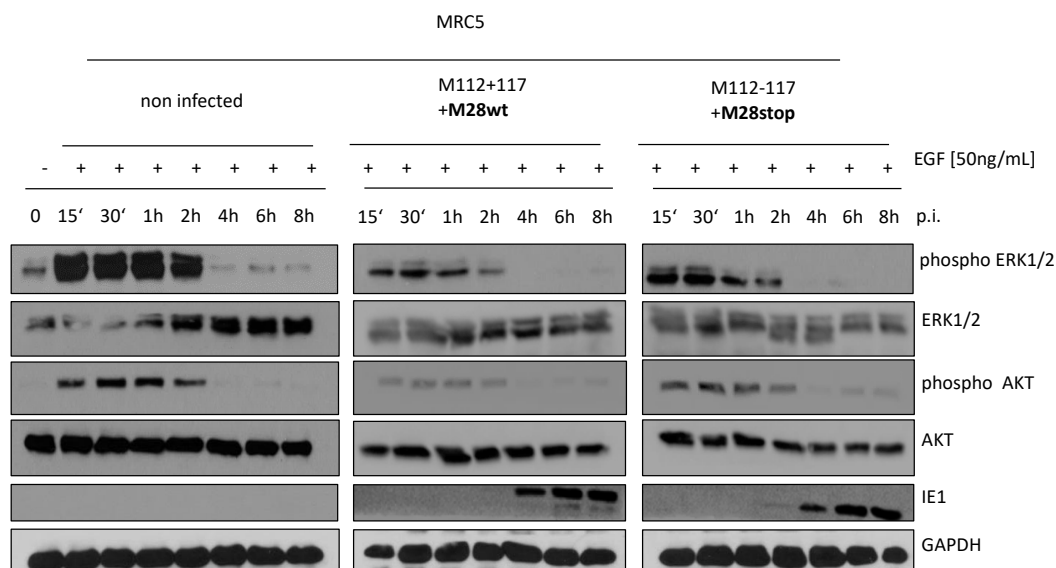
Figure 23: M28wt restricts phosphorylation of ERK1/2 and AKT in human fibroblasts.

MRC5 cells were seeded almost confluent and starved for 24 h without FCS and afterwards treated with 50 ng/mL EGF. Cells were infected with M112-117+M28wt or M112-117+M28stop at MOI 3 $TCID_{50}$/cell in the presence of EGF. Input virus was removed at 2 hpi. and cells were washed 1x with PBS. At the indicated timepoints, cells were harvested in 2x Laemmli buffer and analyzed via immunoblotting and corresponding antibodies. Phospho-ERK1/2 was analyzed at position Y202/204 and AKT phosphorylation was detected at position S473. IE1 was used as an infection control and GAPDH as a loading control.

MRC5 cells infected with M112-117+M28wt showed reduced phosphorylation levels of ERK1/2 and AKT (Figure 23). It was shown that activation of ERK1 resulted in cell cycle progression and facilitation of viral replication of HSV-1 [163]. ERK1/2 dependent activation of the pro-survival MCL-1 protein prevented HCMV latently infected cells from cell death [157]. Two mechanism, which might be beneficial for replication of MCMV in human fibroblasts. Therefore, it was worth to investigate whether ERK1/2 and AKT might be important for viral replication. I hypothesized that inhibition of ERK1/2 and AKT might restrict viral replication of M112-117+M28stop in human fibroblast.

In order to proof this hypothesis, replication kinetics in the presence of inhibitors specific for MEK1/2 and PI3K, upstream of ERK1/2 and AKT, were performed. Cells were infected at low MOI $TCID_{50}$/cell, 2 hours pi. virus inoculum was removed, and cells were left either untreated (DMSO) or incubated with the MEK1/2 inhibitor U0126 and the PI3K inhibitor LY294002, respectively. Cells were maintained throughout the complete experiment with the inhibitors, which were replaced every 48 hours. As shown in Figure 24, the replication of M112-117+M28stop was impaired in presence of the inhibitors U0126 or LY294002, and the peak titer of 10^4 $TCID_{50}$/mL was reached two days later than in non-treated cells. Interestingly, at

day 5 post infection U0126 as well as LY294002 reduced viral replication of M112-117+M28stop more than 10-fold (Figure 24). These results confirm the previous results of the phosphorylation assay, suggesting that the presence of M28 reduced activation of ERK1/2 and AKT, which restricts replication in human fibroblasts.

Figure 24: **Inhibition of ERK1/2 or AKT leads to impaired replication in human fibroblasts.**

A: MRC5 cells were infected at MOI 0.02 TCID$_{50}$/cell with M112-117+M28wt or M112-117+M28stop and maintained with 10nM U0126 after the virus inoculum was removed after 2 hpi. Supernatant was collected every 2 days and media replaced with fresh media containing the inhibitor or DMSO as control **B**: MRC5 cells were infected as described above but maintained with 10nM LY294002 after the input was removed after 2hpi. Supernatant was collected every 2 days and media replaced with fresh media containing the inhibitor or DMSO as control. Viral titers were determined by titration of the supernatant and shown as means ± SEM. DL detection limit

5.3.8 Knockdown of SHC1 impairs viral gene expression and replication

Since the previous findings suggested that activation of ERK1/2 and AKT are important for efficient replication of MCMV in human fibroblasts, most likely via a SHC1 mediated mechanisms, I wanted to investigate the impact of SHC1 on viral gene expression and viral replication in human fibroblasts. For this purpose, the expression of SHC1 was transiently silenced in MRC5 cells, by using specific siRNA. 48 hours later, cells were infected with M112-117+M28wt or M112-117+M28stop at high MOI. The expression of the viral genes IE1, E1 and the late protein gB was analyzed by immunoblotting.

As shown in Figure 25, IE1 and E1 proteins were expressed in cells infected with either M112-117+M28wt or M112-117+M28stop irrespective of the SHC1 knockdown. Interestingly E1 expression was stronger in both infected SHC1 knockdown cells, even though at 48 hours pi. the expression of E1 proteins decreased in both mutant infected cells. This might be explained by the fact that also gB, a late protein is not detectable in SHC1-knockdown cells, neither in M112-117+M28wt nor in M112-117+M28stop infected cells. These results might indicate a

delayed or non-progressive infection (Figure 25). In summary, infection with M112-117+M28stop indicates that viral gene expression is impaired in SHC1 knockdown cells. The results suggest that E1 protein expression accumulates and gB expression is inhibited or delayed, when SHC1 is knocked down (Figure 25). These results suggest that SHC1 is needed for efficient late gene expression of MCMV in human fibroblasts.
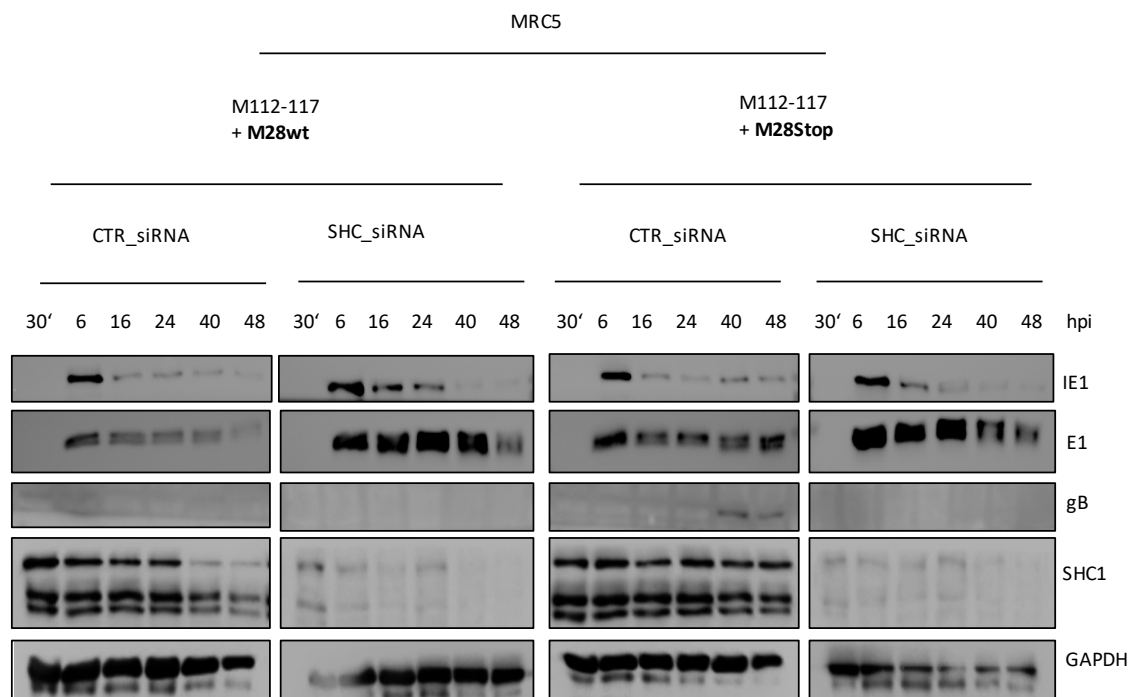
Figure 25: Knockdown of SHC1 affects viral late gene expression in human fibroblasts.

MRC5 cells were transfected with 30μM siRNA_SHC1 or siRNA_scramble (CTR) for 48 h and infected at MOI 3 $TCID_{50}$/cell. Virus inoculum was removed at 2 hpi., replaced by fresh media and samples were collected at the indicated timed points. Viral gene expression was analyzed via immunoblotting. Efficient knockdown was determined via total level of SHC1, and GAPDH was used as a loading control.

To verify whether knockdown of SHC1 impacts viral late gene expression and therefore viral replication in human fibroblasts, replication kinetics were performed at low MOI. Previous results suggested that only in SHC1-knockdown cells, infected with M112-117+M28stop, viral replication is impaired or delayed when M28 is not present.

First of all, the expression control of SHC1 showed that SHC1 is sufficiently knocked down, up to 5 days pi., compared to cells transfected with scramble siRNA (control) (Figure 26C). MRC5 SHC-knockdown cells infected with M112-117+M28wt did not show a drastic difference in viral titers up to day 5 post infection as compared to control cells (Figure 26B). However, when SHC1-knockdown cells were infected with M112-117+M28stop viral titer decreased more than 10-fold at day 5 post infection, in comparison to cells treated with scramble siRNA (Figure

26A). These findings indicate that in the absence of SHC1 viral replication of M112-117+M28stop is restricted in human fibroblasts. The fact that modulation of ERK1/2 and AKT phosphorylation, most likely via SHC1, impairs viral replication in human fibroblasts strengthens the hypothesis that SHC1-downstream signaling is important for crossing the species barrier in human fibroblasts.
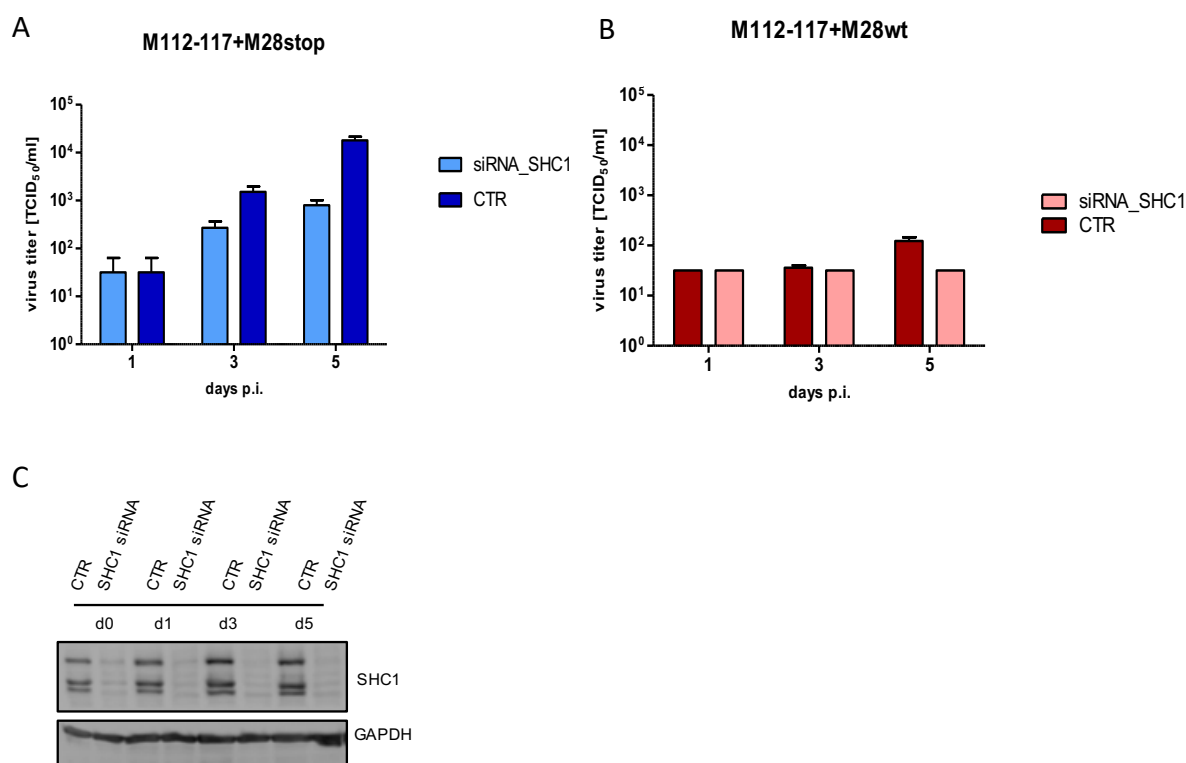
Figure 26: Knockdown of SHC1 leads to a decrease in viral yield in human fibroblasts.

AB: MRC5 cells were transfected with 30μM siRNA_SHC1 or siRNA_scramble for 48 h and infected with the indicated mutants at MOI 0.2 TCID$_{50}$/cell. Input virus was removed after 2 hpi. and viral titers were determined by titration of the supernatant and shown as means $\pm$ SEM. **C:** Efficient knockdown and expression of SHC1 was determined via total level of SHC1, and GAPDH was used as a loading control.

In conclusion, the results showed that M28 interacts with the adaptor protein SHC1 and prevents its phosphorylation in human MRC5 cells but not in murine fibroblasts. Moreover, the presence of M28 restricts activation of ERK1/2 and AKT, downstream of SHC1. Transient knockdown of SHC1 in MRC5 cells impaired replication of an M28-deficient MCMV. These findings suggest that the interaction of M28 with SHC1 blocks EGFR downstream signaling to restrict MCMV replication in human fibroblasts.

6 Discussion

Cytomegaloviruses have a narrowed host range and are strictly species specific. However, the underlying mechanism involved in cross-species infections have remained poorly understood. In the past years, our lab has established a novel system of stepwise adaptation of MCMV to human cells [45]. With this approach, two host range determinants, M112/113 and M117, have been identified and revealed new insights into the molecular mechanisms of the species specificity of MCMV [71, 97]. It was shown that inhibition of apoptosis as well as inhibition of E2F-mediated target gene transcription facilitated viral replication of MCMV in human epithelial cells whereas replication in human fibroblasts was more restricted [71, 80, 97]. However, the underlying mechanisms of why MCMV is more restricted in human fibroblasts have not been elucidated. The aim of this study was to examine the molecular mechanisms involved in the adaptation of MCMV to human fibroblasts through identifying M28 as a host range determinant and characterizing its function in cross-species infection. In this study, I could identify M28 as a novel host range determinant important for fibroblast adaptation. SILAC-based affinity purification combined MS-analysis and Co-IP experiments revealed that, during infection, M28 interacts with the tumor suppressor LIMD1 and the adapter protein SHC1. The interaction with LIMD1 does not alter pRb-phosphorylation and cell cycle regulation hence the biological relevance of LIMD1 interaction remains to be elucidated. The results presented in this work demonstrated that early after infection, M28 interacts with the cellular protein SHC1 to prevent its phosphorylation and further downstream signaling of MAPK/ERK and PI3K/AKT, which in turn restricts viral replicationin human fibroblasts.

6.1 Identification of M28 as a novel host range determinant

While activation of E2F-mediated target gene transcirption is detrimental for MCMV replication in human epithelial cells [97], the molecular mechasnims of the attenuated replication in human fibroblasts has been not addressed. In order to understand the underlying mechanism of adaptation of MCMV to primary human fibroblasts, I constructed different recombinant MCMVs and studied their replication kinetics. Introduction of missense or stop mutations in M28, in addition to those already described in M112 and M117 (Figure 8, Figure 11B), were required for efficient MCMV replication in human fibroblasts. These results confirm preliminary observations that M28 is as an important determinant of the MCMV

species barrier in human fibroblasts [180]. Mutations in M112, M117, and M28 were not sufficient for MCMV to replicate to comparable titers as the human fibroblast-adapted MCMVs (Figure 8). Remarkably, the constructed M112-117+M28 fa-variants did not reach the same peak titer as the adapted MCMV/h1-fa and MCMV/112-117-fa2 thus, suggesting that additional genomic alterations in genes apart from M112, M117 and M28 contribute to MCMV adaptation to human fibroblasts [45, 180]. In a previous study we identified three additional gene regions (m153, m164 and M25) being mutated in MCMV/h1-fa [45, 180]. It would be conceivable that these mutations enhance replication in human fibroblasts. However, those mutations did not appear in the fibroblasts adapted MCMV/112-117-fa2 and would argue against this [45, 180]. It would be worth investigating whether the additional alterations in MCMV/h1-fa and MCMV/112-117-fa2 would facilitate replication to comparable titers as the fibroblast-adapted MCMVs. Nevertheless, introducing an M28 variant into wild type MCMV did not facilitated MCMV replication in MRC5 cells and additional mutations in M112 and/or M117 are required (Figure 8). Interestingly, mutations in M28 appeared only in combination with mutated M117 in all three human cell-adapted MCMV/h1-fa, MMCMV/112-117-fa2 and MCMV/h3 [45] (Table 1). For Influenza virus the mechanism of epistasis was described during adaptations to new hosts. Specific mutations aquired during evolution only apeared to counteract adverse phynotypic effects of other mutations [189, 190]. Thus, a similar mechanism might promote the appearance of M28 mutation in presence of mutated M117. Preliminary results indicated that M117 in combination with M28 is not sufficient to promote efficient replication in MRC5 cells, however it was observed that a truncated M117 mutant was able to replicate to low titers in MRC5 cells [97]. This discrepancy can be explained by differences in the experimental conditions using low MOI infection and no centrifugal enhancement. It was demonstrated that shear stress in endothelial cells, induced by flow, led to phosphorylation of SHC1 [191]. It might be likely that centrifugal enhancement would also lead to phosphorylation of SHC1 and can compensate for M28wt-mediated restriction of SHC1 phosphorylation in M117 mutant-infected MRC5 cells. This would support the hypothesis that M112+M28, or the combination of M112+M117+M28, are required for adaptation to human fibroblasts.

Expression kinetics of different recombinant M28HA-mutants, as well as SHC1-phoshorylation assays revealed that the loss of M28 promoted viral replication in MRC5 cells (Figure 11AB, Figure 22AB), thus indicating that M28 mutations are loss-of-function mutations. Interestingly,

truncation mutants of two other proteins M117 and M139 facilitated replication in human epithelial cells [97], (Puhach, unpublished). A large-scale screen of different human cell-adapted MCMVs would increase knowledge about frequently mutated gene regions that are essential for replication in human cells and would give new insights whether loss of function mutations are commonly acquired during cross-species infection of MCMV.

In the present study I could show that expression of M28 restricts replication of M112-117+M28wt in human fibroblast but not in human epithelial cells (Figure 12). The underlying mechanism of this restriction and the differences between human epithelial cells and fibroblasts are still unclear. A previous study indicated that induction of IFN-β upon infection with MCMV or HCMV is less pronounced in RPE-1 cells as compared to MRC5 cells [45]. While, comparable IFN-β induction was observed in MRC5 infected with the epithelial cell-adapted MCMV (MCMV/h1) or the fibroblast-adapted MCMV (MCMV/h1-fa), thus suggesting that IFN-β levels might not be responsible for the different phenotype [45]. Notably, MCMV/h1 produced larger plaques when IFN-β-neutralizing antibodies were added to infected MRC5 cells [45]. Even though, there was no formal proof for a role of IFN-β during the adaptation in human fibroblasts, some studies would support this hypothesis. Infection of MRC5 cells with a MCMV mutant expressing M28 resulted in diminished phosphorylation of SHC1 (Y317) (Figure 22). A study investigating breast cancer immune suppression demonstrated that cells from transgenic mice defective in phosphorylation of SHC1 (Y313) showed increased STAT1, STAT3 and subsequently absent or low IFN-α, β, γ expression levels [192]. Moreover, activation of MAPK/ERK pathway in RAS-transformed NIH-3T3 cells inhibited reovirus-induced IFN-β expression [193]. It would be interesting to investigate whether M28wt induces elevated IFN-β levels while preventing SHC1 phosphorylation in MRC5 cells. One study showed that hTERT immortalized RPE-1 cells carry an activating mutation in the RAS gene, which likely resulted in keeping RAS in its GTP-bound active state [194]. In this study, I showed that M28wt restricts SHC1-phosphorylation and RAS/MAPK downstream signaling (Figure 22, Figure 24). It might be possible that RPE-1 cells exhibit a modulated or constitutive active RAS signaling resulting in a dispensable function of M28 in RPE-1 cells. Interestingly, M112-117+M28wt was not able to replicate in HFF fibroblasts and introduction of an M28stop mutation resulted only in moderate replication in those cells (Figure 12A). One possible explanation for this phenotype is that cell cycle regulation or MAPK signaling might differ in those cells. This hypothesis is supported by studies indicating that cell cycle regulation and in particular

expression of EGR1, a transcription factor induced downstream of ERK1/2, is involved in senescence, which is differentially regulated in HFF and MRC5 cells [195, 196].

To conclude, M28 could be identified as novel host range determinant important for crossing the species barrier in human fibroblasts while mutations in M112 and M117 contribute to the adaptation, suggesting that an effective adaptation of MCMV to human fibroblasts requires more than one viral factor. Moreover, the results indicate that M28 is important for cross-species infection only in human fibroblasts but not in epithelial cells. It might be feasible that M28 modulates STAT1-mediated IFN-β signaling or cell cycle regulation via interaction with SHC1, however the exact mechanism remains to be elucidated.

6.2 Characterization of MCMV M28 protein

Up to now, only limited data was available of M28 protein. Even though Ashan and colleagues suggested that ORF M28 and m29.1 are expressed from a bicistronic messenger RNA (mRNA) infrequently spliced [197], RNA-seq analysis performed in our lab by Tim Schommartz did not confirm these data. Mass spectrometry analyses performed by Kattenhorn and colleagues demonstrated that the M28 protein is as a virion-associated protein [181]. Expression kinetics, a CHX/ActD release assay and intracellular localization experiments, performed in NIH-3T3 cells infected with HA-tagged MCMV-M28wt, revealed that M28 belongs to the class of early genes and is localized predominantly in the cytoplasm (Figure 9AB, Figure 10). Replication kinetics in mouse embryonic, as well as immortalized murine fibroblasts and endothelial cells, demonstrated that M28 is not essential for replication in murine fibroblasts, but required for efficient replication in endothelial SVEC4-10 cells (Figure 13CD).

The human CMV homolog of M28, pUL29/28 has been described as a virion-associated protein expressed with early kinetics, localized to the nucleus and later in the cytoplasm [182]. Due to the sequence homology of M28 with pUL29/28 I hypothesized, that M28 might share similar protein functions and properties with pUL29/28. Purification of MCMV-M28wtHA virions showed that M28 could be detected in the virion (Figure 22C). In contrast to M28 human homolog pUL29/28, M28 was observed predominantly in the cytoplasm and possibly excluded from the nucleus (Figure 10). Interestingly, two other host range determinants, M112/113 and M117, are also expressed with early kinetics. Both proteins are recruited to viral replication compartments and localize to the nucleus [71, 97]. Even though, it has not been fully elucidated whether M28 can shuttle between the nucleus and cytoplasm during the

course of infection, the fact that M28 interacts with the cytoplasmic protein SHC1 (Figure 20) strengthens the hypothesis that M28 fulfills its functions mainly in the cytoplasm and likely differs from the function of pUL29/28. Notably, the subcellular localization was not altered by introduction of M28(fa) mutation, which excludes mislocalization as a potential mechanism to promote viral replication in human fibroblasts (Figure 10A). Expression kinetics of infected NIH-3T3 cells with different M28 variants revealed that mutations in M28 led to low detectable expression levels in Western blot (Figure 11A). Introduction of a M28stop mutation demonstrated that a complete loss of M28 is favorable for the virus (Figure 11AB). Correlation with SHC1 activity suggests that mutations of M28 affect its protein stability. These data indicate that the replication phenotype is presumable promoted by low abundance of M28 protein.

The data obtained from replication kinetics revealed that the loss of M28 promoted replication in human fibroblasts while M28 expression did not impair replication in primary mouse embryonic as well as immortalized murine fibroblasts (Figure 8, Figure 13AB). Remarkably, another host range determinant, M117, is dispensable for replication in murine fibroblasts *in vitro* but is required for efficient dissemination *in vivo* [97], whereas the large isoform of M112 (E1p87), mutated in M112-117, is essential for replication in NIH-3T3 [184]. Moreover, the spontaneously human cell-adapted MCMV/h did not show a replication defect in murine 10.1 fibroblasts [71]. These data suggest that the function of M28 is less important in murine fibroblasts *in vitro*. Remarkably, in immortalized murine SVEC4-10 cells, expression of M28 was required for efficient replication and loss of the protein resulted in 10-fold decrease of viral titer (Figure 13CD). However, the underlying mechanism of the different replication property of MCMV-M28stop in murine endothelial cells remains to be elucidated, although the observation might be explained by cell-type specific viral tropism in endothelial cells. Interestingly, another MCMV protein, m139, is involved in cross-species infection. A deletion of the gene region m139 resulted in a replication defect in SVEC4-10 cells (Puhach, unpublished). This could indicate some overlapping function. However, the molecular mechanism of m139 during cross-species infection has not been further studied.

In conclusion, M28 is a virion-associated protein expressed with early kinetics and likely fulfills its function in the cytoplasm by being excluded from the nucleus. Moreover, mutations in M28 likely affect the stability of the protein and loss of the protein impairs only replication in murine endothelial cells, whereas the function of M28 in murine fibroblasts is less important.

6.3   Identification of LIMD1 as an interaction partner of M28

In order to understand the molecular mechanism of action of M28, a SILAC-based affinity purification and MS approach, using isotope labeled NIH-3T3 cells, was performed. With this approach, potential interaction partner could be identified to reveal new insights into protein functions. SILAC-based AP-MS has been successfully established to study interaction partners of MCMV [198].   The screening discovered several potential interaction partners, and two candidates, LIMD1 and SHC1, were investigated in more detail (Table 2). Interestingly, when cells were infected with the mutant M28 virus, no potential interaction partner could be found in the screen (data not shown). A feasible explanation might be that mutations in M28 resulted in low stable state expression (Figure 11AB). Due to its low abundance or impaired folding, most likely only limited proteins could stably interact with M28 and did not appear in the screen. The speculation that M28 is degraded would need further investigation by performing expression analysis in the presence of lysosomal or proteasomal inhibitors or pulse chase experiments.

Several studies observed overexpression of LIMD1 in malignant tumors, highlighting its role in cell cycle regulation [117, 186]. LIMD1 is a tumor suppressor and cell cycle regulator, which interacts with pRb resulting in E2F-mediated target gene inhibition [115]. Moreover, in the context of herpesvirus infection, LIMD1 interacts with the LMP1 protein of the gamma-herpesvirus EBV to regulate latency [122], suggesting that LIMD1 plays a potential role during MCMV infection to regulate the cell cycle. Firstly, the interaction of LIMD1 with M28wt was confirmed in mouse and human fibroblasts whereas the mutated form of M28mut(fa) did not interacted with LIMD1 (Figure 15AB). In order to analyze whether M28 could regulate the cell cycle upon binding to LIMD1, flow cytometry analysis of transfected NIH-3T3 or HEK293 with M28wt or M28mut(fa) was performed. The results demonstrated that expression of M28mut(fa) resulted in 10% more cells accumulating in G1 phase to a similar extent to those expressing the positive control pUL117, whereas only a small proportion of cells, expressing M28wt, progressed through the cell cycle (Figure 17). The fact that only a limited number of cells accumulated in G1 phase in M28mut(fa) expressing cells, suggests that M28 does not alter the cell cycle via interaction with LIMD1 or only to a minor extent. Human MRC5 fibroblasts infected with M28wt or fa-specific mutant did not show differences cell cycle regulation (Figure 18). Hence there is no evidence that M28 modulates the cell cycle via interaction of LIMD1 in transfected or infected cells. The results obtained in this study indicate

that the function of M28 differs from the human CMV homolog of M28 pUL29/28, which is able together with pUL38 to arrest the cell cycle in G0/G1 phase [188].

As previously mentioned, pRb is important for cell cycle progression. In uninfected cells at late G1 and S phases, pRb is hyperphosphorylated by CDKs to promote cell cycle progression. During HCMV infection, this process is modulated in at least two steps: pRb is targeted by pp71 for proteasomal degradation [108], and in addition, pUL97 phosphorylates pRb at CDK specific target sites [109] thus resulting in induction of E2F-responsive genes. However, a protein fulfilling this function during MCMV infection is not known. Activation of E2F-mediated gene transcription was detrimental for replication in human epithelial cells [97]. The reason why activation of E2F-mediated transcription is detrimental for the replication in human cells still needs to be elucidated. One might speculate that mutations in M117 arrest MRC5 cells too late or too early at G1 or G2 phase and thus restricts efficient replication. M28 was thought to be a potential candidate to promote pRb phosphorylation and progression of the cell cycle, via its interaction with LIMD1. At the time of infection of MRC5 cells, pRb was hyperphosphorylated (early G1 or late G1/S phase), but dephosphorylated at 6-9 hours and finally accumulated in a hypophosphorylated state at 24 hours after infection, regardless of M28 mutation (Figure 19). These data suggest that infection of MRC5 cells with M112-117 mutants results in accumulation of cells with hypophosphorylated pRb (G1 or G2 phase) irrespective of M28 interaction with LIMD1. The hypothesis that M28 activates E2F-mediated gene transcription via binding to LIMD1 and release of pRB to promote cell cycle progression could be not confirmed during this study and needs further investigations. However, it would be still possible that a complete loss of M28 promotes pRb phosphorylation via a LIMD1 independent mechanism.

6.4 M28 interacts with SHC1 and restricts viral replication in human fibroblasts

The second promising interaction partner of M28 identified via SILAC-based AP-MS was the SHC1 adapter protein (Table 2). Upon stimulation of EGFR, the adapter protein SHC1 is tyrosine-phosphorylated at position Y239/240 and Y317, activates mitogen-activated protein kinases (MAPK) and phosphoinositide-3-kinase/AKT (PI3K/AKT) signaling pathways, which are involved in cell cycle regulation, proliferation and survival [125]. Results obtained in this study showed that M28wt interacts with SHC1 during infection while presence of M28 prevents

phosphorylation of SHC1 at position Y239/240 and Y317 and restricts further downstream signaling of MAPK and PI3K, presumably via a SHC1 dependent mechanism (Figure 20, Figure 22, Figure 24). In primary MEFs, the phosphorylation of SHC1 was not impaired (Figure 21). Co-IP experiments demonstrated that M28wt interacts with SHC1 during infection in murine and human fibroblasts, whereas mutations in M28 impaired the interaction (Figure 20). Moreover, introduction of different M28 variants into M112-117+M28wt revealed that the C-terminus of the protein is likely to be important for efficient replication in human fibroblasts (Table 1). Introduction of deletions into M28 would give insights into whether the C-terminus is important for interactions with the adapter protein SHC1 to promote viral replication.

Several studies have shown that other viral proteins interact with cellular adapter proteins. Felicia Goodrum's group demonstrated that pUL135 of HCMV regulates EGFR signaling and trafficking via interactions with another host adapter protein CIN85, to facilitate reactivation from latency [154, 155]. Remarkably, sequence alignment of pUL135 and M28 identified a conserved proline-rich SH3 binding motif (PxxxPR), which is important for binding to CIN85 [155]. Interestingly, during infection with another herpesvirus, protein VP11/12 of HSV-1 interacts with SHC1 [144]. More recently, an interactome study of HCMV identified pUS22 as a potential interaction partner of SHC1 [199]. The HCMV homolog of M28, pUL29/28 was described as a US22 family protein member, and it is likely that M28 exhibits a similar function as US22. These studies show that interaction of viral proteins with host adapter proteins is a common strategy to manipulate the host cell.

Van der Geer and colleagues observed that tyrosine phosphorylation of SHC1 at position Y239/240 and Y317 leads to the activation of further downstream signaling [135]. In infected MRC5 cells stimulated with EGF, phosphorylation of SHC1 was inhibited when M28wt was present, indicating that the interaction of M28wt with SHC1 diminished phosphorylation (Figure 20). This phenomenon was observed early (15 min) after infection suggesting that the inhibitory effect was likely caused by the virion associated M28 and not by the *de novo* synthesized protein (Figure 22C). Even though, this study and Kattenhorn *et al.* detected M28 as a virion-associated protein [181] this aspect should be verified in our setting by performing experiments with UV-inactivated MCMVs. Tyrosine phosphorylation of SHC1 at position 239/240 and 317 serve as binding sites for GRB2, which is recruited to the plasma membrane upon stimulation with RTKs [135, 136]. I this study, I investigated whether presence of M28 prevents phosphorylation of SHC1 and subsequent impaired interaction with GRB2. Despite

several attemps, GRB2 could not be affinity purified in Co-IP experiments (data not shown). Alternatively, a glutathione-S-transferasen (GST)-tagged GRB2 protein can be used to affinity purifiy GRB2 instead of purifiying endogenous GRB2. In addition, the use of a fluorophore-labeled GRB2 protein would allow to detect recruitment of GRB2 to the plasma membrane in presence of absence of M28. Hence, primary MRC5 cells are difficult to transfect and do not tolerate additional starvation as well as they have only limited passage capacity, this question can be only addressed in immortalized cells.

Surprisingly, SHC1 phosphorylation was not altered in primary MEFs infected with MCMV-M28wt nor MCMV-M28stop (Figure 21), irrespective of low or high EGF concentrations (data not shown). In non-infected primary MEFs, SHC phosphorylation was slightly stronger (Figure 21), which might lead to the speculation that MCMV itself can phosphorylate SHC1, even though preliminary experiments performed under serum deprived conditions (data not shown) did not confirmed this hypothesis. Since EGFR-dependent phosphorylation of SHC1 has been described in primary MEFs [200], I investigated whether the expression levels of SHC1 or EGFR differ in MEFs and MRC5 cells. Expression analysis of different cell types revealed that SHC1 expression indeed slightly differed in primary MEFs as compared to MRC5 cells, whereas differences in abundance of EGFR were more pronounced (Figure 22D). Although, phosphorylation of SHC1 via EGFR was described in primary MEFs and this mechanism seem to be conserved among other cell types [200], this observation was unexpected. Altogether, differences in SHC1 and EGFR expression levels might explain why primary MEFs responded less than MRC5 to EGF stimulation, and differences cannot be detected in Western blot (Figure 22D). Moreover, it could be hypothesized that M28 binds to higher affinity to EGFR than SHC1, and phosphorylation of SHC1 is mediated by another receptor at the plasma membrane. It was shown that phosphorylation of SHC1 can be also mediated by other RTKs via Integrins [131, 201, 202], thus suggesting that SHC1 phosphorylation is mediated by another receptor in primary MEFs. Moreover, it might be possible that the interaction of M28 with SHC1 is only transient or impaired in primary MEFs. In general, the results demonstrated that phosphorylation of SHC1 returns to basal levels after 4 hours post infection. This could be explained by the virus inoculum being replaced by new media without EGF (Figure 21). To conclude, these results would be in line with the fact that the presence of M28 also did not affect viral replication in primary MEFs as well as in NIH-3T3 cells (Figure 13AB). In primary MEFs no aberrant phosphorylation of SHC1 was observed during MCMV-M28stop infection

(Figure 21). The role of SHC1 has been addressed in SHC1 knockout mice, while knockout of SHC1 resulted in embryonic lethality after 11.5 days [200, 203] thus, it would be worth investigating whether infection with M28stop does lead to attenuated replication in mice. Moreover, phosphorylation levels of SHC1 need to be further investigated in SVEC4-10 cells. Infection of SVEC4-10 cells with M28stop mutant reduced viral titers by 10-fold (Figure 13CD). Preliminary experiments of infected SVEC4-10 cells did not show altered phosphorylation levels of SHC1 at early timepoints however this need to be ivestigated under experimental conditions. Taken together, these results suggest that the function of M28 is less important in murine fibroblasts.

Nevertheless, the impact of SHC1 on viral gene expression and replication was investigated in cross-species infection. Transient knockdown of SHC1 in MRC5 cells impaired viral late gene (gB) expression of an M28-deficient MCMV as well as its replication (Figure 25, Figure 26). This would be consistent with previous findings that showed that human cells infected with MCMV resulted in altered or delayed viral late gene expression [71, 80]. Notably, mutation in M112/113 as well as M117 resulted in a delayed replication phenotype [71, 97], which differs from the replication property observed for the triple mutant M112-117+M28stop (Figure 11). These results suggest a pro-viral function of SHC1 during cross-species infection in human fibroblasts.

6.5 M28 restrains downstram signaling of SHC1

Phosphorylation of SHC1 at position Y239/240 and Y317 stimulates and activates RAS-MAPK/ERK and PI3K/AKT pathways. Upon stimulation with EGF, phosphorylation levels of ERK1/2 (Y202/Y204) and AKT (S473) were reduced in MRC5 cells infected with M112-117+M28wt as compared to M112-117+M28stop (Figure 23), suggesting that the presence of M28 restrains phosphorylation of ERK1/2 and AKT downstream of SHC1. These results are consistent with published data obtained by infection experiments with HCMV leading to phosphorylation of ERK1/2 and AKT [32, 162]. A similar mechanism could be proposed for MCMV. Later during infection (8 hours pi.), phosphorylation of ERK1/2 and AKT was almost not detectable and in non-infected and infected cells, had returned to basal level (Figure 23). This can be explained by the fact that cells were only stimulated once with EGF before infection, which does not result in sustained activation.

Nevertheless, by inhibiting PI3K and MEK1/2 using the inhibitor LY294002 and U0126, respectively, viral replication was impaired and delayed in MRC5 cells infected with M112-117+M28stop (Figure 24). These observations suggest that inhibition of MEK1/2 and PI3K, downstream of SHC1, restrict viral replication of M112-117+M28stop in MRC5 cells. Compensatory effects of the inhibitor on PI3K or MAPK pathways could explain reasons for the delayed peak titer or transient replication inhibition. It was described that inhibition with U0126 can lead to a compensatory activation of EGFR mediated activation of AKT [204, 205]. Moreover, LY294002 treatment of HCMV infected cells led to a delayed replication phenotype [166], which is consistent with results obtained in this study. As SHC1 targets both branches of the pathway, it would be possible that inhibition of both PI3K and MEK1/2 would have additive effects and completely abolish replication in MRC5 cells. However, this would need further investigation. Nevertheless, activation of ERK in HCMV latently infected cells, early during infection, induced the anti-apoptotic gene MCL-1 and protected cells from cell death [157]. Such a mechanism might be favorable during cross-species infection in human fibroblasts. Interestingly, by inhibiting ERK signaling or disrupting STAT1-mediated IFN-β induction during a myxoma virus (poxvirus family) infection, this virus was able to cross the species barrier from rabbit to primary MEFs [206]. While ERK1/2 activation seems to be detrimental for cross-species infection of myxoma virus, several other viruses, such as HCMV and Influenza, exploit ERK1/2 signaling to promote replication [160, 207].

Activation of ERK1/2 could modulate cell cycle via induction of cyclin D1 and CDK4 thus promoting G1/S phase progression [208], which could in turn support MCMV replication in human fibroblasts. It is described that ERK1 activation is supportive for viral replication of HSV, resulting in cell cycle progression towards G1/S phase [163]. To speculate, M28wt expression might inhibit cell cycle progression and arrest cells at early G1 phase via an ERK-dependent mechanism. However, this would require sustained or at least two phases of ERK1/2 activation [208]. Moreover, Wiebusch *et al.* demonstrated that MCMV arrests the cell cycle by *de novo* expression of MCMV viral genes [101], therefore it would be worth investigating whether *de novo* expression of M28 can impair SHC1 downstream signaling at later times in the presence of EGF.

Furthermore, PI3K/AKT can modulate other transcriptions factors like AP-1 [125], which is able bind to the promoter region of the MIEP [209] or inhibits other pro-apoptotic BCL-2 family members [210]. This could be an advantage for replication of MCMV in human fibroblasts to

prevent induction of apoptosis in foreign hosts [71, 80]. Moreover, activation of AKT and its phosphorylation leads to a transient induction of the cyclin inhibitor p21^{cip} and progression of cells from G1 to S phase [211]. It is possible that reduced phosphorylation levels of ERK1/2 by M28wt could lead to reduced levels of cyclin D and a cell cycle arrest at early G1 phase before passing the restriction point, which would result in an abortive replication. It is well known that at early G1 phase, the cell cycle is only promoted by mitogens [212], thus indicating that early cell cycle regulation depends on M28 at early time points. Moreover, activation of ERK1/2 can activate nuclear targets such as c-fos or c-myc to promote cell cycle progression [125], which would be supportive for replication in human fibroblasts.

Taken together these findings suggest that the interaction of M28 with SHC1 restricts MCMV replication during cross-species infection in human fibroblasts while preventing SHC1 phosphorylation and further downstream signaling of MAPK/ERK and PI3K/AKT. This mechanism might inhibit apoptosis, IFN-β induction or promote cell cycle regulation early within the G1 phase to promote crossing the species barrier in human fibroblasts.

6.6 Concluding remarks

Cytomegaloviruses are described as strictly species specific viruses with a very narrow host range and normally, CMVs can only replicate in cells of their own or a very closely related host species [20]. Our group has established a system to adapt murine CMV to human epithelial cells and successfully identified new host range determinants. However, we observed that an epithelial cell-adapted MCMV did not completely cross the human species barrier and its replication remained attenuated in human fibroblasts [45, 71, 97].

This study aimed to understand why MCMV adaptation was more restricted in human fibroblasts. Preliminary studies indicated that M28 is an important factor of the species specificity. Therefore, investigating the molecular mechanism of M28 as a potential host range determinant was of particular interest. In the present study, I could identify M28 as a novel host range factor being important for cross-species infection in human fibroblasts. Mutations as well as the complete lack of M28 protein, in addition to mutations in M112+M117, promoted replication in human MRC5 and HFF fibroblasts. M28 was classified as an early protein, demonstrated to be incorporated into the virion, and localized predominantly in the cytoplasm, whilst interacting with two cellular proteins LIMD1 and SHC1. While the impact of the M28-LIMD1 interaction during infection remains unknown, I could show that upon EGFR

stimulation M28 interacts with SHC1 early during infection and consequently prevents its phosphorylation at position Y239/240 and Y317. The diminished phosphorylation of SHC1 restricts further downstream activation of ERK1/2 and AKT, which is detrimental for replication in human fibroblasts. Nevertheless, a transient knockdown of SHC1 in MRC5 cells resulted in impaired replication of M28 deficient virus, thus highlighting SHC1 as pro-viral factor during cross-species infection in human fibroblasts.

In the last 50 years the underlying mechanism of the species specificity of CMV have been not extensively investigated. However, due to emergence of zoonotic viruses like influenza, SARS or Ebola viruses, which pose health risk for the worldwide population, understanding general restricting mechanisms of cross-species infections are of particular interest. Moreover, understanding the molecular mechanism of the species specificity of CMV are of high importance as no suitable mouse model, apart from humanized mice, exist to study HCMV *in vivo*. New insights into the underlying mechanism can be applied to investigate the mechanism restricting HCMV replication in murine cells. The novel findings in this study regarding cross-species infection of MCMV in human fibroblasts, cells in which HCMV is usually propagated in, will help to study HCMV adaptation to murine cells in the future. The potential to study HCMV in mice in the future would generate new possibilities to study antivirals or vaccines against HCMV.

7 Material

7.1 Cell lines and cell culture media

Cell line	Description	Reference/Supplier
10.1	Spontaneously immortalized mouse embryonic fibroblasts from BALB/c mice, defect in p53	[213]
HFF	Primary human foreskin fibroblasts	Prof. Thomas Mertens Institute of Virology, Ulm University Medical Center, Ulm
hTERT-RPE-1 (RPE-1)	Human telomerase reverse transcriptase (hTERT) immortalized human retinal pigmented epithelial cells	ATCC: CRL: 4000
MRC5	Primary human embryonic lung fibroblasts	ATCC: CCL 171
NIH-3T3	Murine embryonal fibroblasts from NIH/Swiss, spontaneously immortalized	ATCC: CRL-1658
Primary MEF	Primary mouse embryonic fibroblasts (MEF) were isolated from 13.5 days old C56BL/6 embryos	Isolation of embryos followed standard procedures described in [97]
SVEC4-10	Murine endothelial cells, immortalized using SV40 large T antigen	ATCC (CRL-2181)
HEK293A	Human embryonic kidney epithelial cells, subclone of 293 cells	Invitrogen (R705-07)

7.1.1 Cell culture media and solutions

Description	Reference/Supplier
SILAC DMEM heavy (R6K6)	DMEM for SILAC + 10 % (v/v) dFCS and 1 % (v/v) penicillin/streptomycin additionally: 84 mg/l L-arginine-$_{13}C_6$, 143 mg/l L-lysine-$_{13}C_6$, 200 mg/l L-proline, 584 mg/l stable L-glutamine sterile filtered
Dulbecco's Modified Eagels Medium (DMEM) with D-Glucose and L-Glutamin	Gibco® Life technologies
Dulbecco's phosphate buffered saline 1x (PBS)	Sigma Aldrich
Fetal bovine serum, dialysed (dFBS)	Thermo Fisher Scientific
Fetal Calf Serum (FCS)	PAN Biotech GmbH
Newborn calf serum (NCS)	Pan Biotech GmbH
OptiMEM-I	Gibco® Life technologies
Penicillin-Streptomycin (10mg/ml)	Sigma Aldrich
Recombinant human EGF (animal free protein)	R&D Systems
SILAC DMEM	Sigma Aldrich
SILAC DMEM light (R0K0)	DMEM for SILAC + 10 % (v/v) dFCS and 1 % (v/v) penicillin/streptomycin additionally: 84 mg/l L-arginine, 143 mg/l L-lysine, 200 mg/l L-proline,584 mg/l stable L-glutamine sterile filtered
Tetracyclin free FCS	Pan Biotech GmbH
Trypsin-EDTA-Solution 1x	Sigma Aldrich -Life Science
Virion purification	
NaPO$_4$-Buffer (0,04 M)	8 mM NaH$_2$PO$_4$•H$_2$O 32 mM Na$_2$HPO$_4$•(H$_2$O)$_2$ pH 7,4
15 % Sodium tartrate	15 % (w/v) Na$_2$Tartrate•(H$_2$O)$_2$ 30 % (v/v) Glycerol in 0,04 M NaPO$_4$-Buffer pH 7,4
35% Sodium Tartrate	35 % (w/v) Na$_2$Tartratet•(H$_2$O)$_2$ in 0,04 M NaPO$_4$-Buffer pH 7,4

7.2 Bacteria and bacteria culture media

Strain	Description	Reference/Supplier
E.*coli* GS1783	DH10B *λ cl*857 Δ (cro-bioA) <>*araC*-PBAD*IScel*	(Tischer et al. 2010)
E.*coli* DH10 B	F- mcrA Δ(mrr-hsdRMS-mcrBC) Φ80dlacZΔM15 ΔlacX74 endA1 recA1 deoR Δ(ara,leu)7697 araD139 galU GalK nupG rpsL λ-	Thermo Fisher Scientific

7.2.1 Bacteria cell culture media

Description	Reference/Supplier
LB-Media 1 % Bacto tryptone 0,5 % Yeast extract 0,5 % NaCl	Roth
LB-Agar-plates 1 % Bacto tryptone, 0,5 % Yeast extract 0,5 % NaCl 15 g/L Agar-Agar	Roth

7.2.2 Antibiotics

Description	Reference/Supplier
Chloramphenicol 15µg/ml	Roth
Kanamycin 50µg/mL	Roth
Penicillin 100ug/mL	Sigma Aldrich
Streptomycin 100µg/mL	Sigma Aldrich
Blasticidin 5µg/mL	Invivogen
Doxycycline 1µg/mL	Biomol
Zeocin	Invivogen

7.3   Viruses

Virus	Description	Reference
MCMV-wt Strain Smith- GFP	Recombinant murine CMV cloned as BAC with an expressing green fluorescent protein (GFP)	[214]
M112-117+M28wt	Recombinant murine CMV cloned as BAC with GFP and mutations in M112 and M117 170 055 C->A	Eléonore Ostermann (unpublished data)
M112-117+ M28fa	Recombinant murine CMV M112-117mut cloned as BAC with GFP and additional mutation in M28 L166Q	[180]
M112-117+ M28fa2	Recombinant murine CMV M112-117mut cloned as BAC with GFP and additional mutation in M28 E300K	constructed in this study
M112-117+M28stop	Recombinant murine CMV M112-117mut cloned as BAC with GFP and additional stop mutation in M28 E18stop	constructed in this study
M112-117+M28wtHA	Recombinant murine CMV M112-117mut cloned as BAC with GFP and C-terminal HA-Tag	[180]
M112-117+M28faHA	Recombinant murine CMV M112-117mut cloned as BAC with GFP and additional mutation in M28 L166Q and C-terminal HA-Tag	[180]

M112-117+M28fa2HA	Recombinant murine CMV M112-117mut cloned as BAC with GFP and additional mutation in M28 E300K and C-terminal HA-Tag	constructed in this study
M112-117+M28h3HA	Recombinant murine CMV M112-117mut cloned as BAC with GFP and additional mutation in M28 G360V and C-terminal HA-Tag	constructed in this study
MCMV-M28wtHA	Recombinant murine CMV cloned as BAC with GFP and a M28 C-terminal HA-tag	[180]
MCMV-M28fa2HA	Recombinant murine CMV cloned as BAC with GFP and additional mutation in M28 E300K and C-terminal HA-Tag	constructed in this study
MCMV-M28stop	Recombinant murine CMV cloned as BAC with GFP and additional stop mutation in M28 E18stop	constructed in this study
MCMV/h1 (GFP)	Spontaneously occurred human adapted MCMV-GFP after 15 days culturing in RPE-1 cells	[71]
MCMV/h3 (GFP)	Spontaneously occurred human adapted MCMV-GFP after 15-21 days culturing in RPE-1 cells	[45]
MCMV/h1-fa (GFP)	Human fibroblast-adapted MCMV/h occurred during IFN-Antibody treatment 14 d.p.i	[45]
MCMV/112-117/fa2 (GFP)	Human fibroblast adapted MCMV/M112mut-117mut-GFP isolated after 4 weeks passaging on MRC5	[180]

MCMV-M45HA (rev)	MCMV Smith pSM3fr-MCK-2fl with reinserted M45 full length ORF including a C-terminal HA tag	[215]
MCMV-m142HA	Recombinant murine CMV cloned as BAC with GFP and with m142 HA-tag	[64]

7.4 Plasmids

Plasmid	Description	Reference/Supplier
pEPKanS	Template plasmid for "en passant" mutagenesis with I-*Sce*I-*aphAI cassette*	[216]
pcDNA3	Plasmid expression vector with CMV promoter and neo and ampicillin resistance	Invitrogen
pcDNA3_M28wt_HA	pCDNA3_M28WT cloned with HindIII and MfeI and C-terminal HA-tag	constructed in this study
pcDNA3_M28fa_HA	pCDNA3_M28fa cloned with HindIII and MfeI and C-terminal HA-tag	constructed in this study
pcDNA3_UL117_HA	pCDNA3_UL117 (HCMV) cloned with HA-tag	Osterman et al. unpublished

7.5 Oligonucleotides

Primer	Sequence	Application
M28mut fw (fa-specific)	GTCATCTCGGAGGACCGCTCGCTAC AGCGGTAGCCAAGCTGCTTTTCTAC GTCGAACGTGTAGGGATAACAGGG TAATCGATTT	*en passant* mutagenesis primer M28 L166Q
M28mut rev (fa-specific)	GATGCCGATAACATCTGTCCCACGTT CGACGTAGAAAAGCAGCTTGGCTAC CGCTGTAGCGCCAGTGTTACAACCA ATTAACC	*en passant* mutagenesis primer M28 L166Q
MCMV_M28mut_fa2_fw	ACCCGTCCGGGCACCACCTGGCCCA ATCTCAAACTCTCTTTATCACCGACC ATGAAATAGCTAGGGATAACAGGGT AATCGATTT	*en passant* mutagenesis primer M28 E300K
MCMV_M28mut_fa2_rev	GTTTATGGGCGAGTTCTTCGGCTATT TCATGGTCGGTGATAAAGAGAGTTT GAGATTGGGCCGCCAGTGTTACAAC CAATTAACC	*en passant* mutagenesis primer M28 E300K
M28_h3mut_fw	GTAGGGCTGCAGGTTGATCCTGAGC CGGTCCCGGAGGAATACCGCTATCG TGTTGGCCACTAGGGATAACAGGGT AATCGATTT	*en passant* mutagenesis primer M28 G360V
M28_h3mut_rev	GCGGCGCCCGCGTCTTGAAGGTGGC CAACACGATAGCGGTATTCCTCCGG GACCGGCTCAGCCAGTGTT ACAACCAATTAACC	*en passant* mutagenesis primer M28 G360V
MCMV_M28stop_fw	AGCTGTCGGTATGCGGATCATCAGC GACGACGACCTCGATTAGGTGTTCC TTCGCGACGATAGGGATAACAGGGT AATCGATTT	*en passant* mutagenesis primer M28 E18stop
MCMV_M28stop_rev	CGACAGGGTCCCCCTGTTCATCGTC GCGAAGGAACACCTAATCGAGGTCG TCGTCGCTGAGCCAGTGTT ACAACCAATTAACC	*en passant* mutagenesis primer M28 E18stop
M28 fw-HA-tag C-terminal	AACTGCAAGAGAGGGGAAAAGCGG TCGATCCCAGCCGTCAAGCGTAGTC TGGGACGTCGTATGGGTATAGGGAT AACAGGGTAATCGATTT	*en passant* mutagenesis primer M28HAtag C-term
M28 rev-HA-tag C-terminal	GGGATAGCCGAGACCTGCGTGCCCA CGCTCGGGTACCCATACGACGTCCC AGACTACGCTTGACGGCTGGGATCG ACCGCGCCAGTGTTACAACCAAT TA	*en passant* mutagenesis primer M28HAtag C-term

Kan rev	CCCGTTGAATATGGCTCAT	Sequencing primer cointegrates *en passant* mutagenesis
M28_pcDNA_HindIII_ fw	TATAAAGCTTATGAGCCTGGAAGCT GTCGG	cloning M28HA
M28_pcDNA_MfeI_ rev	TTAACAATTGTCAAGCGTAGTCTGG GACGT	cloning M28HA

*underlined pEPKanS sequence; all primers were supplied by Life Technologies

siRNAs

Description	Sequence	Reference/Supplier
siGENOME non-targeting SMART pool#2	#1UAAGGCUAUGAAGAGAUAC #2AUGUAUUGGCCUGUAUUAG #3AUGAACGUGAAUUGCUCAA #4UGGUUUACAUGUCGACUAA	Dharmacon/Horizon
siGENOME SHC1 human SMARTpool (6464)	#1CCAAAGACCCUGUGAAUCA #2GAUGAUCCCUCCUAUGUCA #3GAGUUGCGCUUCAAACAAU #4CAGCCGAGUAUGUCGCCUA	Dharmacon/Horizon

7.6 Antibodies

Antigen	Description/ clone	Species	Application	Reference/ Supplier
Primary antibodies				
HA	3F10	Rat	1:1000 (WB) 1:300 (IF)	Roche
HA	16B12	Mouse	1:1000 (WB)	Covance research
HA	Cat.no H 6908	Rabbit	1:1000 (WB)	Santa Cruz
GAPDH	14C10	Rabbit	1:1000 (WB)	Cell Signaling
MCMV IE1	Chroma101	Mouse	1:1000 (WB)	Stipan Jonjic (Univ.of Rijeka)

MCMV E1	Chroma 103	Mouse	1:1000 (WB)	Stipan Jonjic (Univ.of Rijeka)
MCMV gB	HR-MCMV-05	Mouse	1:1000 (WB)	Stipan Jonjic (Copri)
β-actin	Ac-15	Mouse	1:1000 (Wb)	Sigma Aldrich
β-actin	Ac-15	Mouse	1:1000 (Wb)	Sigma Aldrich
AKT		Rabbit	1:1000 (WB)	Cell Signaling
EGFR		Rabbit	1:1000 (WB)	Millipore
ERK1/2	L34F12	Mouse	1:2000 (WB)	Cell Signaling
GAPDH	14C10	Rabbit	1:1000 (WB)	Cell Signaling
HA	3F10	Rat	1:1000 (WB) 1:300 (IF)	Roche
HA	16B12	Mouse	1:1000 (WB)	Covance research
HA	H6908	Rabbit	1:1000 (WB)	Sigma Cruz
LIMD1	E-10	Mouse	1: 3000 (WB) 1:100 (IP)	Santa Cruz
MCMV E1	Chroma 103	Mouse	1:1000 (WB)	Stipan Jonjic (Univ.of Rijeka)
MCMV gB	HR-MCMV-05	Mouse	1:1000 (WB)	Stipan Jonjic (Copri)
MCMV IE1	Chroma101	Mouse	1:1000 (WB)	Stipan Jonjic (Univ.of Rijeka)
Phospho ERK1/2 (Thr202/Tyr204)	E10	Mouse	1:1000 (WB)	Cell Signaling
Phospho SHC1 Y239/240		Rabbit	1:500 (WB)	Cell Signaling
Phospho SHC1 Y317		Rabbit	1:5000 (WB)	Cell Signaling
Phospho Akt S 473		Mouse	1:2000 (WB)	Cell Signaling
Rat-IgG	anti-rat HRP-coupled	Goat	1:3000 (WB) 1:500 (IF)	Jackson Immuno-Research
pRb	G3-245	Mouse	1:500 (WB)	BD Bioscience
SHC1	PG-797	Mouse	1:500 (WB) 1:100 (IP)	Santa Cruz
SHC1	30/SHC	Mouse	1:1000 (WB)	BD Bioscience

M45		Mouse	1:50	Stipan Jonjic (Univ.of Rijeka)
Secondary antibodies				
Mouse IgG-light chain	anti-mouse HRP light chain	Goat	1:3000 (WB)	Jackson ImmunoResearch
Mouse-IgG	anti-rat HRP-coupled	Goat	1:5000 (WB)	Dako
Mouse-IgG	anti-mouse HRP-coupled	Goat	1:3000 (WB)	Jackson ImmunoResearch
Rabbit IgG	anti-rabbit HRP-coupled	Goat	1:3000 (WB)	Jackson ImmunoResearch
Rabbit IgG-light chain	Anti-rabbit HRP light chain	Goat	1:3000 (WB)	Jackson ImmunoResearch
Rabbit-IgG	anti-rabbit HRP-coupled	Goat	1:5000 (WB)	DAKO
Rat IgG	anti-rat AlexaFlour 555-coupled	Goat	1:500 (IF)	Life technologies
Mouse IgG	anti-mouse AlexaFlour 647-coupled	Goat	1:500 (Flow cytometry)	Life technologies

7.7 Enzymes

Description	Reference/Supplier
Dream Taq Green DNA Polymerase	Thermo Fisher Scientific
Fast alkaline phosphatase	Thermo Fisher Scientific
Fast Digest restriction enzymes (10U/µl)	Thermo Fisher Scientific
PRECISIOR High Fidelity DNA Polymerase	BioCat
Proteinase K	Thermo Fisher Scientific
RevertAid H Minus Reverse Transcriptase	Thermo Fisher Scientific
RNAse A	Applichem
T4-DNA-Ligase and buffer	Thermo Fisher Scientific
TURBO™ DNase	Ambion Life Technologies

7.8 Marker

Description	Reference/Supplier
PageRuler™ Prestained Protein Ladder	Thermo Fisher Scientific
Generuler™ 1kb DNA Ladder	Thermo Fisher Scientific

7.9 SILAC-reagents

Description	Reference/Supplier
L-arginine	Sigma-Aldrich
L-arginine-$^{13}C_6$	Sigma-Aldrich
L-lysine	Sigma-Aldrich
L-lysine-$^{13}C_6$	Sigma-Aldrich
Proline	Sigma-Aldrich
stable L-glutamine	Sigma-Aldrich

7.10 Kits

Description	Reference
BCA Protein Assay	Thermo Fisher Scientific
complete™mini, EDTA-free Protease Inhibitor cocktail	Roche
dNTP-Mix	Promega
ECL Western Detection Reagents	Amersham Biosciences
HA-affinity Matrix-rat covalent 3F10	Roche
Hiperfect	Qiagen
Innuprep DNA- Mini Kit	Analytic Jena
Lumigen TMA-6	Bioquote
NucleoBond Gel and PCR Clean-up	Macherey-Nagel
NucleoBond Xtra Midi	Macherey-Nagel
Polyfect	Qiagen
protein G or A agarose beads	Roche
Whatman® gel blotting paper, grade GB003	Sigma-Aldrich

7.11 Buffer and Solutions

Description	
TE9 buffer	50 mM Tris 20 mM EDTA pH 9.0 10 mM NaCl
BAC DNA extraction (Mini-Prep) S1-Buffer S2-Buffer S3-Buffer Tris elution buffer	50 mM Tris, 10 mM EDTA, 100 µg/ml RNase A, pH 8.0 200 mM NaOH, 1 % (v/v) SDS 2,8 M KAc pH 5,1 with AcOH 10mM Tris pH 8.5
Agarose Gelelectrophoresis Agarose gels TAE buffer TBE buffer	1% or 0,6% Agarose in TBE or TAE buffer 2 M Tris, 50 mM EDTA, 5,7% AcOH, pH 8,0 445 mM Tris, 20 mM EDTA, 445 mM Borat pH 8,0
SDS-Polyacrylamide gel electrophoresis (SDS-PAGE) Gel buffer 4x Laemmli loading buffer Anode buffer Cathode buffer RIPA lysis buffer	3M Tris-HCL pH 8.45 0.3% SDS 0,3 M Tris pH 6,8 12 % SDS 40 % Glycerol 0,02 % Bromophenolblue 20% ß-Mercaptoethanol 1M Tris-HCL pH 8,9 1M Tris-HCL 1M Tricine 1%SDS 50 mM Tris 150 mM NaCl 1 % Triton X-100 0,1 % SDS 1 % Deoxycholat

NP-40 (500mL)	50M Tris pH7,5 150M NaCl 1% NP-40
Western Blot Transfer buffer	50mM Tris 40mM Glycine 0.04% SDS 20% Methanol
TBS-Tween buffer (10x) Blocking buffer milk or BSA in TBS-T	100mM Tris 1.5 M NaCl pH7.5 1.5% Tween20 4% milk or 4% BSA in TBS-T-buffer
Immunoprecipitation minimal washing buffer (sterile filtered for SILAC samples) SILAC sample buffer (sterile filtered)	50 mM Tris 150 mM NaCl 50 mM Tris 150 mM NaCl 1 % (v/v) SDS
IP-Washing buffer #1 IP-Washing buffer #2 IP-Washing buffer #3	50 mM Tris*-HCl, pH 7.5; 150 mM sodium chloride; 1% Nonidet P40*; 0.5% sodium deoxycholate; 1 tablet complete protein inhibitor cocktail/50 ml 50 mM Tris*-HCl, pH 7.5; 500 mM sodium chloride; 0.1% Nonidet 40*; 0.05% sodium deoxycholate 50 mM Tris*-HCl, pH 7.5; 0.1% Nonidet P40*; 0.05% sodium deoxycholate

Immunoflourescence	
Fixation	4%PFA in PBS pH7,5
Aldehyde blocking	50mM NH$_4$Cl in PBS
Permeabilization	0.3% Trition x-100 in PBS
Blocking buffer	0.2% Gelatine in PBS
Flow cytometry	
PI (propidium iodide) solution	1mg/mL PI containing ribonuclease and Triton X-100

7.12 Chemicals

Description	Reference/Supplier
Actinomycin D	Sigma
Borat	Roth
Bromphenolblue	Roth
Chloroform	Roth
Cycloheximide (CHX)	Sigma
DAPI	Sigma Aldrich
Deoxycholat	Roth
Draq5	BioStatu Limeted
Ethidiumbromide	Serva
Gelatine	Merck
Glycerine	Roth
L- (+) Arabinose	Sigma- Aldrich
LE Agarose	Biozym
Leptomycin B	Sigma Aldrich
LY294002	Cell Signaling
Methanol	Roth
N, N, N', N' –Tetramethylendiamin (TEMED)	Roth
Paraformaldehyd	Roth
Phenol	Roth
Phosphonoacetic acid (PAA)	Sigma
Polyfect Transfection Agent	Qiagen
Protease inhibitor Aprotinin	Sigma-Aldrich
Protease inhibitor Leupeptin	Sigma

Protease inhibitor Pefablock	Sigma
Rothiphorese Gel 30 (37.5:1) (acrylamide:bisacrylamide)	Roth
SDS	Roth
β-Mercaptoethanol	Roth
Tris	Sigma
Triton X-100	Roth
Tween20	Roth
U0126	Cell signaling

7.13 Equipment and special material

Description	Reference/Supplier
Axiovert 40 CFL Fluorescence-Microscope HXP 120 C	Zeiss
BD FACS CANTO II	BD Bioscience
Beckmann ultracentrifuge L-70	Beckmann
Centrifuge 5415D	Eppendorf
Centrifuge 5415R	Eppendorf
Electroporation cuvettes	Eurogentec
Equipment	
FLUOstar Omega	BMG LABTECH
Fusion Sl-4 3500 Wl molecular imaging	Peqlab
Gel doc XR+ system	BioRad
Gene Pulser Xcell	BioRad
Hybond ECL/Nitrocellulose Membrane	GE Healthcare
NanoDrop ND-1000 Spectrometer	Peqlab
Nicodenze	Axa-Shield
Nikon A1 confocal laser scanning microscope (cLSM)	Nikon
Nikon C2$^+$ confocal microscope	Nikon
pH-meter 211	Hanna Instruments
Primo Vert Microscope	Zeiss
Shaking incubator HT (bacteria)	Infors

Sorvall RC 6+ Zentrifuge	Thermo Fisher Scientific
TC20™ automated cell counter	BioRad
Thermomixer comfort 555	Eppendorf
Trans-Blot turbo transfer system	BioRad
Whatman paper	Roth
Zeiss LSM510 META/FCS	Zeiss

8 Methods

8.1 Cell culture and virology methods

8.1.1 Cell culture

All cell lines as well as primary cells were cultured in Dulbecco's modified Eagle's media (DMEM) supplemented with 5 or 10% fetal calf serum (FCS) or 10% newborn calf serum (NCS) and 1% penicillin/streptomycin. Cells were incubated at 37°C, 80% humidity and 5% CO_2 and passaged once they reached 80% confluence. Therefore, cells were first washed with prewarmed phosphate buffered saline (PBS) before adding 2-3ml Trypsin/EDTA in order to detach adherent cells from the culture plate. Once the monolayer was detached, cells were resuspended with appropriate volume of fresh DMEM, supplemented with serum, to inactivate trypsin and splitted according to their replication properties. In order to seed cells, 10μl of resuspended cells were counted and the appropriate volume of cells was added to fresh culture media (cell counter TC10, BioRad). All cell culture procedures were performed under sterile conditions using a sterile bench (HeraSafe, Heraeus).

8.1.2 Thawing and freezing of cells

In order to freeze cells, a confluent monolayer of one plate (145mm^2) was trypsinized, resuspended in 10ml completed DMEM and cells were pelleted (5min, 500g at RT). The cell pellet was washed and resuspended in 3ml FCS containing 10% DMSO and transferred into 3 cryotubes for short term storage at -80°C or long-term storage at -196°C (liquid nitrogen). Cells were thawed using a water bath at 37°C and were immediately transferred in 15ml tubes with 10ml of prewarmed growth media, followed by a centrifugation step (5min, 200g at 37°C) to remove residual DMSO. Afterwards, cells were resuspended with 10ml of prewarmed DMEM and seeded in a 100mm^2 culture dish. When cells were attached to the culture plate, media was replaced by fresh media.

8.1.3 Stable isotope labelling with amino acids of cell culture (SILAC)

In order to identify specific interaction partners of proteins of interest, a SILAC based affinity purification and mass spectrometry (AP-MS) approach was used. The technique is based on the different labelling of mammalian cell cultures with heavy and light amino acid isotopes by using specialized media. The different labelling with heavy isotopes ensures a difference in

97

mass detectable in the spectrometer. This allows identification of specific interaction partners when different conditions are compared. In this study infected cells with non-tagged MCMV-M28wt were compared to tagged MCMV-M28wtHA. Therefore, NIH-3T3 or HFF cells were cultured for at least 8 passages, in SILAC DMEM+ 10% dialysed FCS containing heavy labelled $^{13}C_6$ L-arginine, $^{13}C_6$ L-lysine and unlabelled proline, to ensure 97% of incorporation of labelled amino-acid during protein turnover. The corresponding light culture was supplemented with light L-arginine, L-lysine and proline. Afterwards, cells (heavy and light) were seeded $3x10^5$ cells/well (NIH-3T3) or $1x10^5$ (HFF) (6-well) and were infected with either MCMV-M28wt or MCMV-M28wtHA using centrifugal enhancement (1500g, 30min at 37°C). To reduced false negative and positive results a so-called label-switch was performed, meaning heavy and light cultures were once infected with the tagged or non-tagged virus respectively, each in duplicates.

8.1.4 Transfection of cells with plasmid DNA

To transfect plasmid DNA, cells were seeded $3x10^5$ per well (6-well) or x 10^6 cells per $100mm^2$ dishes and transfected with 1-3µg DNA using Lipofectamine (Thermo Fisher Scientific) according to the manufacture's protocol. Therefore, 1-3µg DNA was diluted in 100µl of OptiMEM and incubated for 10min at RT. In parallel 100µl OptiMEM were incubated with 10µl Lipofectamine. Afterwards, samples were pooled, slightly vortexed and incubated for additional 20min at RT. Afterwards, the mixture was gently added to the cells. Transfected cells were incubated at least for 24-48h before harvesting.

8.1.5 Transfection of cells with siRNA

To establish a transient knockdown of cells the principle of RNA-interference using small interfering RNA (siRNA) was employed. A complementary sequence of the target gene was designed, which couples with mRNA and therefore prevents expression of messenger RNAs (mRNAs) [217]. With this technique expression of specific genes can be transiently and efficiently downregulated. To improve efficient silencing of the target gene, a pool of 4 different siRNAs was used (Dharmacon). In addition, scramble siRNA with an unspecific target was applied to ensure no off- target effect as well as using an appropriate control system. For this purpose, siRNA was transfected using the transfection kit Hiperfect (Qiagen) according to the manufacture's protocol. First of all, suitable concentrations of siRNA were tested in

Western blot. This ensures efficient silencing of the gene while keeping siRNA-concentration as low as possible. After selection of the suitable concentration 30nM of siRNA was diluted in the total volume of 100μl DMEM and vortexed for 5s. Afterwards, 6μl of Hiperfect was added to the solution, vortexed again for 10s and incubated for 10min at RT. Meanwhile, cells were trypsinized and seeded with a density of $0,8x10^5$ per well (12-well). siRNA mixtures were added to a total volume of 1100μl cell suspension, immediately after seeding.

8.1.6   Transfection of BAC-DNA and virus reconstitution

To reconstitute MCMV from BAC-DNA, $1,5 x10^5$ murine 10.1 cells were seeded on a 6-well plate and transfected the next day with 3μg fresh BAC-DNA using Polyfect (Qiagen) according to the manufacture's protocol. By using the transfection reagent Polyfect, DNA binds to the reagent and forms complexes, which can enter the cells. BAC-DNA was mixed with 100μL non-supplemented DMEM incubated for 5 min at RT. Afterwards, 10μL Polyfect was added to the mixture followed by an additional incubation step for 20min at RT. 500μL DMEM was added to the mixture and gently transferred to the cells. Virus reconstitution was monitored for the next 3-7 days. When small foci and a cytopathic effect could be observed, cells were splitted and further expanded. The virus reconstitution was completed after 14 days and virus supernatant was harvested for a virus stock.

8.1.7   Preparation of virus stocks

For the preparation of a MCMV virus stocks, 5-10 plates ($145mm^2$) with $2x10^6$ cells (10.1 cells) were infected with a multiplicity of infection (MOI) of 0.025 $TCID_{50}$/cell and incubated for 6-8 days. 3- and 6-days post infection virus supernatant was collected, and cell debris removed by centrifugation (15min, 6000g at 4°C). Afterwards, the infectious supernatant was transferred into a new 250ml tube and centrifuged again (4h, 27000g at 4°C). After centrifugation, supernatant was discarded, and the virus pellet was resuspended in 300μl of DMEM (10% FCS or w/o FCS) overnight at 4 °C. The next day, the pellet was resuspended in 2mL DMEM and additionally purified by adding 18mL PBS with 10% nicodenze. After resuspension, the virus solution was additionally ultra-centrifuged at 27000rpm for 90min at 4°C (Beckmann Ultracentrifuge, rotor 70Ti). The residual pellet was resuspended in 300μL DMEM with optional FCS and incubated overnight at 4°C. Next day, the virus pellet was resuspended, aliquoted and stored at – 80°C.

8.1.8   Gradient purification of virions

First, a virus stock of 10-15 dishes ($15cm^2$) was prepared and viral supernatant was collected at day 5-6 when infected cells showed a clear cytopathic effect. $5x10^5$ cells were lysed using RIPA buffer and collected for further analysis and stored at -20°C. In a second step, cells and cell debris from the virus stock supernatant were removed by centrifugation for 15min 6000g 4°C. Afterwards, virus particles were pelleted from supernatant in a precooled centrifuge 27000 rpm for 90min at 4°C (Beckmann, rotor 70Ti). Afterwards, the residual supernatant was removed and resuspended with 250µl 0,04M sodium phosphate buffer overnight at 4°C and then filled up to 2mL with the same buffer. To ensure sufficient resuspension of the viral particle solution, the complete volume was resuspended again by pipetting up and down for at least 30 times. Afterwards, fresh gradients were prepared using 15% sodium/glycerol tartrate and 30% sodium tartrate solution. Both solutions were mixed with a standard gradient maker with constant circulation of both chambers using a magnetic field. The solution was collected in semi-soft Beckmann centrifugal tubes via a thin plastic tube. The freshly prepared gradient was immediately used and 2mL of the viral particle solution was gently layered on top of the gradient by avoiding any drops. The prepared gradient with the overlayered virus suspension was centrifuged without brake at 23000rmp for 45min at 10°C (Beckmann, Swinging rotor SW41Ti). After centrifugation the middle band of the gradient containing the virions was aspirated with a syringe and transferred to a new tube. The suspension containing the virions was resuspended in 18mL PBS and pelleted again for 60min at 23000rpm at 4°C. The pelleted virions were lysed in RIPA buffer for 15min and protein concentration was measured (BCA) including the lysed samples. Equal protein concentration was analysed via SDS-PAGE and Western Blot.

8.1.9   Infection of cells and virus quantification

To determine viral replication and the quantification of infectious particles, the tissue culture infectious dose ($TCID_{50}$), calculated by the Spearman-Karber method, was used [218] . The $TCID_{50}$ is described as a dilution of virus particles, which are required to infect 50% of a defined number of cells. Therefore, $2x10^3$ 10.1 cells per well were seeded in a 96-well plate with 10% DMEM+ 10% FCS. The cells were infected with 100µl of a logarithmic serial dilution 10^3-10^{10} in triplicates with and without centrifugal enhancement (30min, 1000g at 37°C) [219]. The

infected cells were monitored 6-7 days post infection and the number of wells, showing a cytopathic effect was counted for each dilution and $TCID_{50}$ was calculated.

For infection experiments, cells were infected by using a defined multiplicity of infection (MOI) based on the infectious titer of a virus stock ($TCID_{50}$/mL). By using the following equation, the defined volume of virus stock was defined and added to the cells.

$$\frac{(\text{number of cells}) \times \text{MOI}}{\text{TCID50/mL}} = \text{volume of virus stock in mL}$$

8.1.10 Viral replication kinetics

To investigate different replication properties of viruses, for instance in different cell types, viral replication kinetics were performed. To perform a growth kinetic at low MOI (0.1-0.2 $TCID_{50}$/cell), 1.5 x10^5 cells/well were seeded in a 6-well plate and inoculated with the appropriate dose of virus without centrifugal enhancement. All virus replication kinetics were done in triplicates. 4 hours post infection viruses entered the cells. Virus inoculum was removed by washing 1x with PBS and fresh completed DMEM was added to the cells. The initial virus input and the virus supernatant were collected and determined every second day via the $TCID_{50}$ method. The viral replication kinetics were monitored for 7-14 days p.i..

8.2 Molecular Methods

8.2.1 Preparation of electro competent bacteria

For preparation of electro competent bacteria 200ml of LB-Media, supplemented with appropriate antibiotics, was inoculated with 5-10ml (overnight culture) of E.*coli* and incubated at 30°C (GS1783) or 37°C (DH10B) with constant shaking. If not differently clarified, all constant shaking steps were proceeded at 160rpm using a HR shaking incubator. When the bacteria culture reached the exponential phase at OD_{600} of 0.5-0.6, they were immediately cooled on ice for 20min. While bacteria GS1783 were heat shocked (shaking) at 42°C for 15min to induce the expression of Red genes, DH10B were further proceeded without heat shock. After the cooling step, cells were centrifuged (10min, 5000g at 4°C). The pellets were washed with 100ml sterile dH_2O and centrifuged again, followed by an additional washing step with dH_2O. The pellets were centrifuged again, resuspended in 10ml cold and sterile 10% glycerol

and centrifuged (10min, 5000g at 4°C). The resulting pellet was resuspended in 1.2ml cold sterile 10% glycerol, aliquoted and frozen at -80°C.

8.2.2 Transformation of electrocompetent bacteria

In order to introduce DNA into bacteria they were transformed via electroporation. Therefore, 50µL of frozen electrocompetent bacteria were thawed on ice and incubated for 10min on ice with 2-4 µl of ligation product or 100-200ng of linear PCR product. Afterwards, bacteria were transferred to 2mm electroporation cuvettes and pulsed with 2000V 25 µF and 200 Ω. Immediately after, pulsed bacteria were transferred in 1ml prewarmed LB-media to a fresh tube and incubated at 30 or 37°C with constant shaking for 1h. Cultured bacteria were then pelleted, resuspended in 200µl LB-media, plated and incubated for 24- 32 hours at 30°C (GS1783) or 37°C (DH10B).

8.2.3 Cloning of pcDNA-M28wt-HA

To investigate M28 protein expression in uninfected cells, a plasmid inserted with the gene region of M28, including a C-terminal HA-Tag, was constructed. Therefore, the mammalian expression vector pcDNA3 was used. A PCR product was generated by using specific primers, including a restriction site for XhoI and MfeI, using BAC-MCMV-M28wtHA as a template. The PCR-amplified M28-insert was ligated using a T4-Ligase from Thermo Fisher Scientific in the ration 1:5 to vector in a total volume of 20µL, according to the manufacturer's protocol. After ligation, 4µL of the ligated construct was transformed into electro-competent DH10B bacteria and plated on agar-plates containing ampicillin. Positive clones were selected and screened via restriction analysis and Sanger sequencing.

8.2.4 Extraction of plasmid DNA (mini-Prep)

Plasmid DNA was isolated from 5mL of LB-media containing the indicated bacteria by using a mini-Plasmid extraction Kit (Macherey-Nagel). 4ml of overnight bacteria culture was pelleted and proceeded according to the manufacturer's protocol. 1mL of mini-DNA culture was kept for inoculation of a midi-culture. Plasmid DNA was eluted in 30µl EL-buffer.

8.2.5 Extraction of BAC-DNA (mini-Prep)

In order to extract BAC-DNA the principle of alkaline lyses was used. 5mL of LB-Media with the suitableappropriate antibiotic was inoculated with a single picked colony and incubated

overnight at 30°C with constant shaking. 4mL of the overnight culture was centrifuged (1min, 6000g at 4°C). Afterwards, the bacteria pellet was resuspended in 300µl S1 buffer. After resuspension, the bacteria were lysed with 300µl S2 buffer, inverted and incubated for 3-4min at RT. 300µl of S3-buffer was added and the sample was incubated for 8min on ice to precipitate proteins and bacterial chromosomal DNA. The neutralization was followed by a centrifugation step (20min, 11000g at 4°C) to pellet precipitated proteins. Afterwards, 800µl of the supernatant containing the BAC-DNA was transferred to fresh tubes and BAC-DNA was precipitated by using 640µl of isopropanol followed by additional centrifugation (30min 1500g at 4°C). Supernatant was removed and the BAC-DNA pellet was washed two times with 500µl of 70% Ethanol. The extraction was completed by removing residual Ethanol and drying the DNA pellet at RT. Finally, the DNA pellet was resolved in 50µl 10mM Tris pH 8.0 or TE buffer at 37°C with 1h constant shaking (Thermomixer 300rmp) or incubated overnight at 4°C.

8.2.6 Extraction of plasmid DNA or BAC-DNA (midi-Prep)

In order to extract BAC or plasmid DNA for larger scales, 200ml of LB-Media, and suitable antibiotics, were inoculated with 50µl of bacteria culture (mini-prep) and incubated overnight at 30°C or 37°C with constant shaking. The extraction of DNA was performed according to the manufacturer's manual with the NucleoBond Midi Xtra Kit (Macherey-Nagel). DNA was eluted in 150µl 10mM Tris pH 8.0 or TE buffer and incubated for 1h at 37°C with constant shaking or at incubated at 4°C overnight.

8.2.7 Storage of bacteria

For long time storage of bacteria containing BACs or plasmids, 700µL of bacteria culture was mixed with 300µL 86% Glycerol (v/v) and stored at -80°C.

8.2.8 Polymerase chain reaction (PCR)

PCR was performed by using either Dream Taq polymerase or Precisor polymerase according to the manufacturer's protocol. Dream Taq polymerase was only used for BAC mutagenesis and Precisor DNA Polymerase was used for amplification before sequencing or cloning purposes. The general PCR set up and cycle parameters are described below.

Reagent	volume
5xGC-buffer	10μL
dNTPs	0,75μL
Template	10-50ng
Primers (20μL)	2μL
DNA Polymerase	1μL
DMSO (optional)	1,5μL
ddH$_2$O	up to 50μL

Standard cycling condition

Cycling step	Temperature	Time	Number of cycle(s)
Initial denaturation	98°C	2min	1
Denaturation	98°C	30s	
Annealing	2-5°C lower than Tm of primer	30s	35x
Extension	72°C	30s/kb	
Final extension	72°C	5min	1
Cooling	4°C	∞	

8.2.9   Restriction digestion of DNA

BAC or plasmid DNA of interest was analyzed by using restriction digestion with suitable fast digest enzymes according to manufacturer's protocol (Thermo Fisher Scientific). To analyze BAC DNA, 1-2μg DNA was digested for 1h at 37°C and analyzed on a TBE-gel overnight at 40V. In order to analyze plasmid DNA, 1μg DNA was digested for 20min at 37°C and analyzed on an agarose gel. For prior ligation, vector DNA was treated additionally with 1μL Fast Alkaline Phosphatase (AP) according to the guidelines of Thermo Fisher Scientific.

8.2.10   DNA Gel electrophoreses and BAC-Gels

PCR products and digested BAC or plasmid DNA was analyzed on a 1% or TAE or 0,75% (w/v) TBE agarose gel. TAE gels were run for 1h at 120V and TBE gels were run overnight. at 40V, containing 0.5 μg/mL ethidium bromide, respectively. To analyze the size of expected bands 10μl O'GeneRuler (Thermo Fisher Scientific) was used as a standard. Furthermore, bands of

interest were either documented by using an UV transilluminator (GelDoc XR+ BioRad system) or bands were cut out under UV light for purification.

8.2.11 Purification and quantification of DNA fragments

In order to extract DNA fragments from an agarose gel, bands of interest were cut out from the gel. Samples were purified according to the manufacturer's protocol using the NucleoSpin and PCR clean up Kit (Macherey-Nagel). Purified DNA was eluted in 30-50µl TE buffer. Concentration and quality were determined by using the photometer NanoDrop 1000 (Peqlab). The measurement was performed at 260nm and the purity of DNA was determined by the ratio of OD_{260}/OD_{280}. Extracted DNA was stored at 4°C or for long time storage at -20°C.

8.2.12 DNA sequencing

PCR fragments or plasmid DNA were Sanger sequenced by the company Seqlab Microsynth GmbH, Göttingen. For sequencing of lager DNA constructs and BACs, next generation sequencing was performed and analyzed in collaboration with the Research department Prof. Adam Grundhoff (Illumina mySeq).

8.2.13 en-passant BAC mutagenesis

In order to generate recombinant MCMV-BAC mutants, en-passant mutagenesis was performed to introduce specific single nucleotide polymorphisms (SNP) or tags. The principle is based on the insertion of a linear stranded DNA fragment, containing a I-Sce-I-aphAI-cassette, the homologues regions of the gene of interest with the mutation or tag, into a BAC [216]. This method was used because the principle cloning techniques, like restriction and ligation cannot be applied to large DNA constructs such as BACs. The recombination method is based on the Red recombination system. First the target sequence is inserted via homologues recombination followed by cleavage of a marker cassette in the second recombination by the endonuclease SceI. To introduce an HA-tag or point mutations, a pair of mutagenesis primers was designed with 50bp including flanking regions, a sequence duplication and followed by the marker cassette sequence. The target sequence was amplified by PCR using as a template pEPKanS plasmid. The PCR product was digested for 20min at 37°C with DpnI and purified from a TAE-agarose gel using the PCR-clean up kit (Macherey-Nagel).

150ng of the purified sequence was transformed into electrocompetent bacteria GS1783, which harbored already a BAC with either MCMV-wt (GFP) or M112-117+M28wt (GFP). Transformation was performed as described in (8.2.2). Afterwards, bacteria were plated on kanamycin and chloramphenicol agar plates and incubated for 32- 48 hours at 37°C. Single clones were picked and incubated overnight at 37°C in 5mL LB-culture supplemented with chloramphenicol and kanamycin. BAC-DNA was purified according to the protocol described in (8.2.5). Clones were digested with appropriate restriction enzymes and analyzed on a 0.7% TBE BAC gel or via analytical PCR. In a second recombination step positive clones were incubated for 2h in LB-Medium + chloramphenicol/kanamycin and then further cultured for an additional hour after adding 2% (w/v) L-arabinose to induce the SceI-endonuclease. Afterwards, bacteria were transfer to a water bath at 42°C for 20min, with constant shaking, to induce the expression of Red genes. The resulting cleavage of the I-SceI sites results in a new substrate for a second Red recombination. Afterwards, bacteria cultures were transferred back to incubation at 30°C and constant shaking until the OD reached 0.5-06. Bacteria were plated on agar plates, containing only chloramphenicol and 1% L-arabinose, and incubated for 24 hours at 30 °C. Positive clones were screened again using restriction analysis and sequencing to ensure the introduction of the specific point mutations or HA-tags. Positive clones were used to prepare a midi-prep and a subsequent BAC transfection to prepare a virus stock. To ensure that additional mutations were not introduced during BAC-mutagenesis, sequences of MCMV-mutants were analyzed via NGS.

8.3 Protein biochemistry methods

8.3.1 Preparation of cell lysates

In order to prepare cell lysates to analyze proteins via immunoblotting, cells were washed 1x PBS and lysed in 100-200μL 2x laemmli-buffer per well (6-well plate). Afterwards, samples were incubated at 95°C for 10min and transferred for storage at -20°C or directly used for SDS-PAGE. For IP-experiments or to determine protein concentration via a BCA standard, cells were lysed for 15min on ice with RIPA or NP-40 buffer + protease inhibitors. Afterwards, samples were centrifuged to remove cell debris at 4°C for 15min at 11000g. The supernatant containing the proteins was collected. To determine the protein concentration of samples, a BCA assay was performed according to manufacturer's protocol (Thermo Fisher Scientific). Finally, protein concentration was measured via an ELISA omega reader at 562nm absorbance.

To ensure that all samples contain the same amount of protein, RIPA or NP-40 buffer was added to adjust the concentration. 4x laemmli buffer was added to the sample which was then incubated at 95°C for 10min and stored at -20°C or directly used for SDS-PAGE.

8.3.2   (Co-) Immunoprecipitation (Co-IP)

Potential interaction partners of a protein of interest can be investigated via the principle of Co-immunoprecipitation. The principal is based on the binding of an agarose-coupled protein A or G, which binds to a specific antibody, that again binds the protein of interest and its potential interaction partners. First of all, cells were seeded in a 6-well (2-3x10^5 cells per well) and either transfected or infected with HA-tagged M28-MCMV mutants. After 24 hours cells were 1x washed with PBS and then harvested with 160μL NP-40+ cOmplete mini EDTA free protease inhibitor tablets using a cell scraper. Cell lysates were incubated for 15min on ice and then centrifuged to remove cell debris (15min 11000g 4°C). Afterwards, the supernatant containing the proteins was transferred to a fresh 1,5mL tube. 100μL was used to prepare lysate/input controls with 4x Laemmli buffer. The lysate control was incubated at 95°C for 10min and stored at -20°C. The residual 900μL of lysate were first precleared with 20μL protein A or G agarose beads for 60min at 4°C at a rotating platform. This avoids any unspecific binding to the beads. After preclearing, beads were pelleted 30s full speed and supernatant, containing the proteins, was transferred to a fresh tube. Next, the specific antibody against the protein of interest was added to the lysate (mouse/rabbit- HA 1:300) and incubated overnight at 4°C on a rotating platform. After binding of proteins to the antibody, suitable agarose beads were added to the lysate to affinity purify the tagged protein. Afterwards, samples were incubated for additional 2h at 4°C rotating. Next, beads were washed 3x with IP-buffer #1, 2x IP-buffer #2 and 1x IP-buffer #3 with reducing salt concentrations to prepare the elution. After the last washing step, the whole liquid was removed using a fine tip and 120μL of 1x Laemmli buffer was added to the dried beads. To disrupt the binding of beads from the antibody, lysates were incubated for 8min at 95°C. Samples were centrifuges for 30s at full speed to pellet residual beads. Finally, supernatant was transferred to fresh tubes, stored at -20°C or directly used for SDS-PAGE and Western blot.

8.3.3 IP sample preparation for SILAC-mass spectrometry

To prepare samples for SILAC- based affinity purification and mass spectrometry (AP-MS), one set of heavy and light labeled cells were seeded in a 6-well plate with 1-3x10^5 cells per well. Each set of heavy or light cell cultures were infected with MCMV-M28wt or MCMV-M28wtHA, respectively. In all steps, only disposable pipettes and stuffed dips, as well as filtrated buffers were used. The preparation partially differed from the standard protocol. The protein concentration was determined via BCA-assay and the pull down of the M28 protein was performed by using 70µL HA-covalent coupled beads (Roche HA-affinity matrix 3F10). All washing steps were performed using 3x minimal washing buffer. Cell lysates were added with 2x Laemmli buffer following an incubation step for 10 min at 95°C. 10µl of the lysate control as well as 20µL of the IP-sample was kept for a control via SDS-PAGE and Western blot. Heavy and light samples were mixed in the ration 1:1 and stored at -80°C before shipment. All steps of affinity purification and mass spectrometry (AP-MS) analysis were performed in collaboration with Prof. Albert Stickman's group, Stefan Loroch ,at ISAS (Dortmund, Germany).

8.3.4 SDS-PAGE

Protein samples were harvested as described above and analyzed via SDS-PAGE. First, protein samples and a protein ladder (Thermo Fisher Scientific) were concentrated on a 4% stacking gel at 60V for 35min and then separated at 80V for 4h on a 10% resolving gel. If necessary, the SDS-PAGE was cooled on ice. Afterwards, separated proteins were further processed via Western blot (8.3.5). For all SDS-PAGEs the Mini-PROTEAN Tetra Cell-System, (Bio Rad) was used.

<u>10% Resolving Gel</u>

30% Acrylamide (Rotiphorese-Gel 30)	3.3 ml
Gel buffer	3.0 ml
dH2O	1.0 ml
50% Glycerol	2.5 ml
10% APS (Ammoniumpersulfate)	50 µl
TEMED (N,N,N',N'-Tetramethylethylendiamin)	20 µl

4 % Stacking Gel

30% Acrylamide (Rotiphorese-Gel 30)	0.67 ml
Gel buffer	0.67 ml
dH2O	3.67 ml
10% APS (Ammoniumpersulfate)	40 µl
TEMED (N,N,N',N'-Tetramethylethylendiamin)	10 µl

8.3.5 Western blot (semi-dry)

After separation of proteins by SDS-PAGE, SDS-Gels containing the proteins were transferred to a nitrocellulose membrane in order to visualize them later via chemiluminescence. Therefore, 4 pieces of whatman paper were soaked with transfer buffer and were mounted on a cathode of a Trans-Turbo-Blot (BioRad). First two layers of whatman paper were placed on the cathode followed up by a layer of nitrocellulose membrane. The nitrocellulose membrane and also the gel were previously incubated for 3min in transfer buffer. The incubated gel containing the proteins was transferred on top of the membrane and layered with 2 additional soaked pieces of Whatman paper. Residual bubbles or air were removed by rolling the stack before closing the chamber with the anode lid. Proteins were transferred for 60-75min at 2 mA/cm^2. Afterwards, the membrane was washed 1x with TBS-T buffer and blocked with either 4% milk or 4% BSA in TBS-T for 30min at RT. After blocking, the membrane was incubated with the primary antibody against the protein of interest at 4°C overnight, while constantly shaking. Next day, the membrane was rinsed 3x and washed 3x 10min in TBS-T followed by incubation with an HRP-coupled secondary antibody for 1h RT. The membrane was washed again 3x to remove residual antibodies. After all washing steps, the membrane was incubated with 800mL of ECL-solution (Thermo Fisher Scientific) in the dark for 5min at RT. Detection of proteins was performed using a film machine (GE) and x-Ray films or Fusion SL-4 3500WL Molecular Imaging.

8.3.6 Mass spectrometry analysis of SILAC IP samples

The following steps including (8.3.6, 8.3.7) were performed by our collaboration partner Stefan Loroch at ISAS in Dortmund. The detailed and following procedure is cited and described in [97]. Cysteines were reduced in the presence of 10 mM DTT for 30 min at 56°C and alkylated using 20 mM IAA for 30 min at RT in the dark. Proteins were precipitated by

diluting the samples 1:10 with ice-cold ethanol (-40°C) and incubation at -40°C for 1 h. Precipitated proteins were spun down at 20,000 x g for 40 min at 4°C and the pellet was washed with 50 µl ice-cold acetone (-40°C). After 15 minutes of incubation at -40°C, proteins were spun down for 15 min at 20,000 x g and 4°C. The sediment was solubilized in 7.5 µl 2 M guanidinium hydro- chloride (GuHCl) and diluted 1:10 using 50 mM ABC and 1 mM $CaCl_2$. Proteins were digested by adding 5 µl of a 0.1 µg/µl trypsin solution (Sigma-Aldrich T-1426) followed by incubation for 12.5 h at 37°C. The reaction was stopped by adding TFA to a final concentration of 1%. Samples were dried in a vacuum centrifuge, reconstituted in 0.1% TFA and subjected to LC-MS. NanoLC-MS/MS was conducted using a U3000 HPLC system online coupled to a Q Exac- tive HF (both Thermo Scientific). Samples were loaded in 0.1% TFA on a C18 trap column (HiChrom ACE, 100 µm x 2 cm, 5 µm particles) and separated on a C18 main column (HiChrom ACE, 75 µm x 30 cm, 5 µm particles) using a 60 min linear gradient-program from 2.5% to 35% ACN in the presence of 0.1% FA at 60°C and a flow rate of 270 nL/min. The column effluent was introduced to the MS by nanoESI using a PicoTip emitter (new objectives) operated at 1.5 kV. The MS was operated in positive ion-mode using a top15 HCD data-dependent acquisition method with a resolution of 60,000 for MS and a resolution of 15,000 for MS/MS. The normalized collision energy was set to 27 and only ions with an assigned charge state of 2–4 were selected for fragmentation. Automatic gain control target values were set to 106 and 5x104 with maximum ion injection times of 120 and 250 ms for MS and MS/MS, respectively. The dynamic exclusion was set to 12 sec and the m/z = 371.10124 lock mass was used for internal calibration.

8.3.7 Data analysis for mass spectrometry analysis

Database search was done using Mascot v2.4.1 implemented in Proteome Discoverer v1.4 against a merged database comprising all Uniprot entries of *Mus musculus* and all Uniprot/ TreEMBL entries of MCMV strain Smith and K181 (January 2013, 16,799 target sequences). The decoy search option was enabled, and mass error tolerances were set to 10 ppm and 0.02 Da for MS and MS/MS. A maximum of 2 missed cleavages was allowed, oxidation of Met and heavy labelled Arg/Lys was allowed as variable modifications and carbamidomethylation of Cys was set as static modification. Results were filtered for 1% FDR at the PSM level and feature quantification was performed within a 2ppm mass precision window using the precursor ion quantifier. PSM tables were exported and further processed with Microsoft

Excel and R to calculate the number of unique peptides per protein in each condition and median-normalized heavy/light ratios. Proteins identified with 2 unique peptides and a log2 ratio 2,8 in both replicates were considered as potential interaction partners.

8.3.8 Immunofluorescence

To visualize subcellular localizations of proteins immunofluorescence was applied. Therefore, cells were seeded on 4% gelatine pre-coated coverslips with a cell density of 1x10^5 or on impede slides with $4x10^4$ cells per well. Cells were then infected with MCMV mutants at MOI of 1. After 6- 24 hours, cells were washed 1x with PBS and cellular proteins were fixed with 4% paraformaldehyde (PFA) for 20min at RT. Cells were washed again 2x in PBS and aldehyde groups were neutralized with 50mM NH_4Cl in PBS for 15min at RT. After additional 3 washing steps, cells were permeabilized with 0,3% Triton X-100 for 15min at RT. Cells were first washed and then blocked with 0.2 % gelatine for 15min at RT. Afterwards, cells were incubated with the primary antibody (1:300) for 1h at RT. Next, cells were washed again 3x and incubated for 45 – 60 min at RT in the dark with secondary AlexaFlour-conjugated antibody (1:1000) diluted in PBS containing 0.2 % gelatine. The last step was optional, staining of the nucleus with either DAPI or Draq5 (1:1000) in PBS for 10min at RT. To remove residual antibodies or DAPI staining, cells were washed again 3x with PBS. Coverslips were rinsed with water, mounted with 1 drop on an object slide and dried at least for 12 h. Impede slides where kept at 4°C in PBS.

8.3.9 Flow cytometry

Properties of cell populations or single cells can be analyzed via the technique of flow cytometry using specific antibodies. To analyze specific cell cycle stages of transfected cells or MCMV- infected cells, cells were cultivated asynchronized with a density of $8x10^5$ cells per $6cm^2$ dish (transfection) or $3x10^6$ (6-Well). After 24 hours after transfection or infection cells were washed 1x with PBS and then trypsinized with 1mL for 3min at RT. Cells were resuspended in 5mL complemented DMEM with a fine tip to remove all cell clumps and subsequently pelleted at 200g for 5min at RT. The cell pellet was washed with 1mL PBS and again centrifuged at 200g for 5min at RT. Afterwards, the cell pellet was resuspended in 100μL PBS and adjusted to the final volume of 1mL by adding ice-cold 70% ethanol. Samples were gently vortexed during this step and fixed for at least 12h at 4°C. Ethanol was removed and cells were washed with PBS for 300g for 5min at RT. Cells were permebilized with 0,3% Triton-

X100 for 15min at RT. Cells were washed 3x and then stained with primary antibodies against IE1 (1:250) or HA (1:250) in PBS for 30min- 1hour on a rotating platform at RT. This step was followed by additional 3 washing steps and staining of the cells with AlexaFlour-linked secondary antibody (1:500) for 30min rotating at RT. Cells were washed again (300g 5min RT). To determine the cell cycle phases of the cells, the DNA content of cells was measured by using 800 µl propidium iodide (PI) solution which was gently added to the cells under constantly vortexing. The specific gating strategy is shown in (Figure 16). First, cells were gated for the live cells and then for single cells and afterwards for HA or IE1 positive cells. In each experiment 10.000 events were acquired by using a flow cytometer FACS canto II (BD Bioscience). The acquired data was analyzed via Flowjo software.

9 References

1. Jesionek, A., and Kiolemenoglou,B., *Über einen Befund von prozoenartigen Gebilden in den Organen eines heriditarluetischen Fötus.* Munch Med. Wochenschr., 1904. 51(1905-1907).
2. Smith, M.G., Propagation in tissue cultures of a cytopathogenic virus from human salivary gland virus (SGV) disease. Proc Soc Exp Biol Med, 1956. 92(2): p. 424-30.
3. Weller, T.H., *Review. Cytomegaloviruses: the difficult years.* J Infect Dis, 1970. 122(6): p. 532-9.
4. Ogawa, H., et al., Etiology of severe sensorineural hearing loss in children: independent impact of congenital cytomegalovirus infection and GJB2 mutations. J Infect Dis, 2007. 195(6): p. 782-8.
5. Swanson, E.C. and M.R. Schleiss, *Congenital cytomegalovirus infection: new prospects for prevention and therapy.* Pediatric clinics of North America, 2013. 60(2): p. 335-349.
6. Kenneson, A. and M.J. Cannon, Review and meta-analysis of the epidemiology of congenital cytomegalovirus (CMV) infection. Rev Med Virol, 2007. 17(4): p. 253-76.
7. Stagno, S., et al., Congenital cytomegalovirus infection: The relative importance of primary and recurrent maternal infection. N Engl J Med, 1982. 306(16): p. 945-9.
8. Britt, W., Manifestations of human cytomegalovirus infection: proposed mechanisms of acute and chronic disease. Curr Top Microbiol Immunol, 2008. 325: p. 417-70.
9. Cannon, M.J., T.B. Hyde, and D.S. Schmid, Review of cytomegalovirus shedding in bodily fluids and relevance to congenital cytomegalovirus infection. Reviews in medical virology, 2011. 21(4): p. 240-255.
10. Cannon, M.J., D.S. Schmid, and T.B. Hyde, Review of cytomegalovirus seroprevalence and demographic characteristics associated with infection. Rev Med Virol, 2010. 20(4): p. 202-13.
11. Lachmann, R., et al., Cytomegalovirus (CMV) seroprevalence in the adult population of Germany. PloS one, 2018. 13(7): p. e0200267-e0200267.
12. Reeves, M. and J. Sinclair, *Aspects of human cytomegalovirus latency and reactivation.* Curr Top Microbiol Immunol, 2008. 325: p. 297-313.
13. Deayton, J.R., et al., Importance of cytomegalovirus viraemia in risk of disease progression and death in HIV-infected patients receiving highly active antiretroviral therapy. Lancet, 2004. 363(9427): p. 2116-21.
14. Pereyra, F. and R.H. Rubin, Prevention and treatment of cytomegalovirus infection in solid organ transplant recipients. Curr Opin Infect Dis, 2004. 17(4): p. 357-61.
15. Gerna, G., D. Lilleri, and F. Baldanti, *An overview of letermovir: a cytomegalovirus prophylactic option.* Expert Opin Pharmacother, 2019. 20(12): p. 1429-1438.
16. Piret, J. and G. Boivin, Clinical development of letermovir and maribavir: Overview of human cytomegalovirus drug resistance. Antiviral Res, 2019. 163: p. 91-105.
17. Jung, S., et al., Fast breakthrough of resistant cytomegalovirus during secondary letermovir prophylaxis in a hematopoietic stem cell transplant recipient. BMC infectious diseases, 2019. 19(1): p. 388-388.
18. Adland, E., et al., Ongoing burden of disease and mortality from HIV/CMV coinfection in Africa in the antiretroviral therapy era. Front Microbiol, 2015. 6: p. 1016.
19. McGeoch, D.J., F.J. Rixon, and A.J. Davison, *Topics in herpesvirus genomics and evolution.* Virus Res, 2006. 117(1): p. 90-104.
20. Brune, W., Molecular basis of cytomegalovirus host species *specificity.*, in *Cytomaglovirus* M.J. Reddehase, Editor. 2013. p. 322-329.
21. Schleiss, M.R., Developing a Vaccine against Congenital Cytomegalovirus (CMV) Infection: What Have We Learned from Animal Models? Where Should We Go Next? Future virology, 2013. 8(12): p. 1161-1182.
22. Rawlinson, W.D., H.E. Farrell, and B.G. Barrell, *Analysis of the complete DNA sequence of murine cytomegalovirus.* Journal of virology, 1996. 70(12): p. 8833-8849.

23.   Kalejta, R.F., Functions of human cytomegalovirus tegument proteins prior to immediate early gene expression. Curr Top Microbiol Immunol, 2008. 325: p. 101-15.

24.   Kalejta, R.F., *Tegument proteins of human cytomegalovirus.* Microbiol Mol Biol Rev, 2008. 72(2): p. 249-65, table of contents.

25.   Gibson, W., *Structure and formation of the cytomegalovirus virion.* Curr Top Microbiol Immunol, 2008. 325: p. 187-204.

26.   Blut, B.f.G.-A., Humanes Cytomegalovirus (HCMV)- Stellungsnahmen des Arbeitskreises Blut des Bundesministeriums für Gesundheit, in Bundesgesundheitsblatt-Gesundheitsforschung-Gesundheitsschutz. 2000. p. 653-659.

27.   Sinzger, C., M. Digel, and G. Jahn, *Cytomegalovirus cell tropism.* Curr Top Microbiol Immunol, 2008. 325: p. 63-83.

28.   Vanarsdall, A.L. and D.C. Johnson, *Human cytomegalovirus entry into cells.* Current opinion in virology, 2012. 2(1): p. 37-42.

29.   Boyle, K.A. and T. Compton, Receptor-binding properties of a soluble form of human cytomegalovirus glycoprotein B. Journal of virology, 1998. 72(3): p. 1826-1833.

30.   Feire, A.L., H. Koss, and T. Compton, *Cellular integrins function as entry receptors for human cytomegalovirus via a highly conserved disintegrin-like domain.* Proceedings of the National Academy of Sciences of the United States of America, 2004. 101(43): p. 15470-15475.

31.   Isaacson, M.K., A.L. Feire, and T. Compton, *Epidermal growth factor receptor is not required for human cytomegalovirus entry or signaling.* Journal of virology, 2007. 81(12): p. 6241-6247.

32.   Soroceanu, L., A. Akhavan, and C.S. Cobbs, Platelet-derived growth factor-alpha receptor activation is required for human cytomegalovirus infection. Nature, 2008. 455(7211): p. 391-5.

33.   Wang, H.S., Chiu ML, Raab-Traub N, Huang ES., *Epidermal growth factor receptor is a cellular receptor for human cytomegalovirus.* nature, 2003. 424: p. 465-461.

34.   Nguyen, C.C. and J.P. Kamil, Pathogen at the Gates: Human Cytomegalovirus Entry and Cell Tropism. Viruses, 2018. 10(12): p. 704.

35.   Ogawa-Goto, K., et al., Microtubule network facilitates nuclear targeting of human cytomegalovirus capsid. J Virol, 2003. 77(15): p. 8541-7.

36.   Reddehase, M.J., et al., *Murine model of cytomegalovirus latency and reactivation.* Curr Top Microbiol Immunol, 2008. 325: p. 315-31.

37.   Scherer, M. and T. Stamminger, *Emerging Role of PML Nuclear Bodies in Innate Immune Signaling.* J Virol, 2016. 90(13): p. 5850-5854.

38.   Ahn, J.H., W.J. Jang, and G.S. Hayward, The human cytomegalovirus IE2 and UL112-113 proteins accumulate in viral DNA replication compartments that initiate from the periphery of promyelocytic leukemia protein-associated nuclear bodies (PODs or ND10). Journal of virology, 1999. 73(12): p. 10458-10471.

39.   Anders, D.G., et al., Boundaries and structure of human cytomegalovirus oriLyt, a complex origin for lytic-phase DNA replication. Journal of virology, 1992. 66(6): p. 3373-3384.

40.   Anders, D.G. and S.M. Punturieri, *Multicomponent origin of cytomegalovirus lytic-phase DNA replication.* J Virol, 1991. 65(2): p. 931-7.

41.   Jean Beltran, P.M. and I.M. Cristea, *The life cycle and pathogenesis of human cytomegalovirus infection: lessons from proteomics.* Expert review of proteomics, 2014. 11(6): p. 697-711.

42.   Dalod, M., et al., Interferon alpha/beta and interleukin 12 responses to viral infections: pathways regulating dendritic cell cytokine expression in vivo. J Exp Med, 2002. 195(4): p. 517-28.

43.   Browne, E.P., et al., Altered cellular mRNA levels in human cytomegalovirus-infected fibroblasts: viral block to the accumulation of antiviral mRNAs. J Virol, 2001. 75(24): p. 12319-30.

44.   McSharry, B.P., et al., Abrogation of the interferon response promotes more efficient human

cytomegalovirus replication. J Virol, 2015. 89(2): p. 1479-83.

45.   Ostermann, E., et al., Stepwise adaptation of murine cytomegalovirus to cells of a foreign host for identification of host range determinants. Med Microbiol Immunol, 2015. 204(3): p. 461-9.

46.   Takeuchi, O. and S. Akira, *Pattern recognition receptors and inflammation.* Cell, 2010. 140(6): p. 805-20.

47.   Chen, Q., L. Sun, and Z.J. Chen, *Regulation and function of the cGAS-STING pathway of cytosolic DNA sensing.* Nat Immunol, 2016. 17(10): p. 1142-9.

48.   Dell'Oste, V., et al., The interferon-inducible DNA-sensor protein IFI16: a key player in the antiviral response. New Microbiol, 2015. 38(1): p. 5-20.

49.   Compton, T., et al., Human cytomegalovirus activates inflammatory cytokine responses via CD14 and Toll-like receptor 2. J Virol, 2003. 77(8): p. 4588-96.

50.   Boehme, K.W., M. Guerrero, and T. Compton, Human cytomegalovirus envelope glycoproteins B and H are necessary for TLR2 activation in permissive cells. J Immunol, 2006. 177(10): p. 7094-102.

51.   Rossini, G., et al., Interplay between human cytomegalovirus and intrinsic/innate host responses: a complex bidirectional relationship. Mediators of inflammation, 2012. 2012: p. 607276-607276.

52.   Chan, B., et al., The murine cytomegalovirus M35 protein antagonizes type I IFN induction downstream of pattern recognition receptors by targeting NF-kappaB mediated transcription. PLoS Pathog, 2017. 13(5): p. e1006382.

53.   Paulus, C., S. Krauss, and M. Nevels, *A human cytomegalovirus antagonist of type I IFN-dependent signal transducer and activator of transcription signaling.* Proceedings of the National Academy of Sciences of the United States of America, 2006. 103(10): p. 3840-3845.

54.   Le-Trilling, V.T.K., et al., STAT2-Dependent Immune Responses Ensure Host Survival despite the Presence of a Potent Viral Antagonist. Journal of virology, 2018. 92(14): p. e00296-18.

55.   Sun, L., Wu, J., Du, F., Chen, X., & Chen, Z. J. , Cyclic GMP-AMP synthase is a cytosolic DNA sensor that activates the type I interferon pathway. . Science, 2013. 339,6121: p. 786-791.

56.   Paijo, J., et al., cGAS Senses Human Cytomegalovirus and Induces Type I Interferon Responses in Human Monocyte-Derived Cells. PLoS Pathog, 2016. 12(4): p. e1005546.

57.   Lio, C.W., et al., cGAS-STING Signaling Regulates Initial Innate Control of Cytomegalovirus Infection. J Virol, 2016. 90(17): p. 7789-97.

58.   Fu, Y.Z., et al., Human Cytomegalovirus Tegument Protein UL82 Inhibits STING-Mediated Signaling to Evade Antiviral Immunity. Cell Host Microbe, 2017. 21(2): p. 231-243.

59.   Huang ZF, Z.H., Liao BW, Zhang HY, Yang Y, Fu YZ, , *Human Cytomegalovirus Protein UL31 Inhibits DNASensing of cGAS to Mediate Immune Evasion.* Cell Host Microbe, 2018. 11;24(1): p. 69-80.

60.   Fu, Y.Z., et al., Human cytomegalovirus protein UL42 antagonizes cGAS/MITA-mediated innate antiviral response. PLoS Pathog, 2019. 15(5): p. e1007691.

61.   Stempel, M., et al., The herpesviral antagonist m152 reveals differential activation of STING-dependent IRF and NF-kappaB signaling and STING's dual role during MCMV infection. EMBO J, 2019. 38(5).

62.   Amsler, L., M. Verweij, and V.R. DeFilippis, The tiers and dimensions of evasion of the type I interferon response by human cytomegalovirus. J Mol Biol, 2013. 425(24): p. 4857-71.

63.   Balachandran, S., et al., Essential role for the dsRNA-dependent protein kinase PKR in innate immunity to viral infection. Immunity, 2000. 13(1): p. 129-41.

64.   Budt, M., et al., Specific inhibition of the PKR-mediated antiviral response by the murine cytomegalovirus proteins m142 and m143. Journal of virology, 2009. 83(3): p. 1260-1270.

65.   Ostermann, E., et al., Knockout of the Host Resistance Gene Pkr Fully Restores Replication of Murine Cytomegalovirus m142 and m143 Mutants In Vivo. Journal of virology, 2015. 90(2): p. 1144-1147.

66.   Valchanova, R.S., et al., Murine cytomegalovirus m142 and m143 are both required to block

protein kinase R-mediated shutdown of protein synthesis. Journal of virology, 2006. 80(20): p. 10181-10190.

67.   Vincent, H.A., B. Ziehr, and N.J. Moorman, *Mechanism of Protein Kinase R Inhibition by Human Cytomegalovirus pTRS1.* Journal of virology, 2017. 91(5): p. e01574-16.

68.   Tavalai, N. and T. Stamminger, *New insights into the role of the subnuclear structure ND10 for viral infection.* Biochim Biophys Acta, 2008. 1783(11): p. 2207-21.

69.   Negorev, D. and G.G. Maul, Cellular proteins localized at and interacting within ND10/PML nuclear bodies/PODs suggest functions of a nuclear depot. Oncogene, 2001. 20(49): p. 7234-42.

70.   Bernardi, R. and P.P. Pandolfi, *Structure, dynamics and functions of promyelocytic leukaemia nuclear bodies.* Nat Rev Mol Cell Biol, 2007. 8(12): p. 1006-16.

71.   Schumacher, U., et al., Mutations in the M112/M113-coding region facilitate murine cytomegalovirus replication in human cells. J Virol, 2010. 84(16): p. 7994-8006.

72.   Adler M, T.N., Müller R, Stamminger T., Human cytomegalovirus immediate-early gene expression is restricted by the nuclear domain 10 component Sp100. Journal of General Virology, 2011. Jul;92(Pt 7): p. 1532-8.

73.   Tang, Q. and G.G. Maul, Mouse cytomegalovirus immediate-early protein 1 binds with host cell repressors to relieve suppressive effects on viral transcription and replication during lytic infection. Journal of virology, 2003. 77(2): p. 1357-1367.

74.   Ahn, J.H., E.J. Brignole, 3rd, and G.S. Hayward, Disruption of PML subnuclear domains by the acidic IE1 protein of human cytomegalovirus is mediated through interaction with PML and may modulate a RING finger-dependent cryptic transactivator function of PML. Molecular and cellular biology, 1998. 18(8): p. 4899-4913.

75.   Murphy, J.C., et al., Control of cytomegalovirus lytic gene expression by histone acetylation. The EMBO journal, 2002. 21(5): p. 1112-1120.

76.   Nevels, M., C. Paulus, and T. Shenk, *Human cytomegalovirus immediate-early 1 protein facilitates viral replication by antagonizing histone deacetylation.* Proceedings of the National Academy of Sciences of the United States of America, 2004. 101(49): p. 17234-17239.

77.   Tavalai, N., et al., Nuclear domain 10 components promyelocytic leukemia protein and hDaxx independently contribute to an intrinsic antiviral defense against human cytomegalovirus infection. Journal of virology, 2008. 82(1): p. 126-137.

78.   Woodhall, D.L., et al., Human Daxx-mediated repression of human cytomegalovirus gene expression correlates with a repressive chromatin structure around the major immediate early promoter. J Biol Chem, 2006. 281(49): p. 37652-60.

79.   Saffert, R.T. and R.F. Kalejta, Inactivating a cellular intrinsic immune defense mediated by Daxx is the mechanism through which the human cytomegalovirus pp71 protein stimulates viral immediate-early gene expression. Journal of virology, 2006. 80(8): p. 3863-3871.

80.   Jurak, I. and W. Brune, Induction of apoptosis limits cytomegalovirus cross-species infection. EMBO J, 2006. 25(11): p. 2634-42.

81.   Willis, S.N., et al., Proapoptotic Bak is sequestered by Mcl-1 and Bcl-xL, but not Bcl-2, until displaced by BH3-only proteins. Genes & development, 2005. 19(11): p. 1294-1305.

82.   Brune, W. and C.E. Andoniou, Die Another Day: Inhibition of Cell Death Pathways by Cytomegalovirus. Viruses, 2017. 9(9): p. 249.

83.   Arnoult, D., et al., Cytomegalovirus cell death suppressor vMIA blocks Bax- but not Bak-mediated apoptosis by binding and sequestering Bax at mitochondria. Proceedings of the National Academy of Sciences of the United States of America, 2004. 101(21): p. 7988-7993.

84.   Goldmacher, V.S., et al., *A cytomegalovirus-encoded mitochondria-localized inhibitor of apoptosis structurally unrelated to Bcl-2.* Proceedings of the National Academy of Sciences of the United States of America, 1999. 96(22): p. 12536-12541.

85.   Jurak, I., et al., *Murine cytomegalovirus m38.5 protein inhibits Bax-mediated cell death.* Journal of virology, 2008. 82(10): p. 4812-4822.

86.   Norris, K.L. and R.J. Youle, Cytomegalovirus proteins vMIA and m38.5 link mitochondrial

morphogenesis to Bcl-2 family proteins. Journal of virology, 2008. 82(13): p. 6232-6243.

87. Cam, M., et al., Cytomegaloviruses inhibit Bak- and Bax-mediated apoptosis with two separate viral proteins. Cell Death Differ, 2010. 17(4): p. 655-65.

88. Skaletskaya, A., et al., *A cytomegalovirus-encoded inhibitor of apoptosis that suppresses caspase-8 activation.* Proceedings of the National Academy of Sciences of the United States of America, 2001. 98(14): p. 7829-7834.

89. McCormick, A.L., et al., Differential function and expression of the viral inhibitor of caspase 8-induced apoptosis (vICA) and the viral mitochondria-localized inhibitor of apoptosis (vMIA) cell death suppressors conserved in primate and rodent cytomegaloviruses. Virology, 2003. 316(2): p. 221-33.

90. Handke, W., E. Krause, and W. Brune, *Live or let die: manipulation of cellular suicide programs by murine cytomegalovirus.* Med Microbiol Immunol, 2012. 201(4): p. 475-86.

91. Mack, C., et al., *Inhibition of proinflammatory and innate immune signaling pathways by a cytomegalovirus RIP1-interacting protein.* Proceedings of the National Academy of Sciences of the United States of America, 2008. 105(8): p. 3094-3099.

92. Upton, J.W., W.J. Kaiser, and E.S. Mocarski, Cytomegalovirus M45 cell death suppression requires receptor-interacting protein (RIP) homotypic interaction motif (RHIM)-dependent interaction with RIP1. The Journal of biological chemistry, 2008. 283(25): p. 16966-16970.

93. Malumbres, M. and M. Barbacid, *Cell cycle, CDKs and cancer: a changing paradigm.* Nat Rev Cancer, 2009. 9(3): p. 153-66.

94. Sherr, C.J. and J.M. Roberts, CDK inhibitors: positive and negative regulators of G1-phase progression. Genes Dev, 1999. 13(12): p. 1501-12.

95. Henley, S.A. and F.A. Dick, The retinoblastoma family of proteins and their regulatory functions in the mammalian cell division cycle. Cell Div, 2012. 7(1): p. 10.

96. Lomazzi, M., et al., Suppression of the p53- or pRB-mediated G1 checkpoint is required for E2F-induced S-phase entry. Nat Genet, 2002. 31(2): p. 190-4.

97. Ostermann, E., et al., Activation of E2F-dependent transcription by the mouse cytomegalovirus M117 protein affects the viral host range. PLoS Pathog, 2018. 14(12): p. e1007481.

98. Fortunato, E.A., et al., Infection of cells with human cytomegalovirus during S phase results in a blockade to immediate-early gene expression that can be overcome by inhibition of the proteasome. Journal of virology, 2002. 76(11): p. 5369-5379.

99. Salvant, B.S., E.A. Fortunato, and D.H. Spector, Cell cycle dysregulation by human cytomegalovirus: influence of the cell cycle phase at the time of infection and effects on cyclin transcription. J Virol, 1998. 72(5): p. 3729-41.

100. Spector, D.H., *Human cytomegalovirus riding the cell cycle.* Med Microbiol Immunol, 2015. 204(3): p. 409-19.

101. Wiebusch, L., et al., Cell cycle-independent expression of immediate-early gene 3 results in G1 and G2 arrest in murine cytomegalovirus-infected cells. J Virol, 2008. 82(20): p. 10188-98.

102. Wiebusch, L. and C. Hagemeier, The human cytomegalovirus immediate early 2 protein dissociates cellular DNA synthesis from cyclin-dependent kinase activation. EMBO J, 2001. 20(5): p. 1086-98.

103. Bresnahan, W.A., et al., Human cytomegalovirus inhibits cellular DNA synthesis and arrests productively infected cells in late G1. Virology, 1996. 224(1): p. 150-60.

104. Jault, F.M., et al., Cytomegalovirus infection induces high levels of cyclins, phosphorylated Rb, and p53, leading to cell cycle arrest. J Virol, 1995. 69(11): p. 6697-704.

105. Hertel, L. and E.S. Mocarski, Global analysis of host cell gene expression late during cytomegalovirus infection reveals extensive dysregulation of cell cycle gene expression and induction of Pseudomitosis independent of US28 function. J Virol, 2004. 78(21): p. 11988-2011.

106. Sanchez, V., A.K. McElroy, and D.H. Spector, Mechanisms governing maintenance of Cdk1/cyclin B1 kinase activity in cells infected with human cytomegalovirus. J Virol, 2003.

77(24): p. 13214-24.

107. Oduro, J.D., et al., Inhibition of human cytomegalovirus immediate-early gene expression by cyclin A2-dependent kinase activity. Journal of virology, 2012. 86(17): p. 9369-9383.

108. Kalejta, R.F. and T. Shenk, Proteasome-dependent, ubiquitin-independent degradation of the Rb family of tumor suppressors by the human cytomegalovirus pp71 protein. Proceedings of the National Academy of Sciences of the United States of America, 2003. 100(6): p. 3263-3268.

109. Prichard, M.N., et al., Human cytomegalovirus UL97 kinase activity is required for the hyperphosphorylation of retinoblastoma protein and inhibits the formation of nuclear aggresomes. Journal of virology, 2008. 82(10): p. 5054-5067.

110. Qian, Z., et al., Human cytomegalovirus protein pUL117 targets the mini-chromosome maintenance complex and suppresses cellular DNA synthesis. PLoS Pathog, 2010. 6(3): p. e1000814.

111. White, E.A. and D.H. Spector, Exon 3 of the human cytomegalovirus major immediate-early region is required for efficient viral gene expression and for cellular cyclin modulation. Journal of virology, 2005. 79(12): p. 7438-7452.

112. Kadrmas, J.L. and M.C. Beckerle, *The LIM domain: from the cytoskeleton to the nucleus.* Nat Rev Mol Cell Biol, 2004. 5(11): p. 920-31.

113. Smith, M.A., L.M. Hoffman, and M.C. Beckerle, *LIM proteins in actin cytoskeleton mechanoresponse.* Trends in cell biology, 2014. 24(10): p. 575-583.

114. Sharp, T.V., et al., *The chromosome 3p21.3-encoded gene, LIMD1, is a critical tumor suppressor involved in human lung cancer development.* Proceedings of the National Academy of Sciences of the United States of America, 2008. 105(50): p. 19932-19937.

115. Sharp, T.V., et al., LIM domains-containing protein 1 (LIMD1), a tumor suppressor encoded at chromosome 3p21.3, binds pRB and represses E2F-driven transcription. Proceedings of the National Academy of Sciences of the United States of America, 2004. 101(47): p. 16531-16536.

116. Liao, Z.L., et al., [Expression and clinical significance of LIMD-1 gene in adult patients with acute leukemia]. Zhongguo Shi Yan Xue Ye Xue Za Zhi, 2015. 23(1): p. 34-8.

117. Ghosh, S., et al., LIMD1 is more frequently altered than RB1 in head and neck squamous cell carcinoma: clinical and prognostic implications. Molecular cancer, 2010. 9: p. 58-58.

118. Eales, K.L., K.E. Hollinshead, and D.A. Tennant, *Hypoxia and metabolic adaptation of cancer cells.* Oncogenesis, 2016. 5: p. e190.

119. Foxler, D.E., et al., A HIF-LIMD1 negative feedback mechanism mitigates the pro-tumorigenic effects of hypoxia. EMBO molecular medicine, 2018. 10(8): p. e8304.

120. Dimova, D.K. and N.J. Dyson, *The E2F transcriptional network: old acquaintances with new faces.* Oncogene, 2005. 24(17): p. 2810-26.

121. Zhou, J., et al., LIMD1 phosphorylation in mitosis is required for mitotic progression and its tumor-suppressing activity. FEBS J, 2019. 286(5): p. 963-974.

122. Wang, L., et al., LIMD1 is induced by and required for LMP1 signaling, and protects EBV-transformed cells from DNA damage-induced cell death. Oncotarget, 2017. 9(5): p. 6282-6297.

123. Lemmon, M.A. and J. Schlessinger, *Cell signaling by receptor tyrosine kinases.* Cell, 2010. 141(7): p. 1117-34.

124. Haqshenas, G. and C. Doerig, Targeting of host cell receptor tyrosine kinases by intracellular pathogens. Sci Signal, 2019. 12(599).

125. Wee, P. and Z. Wang, Epidermal Growth Factor Receptor Cell Proliferation Signaling Pathways. Cancers (Basel), 2017. 9(5).

126. Ullrich, A. and J. Schlessinger, *Signal transduction by receptors with tyrosine kinase activity.* Cell, 1990. 61(2): p. 203-12.

127. Begley, M.J., et al., EGF-receptor specificity for phosphotyrosine-primed substrates provides signal integration with Src. Nat Struct Mol Biol, 2015. 22(12): p. 983-90.

128. Roepstorff, K., et al., Differential effects of EGFR ligands on endocytic sorting of the receptor. Traffic, 2009. 10(8): p. 1115-27.

129. Ravichandran, K.S., *Signaling via Shc family adapter proteins.* Oncogene, 2001. 20(44): p. 6322-30.

130. Lotti, L.V., et al., Sch proteins are localized on endoplasmic reticulum membranes and are redistributed after tyrosine kinase receptor activation. Molecular and cellular biology, 1996. 16(5): p. 1946-1954.

131. Wary, K.K., et al., The adaptor protein Shc couples a class of integrins to the control of cell cycle progression. Cell, 1996. 87(4): p. 733-43.

132. Gotoh, N., M. Toyoda, and M. Shibuya, Tyrosine phosphorylation sites at amino acids 239 and 240 of Shc are involved in epidermal growth factor-induced mitogenic signaling that is distinct from Ras/mitogen-activated protein kinase activation. Molecular and cellular biology, 1997. 17(4): p. 1824-1831.

133. Ventura, A., et al., The p66Shc longevity gene is silenced through epigenetic modifications of an alternative promoter. J Biol Chem, 2002. 277(25): p. 22370-6.

134. Migliaccio, E., et al., Opposite effects of the p52shc/p46shc and p66shc splicing isoforms on the EGF receptor-MAP kinase-fos signalling pathway. EMBO J, 1997. 16(4): p. 706-16.

135. van der Geer , W.S., Gish GD, Pawson T., The Shc adaptor protein is highly phosphorylated at conserved, twin tyrosine residues (Y239/240) that mediate protein-protein interactions. Current Biology, 1996. 6(11): p. 1435-1444.

136. Salcini, A.E., et al., Formation of Shc-Grb2 complexes is necessary to induce neoplastic transformation by overexpression of Shc proteins. Oncogene, 1994. 9(10): p. 2827-36.

137. Zheng, Y., et al., Temporal regulation of EGF signalling networks by the scaffold protein Shc1. Nature, 2013. 499(7457): p. 166-71.

138. Ingham, R.J., et al., The Gab1 protein is a docking site for multiple proteins involved in signaling by the B cell antigen receptor. J Biol Chem, 1998. 273(46): p. 30630-7.

139. Gu, H., et al., *New role for Shc in activation of the phosphatidylinositol 3-kinase/Akt pathway.* Molecular and cellular biology, 2000. 20(19): p. 7109-7120.

140. Radhakrishnan, Y., et al., Insulin-like growth factor-I stimulates Shc-dependent phosphatidylinositol 3-kinase activation via Grb2-associated p85 in vascular smooth muscle cells. The Journal of biological chemistry, 2008. 283(24): p. 16320-16331.

141. Ahmed, S.B.M. and S.A. Prigent, *Insights into the Shc Family of Adaptor Proteins.* Journal of molecular signaling, 2017. 12: p. 2-2.

142. Dilworth, S.M., et al., Transformation by polyoma virus middle T-antigen involves the binding and tyrosine phosphorylation of Shc. Nature, 1994. 367(6458): p. 87-90.

143. Baughn, L.B. and N. Rosenberg, Disruption of the Shc/Grb2 complex during abelson virus transformation affects proliferation, but not apoptosis. Journal of virology, 2005. 79(4): p. 2325-2334.

144. Strunk, U., et al., Role of Herpes simplex virus 1 VP11/12 tyrosine-based binding motifs for Src family kinases, p85, Grb2 and Shc in activation of the phosphoinositide 3-kinase-Akt pathway. Virology, 2016. 498: p. 31-35.

145. Strunk, U., et al., Role of herpes simplex virus VP11/12 tyrosine-based motifs in binding and activation of the Src family kinase Lck and recruitment of p85, Grb2, and Shc. J Virol, 2013. 87(20): p. 11276-86.

146. Herber, B., et al., Inducible regulatory elements in the human cyclin D1 promoter. Oncogene, 1994. 9(7): p. 2105-7.

147. Manning, B.D. and L.C. Cantley, *AKT/PKB signaling: navigating downstream.* Cell, 2007. 129(7): p. 1261-74.

148. Rössig, L., et al., Akt-dependent phosphorylation of p21(Cip1) regulates PCNA binding and proliferation of endothelial cells. Molecular and cellular biology, 2001. 21(16): p. 5644-5657.

149. Eierhoff, T., et al., The epidermal growth factor receptor (EGFR) promotes uptake of influenza A viruses (IAV) into host cells. PLoS pathogens, 2010. 6(9): p. e1001099-e1001099.

150. Macdonald, C.J., Harris M., Perturbation of epidermal growth factor receptor complex formation and Ras signalling in cells harbouring the hepatitis C virus subgenomic replicon. Journal of General Virology, 2005. 86: p. 1027-1033.

151. Macdonald, A., et al., The hepatitis C virus non-structural NS5A protein inhibits activating protein-1 function by perturbing ras-ERK pathway signaling. J Biol Chem, 2003. 278(20): p. 17775-84.

152. Feire, A.L., et al., The glycoprotein B disintegrin-like domain binds beta 1 integrin to mediate cytomegalovirus entry. Journal of virology, 2010. 84(19): p. 10026-10037.

153. Wang, X., et al., *Integrin alphavbeta3 is a coreceptor for human cytomegalovirus.* Nature medicine, 2005. 11(5): p. 515-521.

154. Buehler, J., et al., Opposing Regulation of the EGF Receptor: A Molecular Switch Controlling Cytomegalovirus Latency and Replication. PLoS Pathog, 2016. 12(5): p. e1005655.

155. Rak, M.A., et al., Human Cytomegalovirus UL135 Interacts with Host Adaptor Proteins To Regulate Epidermal Growth Factor Receptor and Reactivation from Latency. J Virol, 2018. 92(20).

156. Buehler, J., et al., Host signaling and EGR1 transcriptional control of human cytomegalovirus replication and latency. PLoS Pathog, 2019. 15(11): p. e1008037.

157. Reeves, M.B., A. Breidenstein, and T. Compton, Human cytomegalovirus activation of ERK and myeloid cell leukemia-1 protein correlates with survival of latently infected cells. Proc Natl Acad Sci U S A, 2012. 109(2): p. 588-93.

158. Kew, V., M. Wills, and M. Reeves, HCMV activation of ERK-MAPK drives a multi-factorial response promoting the survival of infected myeloid progenitors. J Mol Biochem, 2017. 6(1): p. 13-25.

159. Boyle, K.A., R.L. Pietropaolo, and T. Compton, Engagement of the cellular receptor for glycoprotein B of human cytomegalovirus activates the interferon-responsive pathway. Molecular and cellular biology, 1999. 19(5): p. 3607-3613.

160. Rodems, S.M. and D.H. Spector, Extracellular signal-regulated kinase activity is sustained early during human cytomegalovirus infection. J Virol, 1998. 72(11): p. 9173-80.

161. Harel, N.Y. and J.C. Alwine, Phosphorylation of the human cytomegalovirus 86-kilodalton immediate-early protein IE2. Journal of virology, 1998. 72(7): p. 5481-5492.

162. Johnson, R.A., et al., The role of MKK1/2 kinase activity in human cytomegalovirus infection. J Gen Virol, 2001. 82(Pt 3): p. 493-7.

163. Colao, I., et al., The ERK-1 function is required for HSV-1-mediated G1/S progression in HEP-2 cells and contributes to virus growth. Sci Rep, 2017. 7(1): p. 9176.

164. Melnick, M., et al., Small molecule inhibitors of the host cell COX/AREG/EGFR/ERK pathway attenuate cytomegalovirus-induced pathogenesis. Experimental and molecular pathology, 2011. 91(1): p. 400-410.

165. Cobbs, C.S., et al., Modulation of oncogenic phenotype in human glioma cells by cytomegalovirus IE1-mediated mitogenicity. Cancer Res, 2008. 68(3): p. 724-30.

166. Johnson, R.A., et al., Human cytomegalovirus up-regulates the phosphatidylinositol 3-kinase (PI3-K) pathway: inhibition of PI3-K activity inhibits viral replication and virus-induced signaling. Journal of virology, 2001. 75(13): p. 6022-6032.

167. Chan, G., et al., PI3K-dependent upregulation of Mcl-1 by human cytomegalovirus is mediated by epidermal growth factor receptor and inhibits apoptosis in short-lived monocytes. Journal of immunology (Baltimore, Md. : 1950), 2010. 184(6): p. 3213-3222.

168. Lafemina, R.L. and G.S. Hayward, Differences in cell-type-specific blocks to immediate early gene expression and DNA replication of human, simian and murine cytomegalovirus. J Gen Virol, 1988. 69 (Pt 2): p. 355-74.

169. Kim, K.S. and R.I. Carp, Abortive infection of human diploid cells by murine cytomegalovirus. Infect Immun, 1972. 6(5): p. 793-7.

170. Walker, D. and J. Hudson, Analysis of immediate-early and early proteins of murine cytomegalovirus in permissive and nonpermissive cells. Arch Virol, 1987. 92(1-2): p. 103-19.

171. Walker DG, H.J., Further characterization of the murine cytomegalovirus induced early proteins in permissive and nonpermissive cells. Arch Virol, 1988. 101(3–4):: p. 143-154.

172. Mocarski, E.S.C., C.T., *Cytomegaloviruses and their replication.*, in *Fields Virology 4th edition*, D.M. Knipe, and Howley, P.M., Editor. 2001. p. 2629–2673.

173. Moran, E. and M.B. Mathews, *Multiple functional domains in the adenovirus E1A gene.* Cell, 1987. 48(2): p. 177-8.

174. Cuconati, A. and E. White, Viral homologs of BCL-2: role of apoptosis in the regulation of virus infection. Genes Dev, 2002. 16(19): p. 2465-78.

175. Cosme, R.C., F.P. Martinez, and Q. Tang, Functional interaction of nuclear domain 10 and its components with cytomegalovirus after infections: cross-species host cells versus native cells. PLoS One, 2011. 6(4): p. e19187.

176. Tang, Q. and G.G. Maul, Mouse cytomegalovirus crosses the species barrier with help from a few human cytomegalovirus proteins. J Virol, 2006. 80(15): p. 7510-21.

177. Buhler, B., et al., Characterization of the murine cytomegalovirus early transcription unit e1 that is induced by immediate-early proteins. J Virol, 1990. 64(5): p. 1907-19.

178. Wang, F., et al., Disruption of Erk-dependent type I interferon induction breaks the myxoma virus species barrier. Nat Immunol, 2004. 5(12): p. 1266-74.

179. Child, S.J., et al., Species specificity of protein kinase r antagonism by cytomegalovirus TRS1 genes. Journal of virology, 2012. 86(7): p. 3880-3889.

180. Pawletko, K., Identification and Characterization of Determinants of the Cytomegalovirus Species Specificity, in Biology. 2015, Universität Duisburg-Essen.

181. Kattenhorn, L.M., et al., Identification of proteins associated with murine cytomegalovirus virions. J Virol, 2004. 78(20): p. 11187-97.

182. Mitchell, D.P., et al., Human cytomegalovirus UL28 and UL29 open reading frames encode a spliced mRNA and stimulate accumulation of immediate-early RNAs. J Virol, 2009. 83(19): p. 10187-97.

183. Stade, K., et al., Exportin 1 (Crm1p) is an essential nuclear export factor. Cell, 1997. 90(6): p. 1041-50.

184. Schommartz, T., et al., Functional Dissection of an Alternatively Spliced Herpesvirus Gene by Splice Site Mutagenesis. Journal of virology, 2016. 90(9): p. 4626-4636.

185. Mellacheruvu, D., et al., The CRAPome: a contaminant repository for affinity purification-mass spectrometry data. Nat Methods, 2013. 10(8): p. 730-6.

186. Huggins, C.J. and I.L. Andrulis, Cell cycle regulated phosphorylation of LIMD1 in cell lines and expression in human breast cancers. Cancer Lett, 2008. 267(1): p. 55-66.

187. Spendlove, I., et al., Differential subcellular localisation of the tumour suppressor protein LIMD1 in breast cancer correlates with patient survival. Int J Cancer, 2008. 123(10): p. 2247-53.

188. Terhune, S.S., et al., Human cytomegalovirus UL29/28 protein interacts with components of the NuRD complex which promote accumulation of immediate-early RNA. PLoS pathogens, 2010. 6(6): p. e1000965-e1000965.

189. Gong, L.I., M.A. Suchard, and J.D. Bloom, Stability-mediated epistasis constrains the evolution of an influenza protein. Elife, 2013. 2: p. e00631.

190. Duan, S., et al., Epistatic interactions between neuraminidase mutations facilitated the emergence of the oseltamivir-resistant H1N1 influenza viruses. Nat Commun, 2014. 5: p. 5029.

191. Shyy, J.Y. and S. Chien, *Role of integrins in endothelial mechanosensing of shear stress.* Circ Res, 2002. 91(9): p. 769-75.

192. Ahn, R., et al., The Shc1 adaptor simultaneously balances Stat1 and Stat3 activity to promote breast cancer immune suppression. Nat Commun, 2017. 8: p. 14638.

193. Shmulevitz, M., et al., Oncogenic Ras promotes reovirus spread by suppressing IFN-beta production through negative regulation of RIG-I signaling. Cancer Res, 2010. 70(12): p. 4912-21.

194.   Di Nicolantonio, F., et al., Replacement of normal with mutant alleles in the genome of normal human cells unveils mutation-specific drug responses. Proc Natl Acad Sci U S A, 2008. 105(52): p. 20864-9.

195.   Marthandan, S., et al., Conserved genes and pathways in primary human fibroblast strains undergoing replicative and radiation induced senescence. Biol Res, 2016. 49(1): p. 34.

196.   Marthandan, S., et al., Similarities in Gene Expression Profiles during In Vitro Aging of Primary Human Embryonic Lung and Foreskin Fibroblasts. Biomed Res Int, 2015. 2015: p. 731938.

197.   Ahasan, M.M. and C. Sweet, Murine cytomegalovirus open reading frame m29.1 augments virus replication both in vitro and in vivo. J Gen Virol, 2007. 88(Pt 11): p. 2941-51.

198.   Muscolino, E., et al., Herpesviruses induce aggregation and selective autophagy of host signalling proteins NEMO and RIPK1 as an immune-evasion mechanism. Nat Microbiol, 2020. 5(2): p. 331-342.

199.   Nobre, L.V., et al., Human cytomegalovirus interactome analysis identifies degradation hubs, domain associations and viral protein functions. Elife, 2019. 8.

200.   Lai, K.M. and T. Pawson, The ShcA phosphotyrosine docking protein sensitizes cardiovascular signaling in the mouse embryo. Genes Dev, 2000. 14(9): p. 1132-45.

201.   Mainiero, F., et al., Signal transduction by the alpha 6 beta 4 integrin: distinct beta 4 subunit sites mediate recruitment of Shc/Grb2 and association with the cytoskeleton of hemidesmosomes. EMBO J, 1995. 14(18): p. 4470-81.

202.   Niu, S., H. Xie, and E.E. Marcantonio, Integrin-mediated tyrosine phosphorylation of Shc in T cells is regulated by protein kinase C-dependent phosphorylations of Lck. Mol Biol Cell, 2003. 14(2): p. 349-60.

203.   Ruff-Jamison, S., et al., Epidermal growth factor stimulates the tyrosine phosphorylation of SHC in the mouse. J Biol Chem, 1993. 268(11): p. 7610-2.

204.   Mendoza, M.C., E.E. Er, and J. Blenis, The Ras-ERK and PI3K-mTOR pathways: cross-talk and compensation. Trends in biochemical sciences, 2011. 36(6): p. 320-328.

205.   Yu, C.F., Z.X. Liu, and L.G. Cantley, ERK negatively regulates the epidermal growth factor-mediated interaction of Gab1 and the phosphatidylinositol 3-kinase. J Biol Chem, 2002. 277(22): p. 19382-8.

206.   Wang, F., et al., Disruption of Erk-dependent type I interferon induction breaks the myxoma virus species barrier. Nat Immunol, 2004. 5(12): p. 1266-1274.

207.   Pleschka, S., et al., Influenza virus propagation is impaired by inhibition of the Raf/MEK/ERK signalling cascade. Nat Cell Biol, 2001. 3(3): p. 301-5.

208.   Meloche, S. and J. Pouyssegur, The ERK1/2 mitogen-activated protein kinase pathway as a master regulator of the G1- to S-phase transition. Oncogene, 2007. 26(22): p. 3227-39.

209.   Stamminger, T. and B. Fleckenstein, Immediate-early transcription regulation of human cytomegalovirus. Curr Top Microbiol Immunol, 1990. 154: p. 3-19.

210.   Datta, S.R., et al., Akt phosphorylation of BAD couples survival signals to the cell-intrinsic death machinery. Cell, 1997. 91(2): p. 231-41.

211.   Vanhaesebroeck, B., L. Stephens, and P. Hawkins, PI3K signalling: the path to discovery and understanding. Nat Rev Mol Cell Biol, 2012. 13(3): p. 195-203.

212.   Yamamoto, T., et al., Continuous ERK activation downregulates antiproliferative genes throughout G1 phase to allow cell-cycle progression. Curr Biol, 2006. 16(12): p. 1171-82.

213.   Harvey, D.M. and A.J. Levine, p53 alteration is a common event in the spontaneous immortalization of primary BALB/c murine embryo fibroblasts. Genes Dev, 1991. 5(12B): p. 2375-85.

214.   Angulo, A., P. Ghazal, and M. Messerle, The major immediate-early gene ie3 of mouse cytomegalovirus is essential for viral growth. J Virol, 2000. 74(23): p. 11129-36.

215.   Krause, E., et al., Murine cytomegalovirus virion-associated protein M45 mediates rapid NF-kappaB activation after infection. J Virol, 2014. 88(17): p. 9963-75.

216.   Tischer, B.K., G.A. Smith, and N. Osterrieder, En passant mutagenesis: a two step markerless red recombination system. Methods Mol Biol, 2010. 634: p. 421-30.

217.   Hamilton, A.J. and D.C. Baulcombe, A species of small antisense RNA in posttranscriptional gene silencing in plants. Science, 1999. 286(5441): p. 950-2.

218.   Ramakrishnan, M.A., *Determination of 50% endpoint titer using a simple formula.* World journal of virology, 2016. 5(2): p. 85-86.

219.   Osborn, J.E. and D.L. Walker, Enhancement of infectivity of murine cytomegalovirus in vitro by centrifugal inoculation. J Virol, 1968. 2(9): p. 853-8.

10 Appendix   125

10.1 Curriculum Vitae

Lebenslauf entfällt aus datenschutzrechtlichen Gründen.

10.2 Content of figures and tables

10.3 List of abbreviations

ActD	Actinomycin D
AIDS	Acquired immunodeficiency syndrome
AIM2	Absent in melanoma 2
AKT	Proteinkinase B
AP	affinity purification
AP-1	c-fos and c-jun
BAD	Bcl2-associated agonist of cell death
BAK	BCL-2 antagonist
BAX	Apoptosis regulator BAX
BCL-2	B-cell lymphoma protein 2
CDK	Cylin dependent kinase
cGAS	Cyclic GMP–AMP synthase
CHX	Cycloheximide
CMV	Cytomegalovirus
CREB	Cyclic AMP-responsive element-binding protein 1
DAXX	Death-associated protein
DP	Dimerization protein
E	Early
E2F	E2F transcription factor
EBV	Epstein-Barr virus
EGFR	Epidermal growth factor receptor
elFα2	elFα2-Translation initiation factor
ELK1	ETS domain-containing protein 1
ER	Endoplasmic reticulum
ERK1/2	Extracellular signal-regulated kinases 1/2
GAB1/2	GRB2-associated-binding protein 1 is a protein
gB	Glycoprotein B
GFP	Green fluorescent protein
GRB2	Growth factor receptor-bound 2
GSK-3β	Glycogen synthase kinase 3 beta
HA	Hemagglutinin
HAART	Highly antiretroviral therapy
HCMV	Human cytomegalovirus
HIF-alpha	Hypoxia-inducible factor 1-alpha
HIV	Human immunodeficiency virus
HPC	Hematopoietic progenitor cells
HPI	hours post infection
HPV	Human papilloma virus
HSV-1	Herpes simplex virus 1
IE	Immediate-early
IFI16	Gamma-interferon-inducible protein 16
IFN	Interferon
IFN	Interferon
IKK	IκB kinase
IL	Interleukin
IRF	Interferon regulatory factor

IRS1	Internal repeat short 1
ISG	Interferon-stimulated gene
JAK	Janus kinase
L	Late
LIMD1	LIM domain containing protein I
LTV	Letermovir
MAPK	Mitogen-activated protein kinase
MCL-1	Induced myeloid leukemia cell differentiation protein Mcl-1
MCMV	Murine cytomegalovirus
MDM2	Mouse double minute 2 homolog
MIEP	Major immediate early promoter
MOI	multiplicity of infection
mRNA	messenger RNA
MS	mass spectrometry
mTOR	mammalian target of rapamycin
mTORC	mammalian target of rapamycin complex
ND10	Nuclear domain 10
NES	nuclear export signal
NF-κb	Nuclear factor 'kappa-light-chain-enhancer' of activated B-cells
NLR	Nod-like receptor
ORF	Open reading frame
p204	Phosphoprotein 204
PAMP	Pathogen-associated molecular pattern
PCNA	Proliferating cell nuclear antigen
PCR	polymerase chain reaction
PDGFRα	Platelet-derived growth factor receptor alpha
PDK	3-phosphoinositide-dependent protein kinase
PI3K	phosphoinositide 3-kinase
PI3K	Phosphatidylinositol 3-kinase
PKR	Protein kinase R
PLCγ1	Phospholipase C-gamma-Isoenzyme
PML-NB	Promyelocytic leukemia nuclear body
pRb	Retinoblastoma protein
PRR	Pathogen recognition receptor
PYD	Pyrin domain
RCMV	Rat CMV
RIG-I	Retinoic acid-inducible gene I
RIPK	Receptor interacting protein
RLR	Retinoic acid-inducible gene I like receptor
RTK	Receptor tyrosine kinase
SHC1	SHC-transforming protein 1
SILAC	stable isotope labelling amino acids in cell culture
SOS	Son of sevenless
Sp1	Specificity protein 1
SP100	Sp100 nuclear antigen
STAT	Signal transducer and activator of transcription
STING	Stimulator of interferon genes
TBK1	TANK-binding kinase 1

TCID$_{50}$	tissue culture infectious dose 50 %
TLR	Toll-like receptor
TNF	Tumor necrosis factor
TRS1	Terminal repeat short
vAC	Viral assembly complex
WT	wildtype

10.4 List of hazardous substances

substance	GHS symbol	hazard statements	precautionary statements
2-mercaptoethanol		H301 + H331-H310-H315-H317-H318-H373-H410	P261-P280-P301 + P310 + P330-P302 + P352 + P310-P305 + P351 + P338 + P310-P403 + P233
acetic acid		H226-H314	P280-P305 + P351 + P338-P310
acrylamide		H301-H312 + H332-H315-H317-H319-H340-H350-H361f-H372	P201-P280-P301 + P310-P305 + P351 + P338-P308 + P313
ammonium bicarbonate		H302	P301 + P312 + P330
ammonium persulfate		H272-H302-H315-H317-H319-H334-H335	P220-P261-P280-P305 + P351 + P338-P342 + P311
ampicillin		H315-H317-H319-H334-H335	P261-P280-P305 + P351 + P338-P342 + P311
bis-acrylamide		H302 + H332	
boric acid		H360FD	P201-P308 + P313
chloramphenicol		H350	P201-P308 + P313
cycloheximide		H302-H330-H341	P260-P281-P284-P310
EDTA		H319	P305 + P351 + P338
ethanol		H225-H319	P210-P280-P305 + P351 + P338-P337 + P313-P403 + P235
ethidium bromide		H302-H330-H341	P260-P281-P284-P310
hydrochloric acid		H290-H314-H335	P261-P280-P305 + P351 + P338-P310
isopropanol		H225-H319-H336	P210-P261-P305 + P351 + P338
kanamycin		H360	P201-P308 + P313

leptomycin B		H225 H301 + H311 + H331 H370	P210 P280 P301 + P310 + P330 P302 + P352 + P312 P304 + P340 + P311
liquid nitrogen		H281	P202-P271 + P403-P282
methanol		H225-H301 + H311 + H331-H370	P210-P260-P280-P301 + P310-P311
NP-40		H319+H315	P264+P280
penicillin		H317-H334	P261-P280-P342 + P311
protein A-agarose		H226	
protein G-agarose		H226	
puromycin		H373	
sodium dodecyl sulfate		H315-H318-H335	P280-P304 + P340 + P312-P305 + P351 + P338 + P310
sodium hydroxide		H290-H314	P280-P305 + P351 + P338-P310
streptomycin		H302-H361	P281
TEMED		H225-H302-H314-H332	P210-P280-P305 + P351 + P338-P310
Triton X-100		H302-H319-H411	P273-P280-P301 + P312 + P330-P337 + P313-P391-P501

10.5 Acknowledgments

10.6 Statement of Authorship

I hereby declare on oath, that I have written the present dissertation by my own and have not used other than the acknowledged resources and aids. The submitted written version corresponds to the version on the electronic storage medium. I hereby declare that I have not previously applied or pursued for a doctorate (Ph.D.studies).

Hamburg, 19.02.2020

Kerstin Pawletko